UNIVERSITY OF CAPE TOWN

FACULTY OF ENGINEERING AND BUILT ENVIRONMENT

DEPARTMENT OF ELECTRICAL ENGINEERING

Using Probability Density Functions to Analyze the Effect of External Threats on the Reliability of a South African Power Grid

MILTON EDIMU

Supervisors: Prof. C. T. Gaunt & Dr. R. Herman

Thesis submitted in fulfilment of the requirements for the degree of

Doctor of Philosophy

In

Electrical Engineering

October 2013

Keywords-Bulk Power System, Reliability Analysis, Risk Modelling, Adverse Weather, Probability Distribution Functions

DECLARATION

I know the meaning of plagiarism and declare that all the work in the document, save for that which is properly acknowledged, is my own.

The number of words in the main text of the thesis is less than 80,000.

Signature: Signed by candidate
Signature Removed

Date: 10th October 2013

ABSTRACT

The implications of reliability based decisions are a vital component of the control and management of power systems. Network planners strive to achieve an optimum level of investments and reliability. Network operators on the other hand aim at mitigating the costs associated with low levels of reliability. Effective decision making requires the management of uncertainties in the process applied. Thus, the modelling of reliability inputs, methodology applied in assessing network reliability and the interpretation of the reliability outputs should be carefully considered in reliability analyses.

This thesis applies probability density functions, as opposed to deterministic averages, to model component failures. The probabilistic models are derived from historical failure data that is usually confined to finite ranges. Thus, the Beta distribution which has the unique characteristic of being able to be rescaled to a different finite range is selected.

The thesis presents a new reliability evaluation technique that is based on the sequential Monte Carlo simulation. The technique applies a time-dependent probabilistic modelling approach to network reliability parameters. The approach uses the Beta probability density functions to model stochastic network parameters while taking into account seasonal and time-of-day influences. While the modelling approach can be applied to different aspects such as intermittent power supply and system loading, it is applied in this thesis to model the failure and repair rates of network components. Unlike the conventional sequential Monte Carlo methods, the new technique does not require the derivation of an inverse translation function for the probability distribution applied. The conventional Monte Carlo technique simulates the up and down component states when building their chronological cycles. The new technique applied here focuses instead on simulating the down states of component chronological cycles. The simulation determines the number of down states, when they will occur and how long they will last before developing the chronological cycle.

Tests performed on a published network show that focussing on the down states significantly improves the computation times of a sequential Monte Carlo simulation. Also, the reliability results of the new sequential Monte Carlo technique are more dependent on the input failure models than on the number of simulation runs or the stopping criterion applied to a simulation and in this respect gives results different from present standard approaches.

The thesis also applies the new approach on a real bulk power network. The bulk network is part of the South African power grid. Thus, the network threats considered and the corresponding failure data collected are typical of the real South African conditions. The thesis shows that probability density functions are superior to deterministic average values when modelling reliability parameters. Probability density functions reflect the variability in reliability parameters through their dispersion and skewness. The time-dependent probabilistic approach is applied in both planning and operational reliability analyses. The component failure models developed show that variability in network parameters is different for planning and operational reliability analyses. The thesis shows how the modelling approach is used to translate long-term failure models into operational (short-term) failure models.

DigSilent and MATLAB software packages are used to perform network stability and reliability simulations in this thesis. The reliability simulation results of the time-dependent probabilistic approach show that the perception on a network's reliability is significantly impacted on when probability distribution functions that account for the full range of parameter values are applied as inputs. The results also show that the application of the probabilistic models to network components must be considered in the context of either network planning or operation. Furthermore, the risk-based approach applied to the interpretation of reliability indices significantly influences the perception on the network's reliability performance. The risk-based approach allows the uncertainty allowed in a network planning or operation decision to be quantified.

ACKNOWLEDMENTS

First and foremost, I would like to thank the almighty God for paving the road that has brought me this far. May you continue to shed your light in my life. Amen!

My sincere gratitude goes to the University of Cape Town, particularly my supervisors Prof. C.T. Gaunt and Dr. R. Herman for availing me this opportunity. I appreciate all the guidance and advice provided. I promise to pass on the lessons learnt. The support staff in the Department of electrical Engineering: Marlene, Chris, Phillip, Nicole, Carol and Pierre. Thank you for all your efforts in making my stay at UCT a smooth one. A special thank you to the UCT Postgraduate funding office for the support rendered during the course of this thesis.

I dedicate this thesis to my parents, Prof Adipala Ekwamu and the late Mrs. Theopista Nagujja Adipala. To my mother I miss you still. To my father, thank you for being my inspiration and showing me what it means to be a real man. I would like to thank my wife, Mrs. Pamela Alinda Edimu, for the unending support and encouragement. Thank you for always believing in me. To the rest of my family, I thank you for the prayers. I needed them.

I would also like to thank all the old and new friends I have met during my stay in South Africa. It was an absolute pleasure meeting all of you and thank you for the many needed breaks from this research.

For God and my country…!

TABLE OF CONTENTS

LIST OF FIGURES

LIST OF TABLES

ACRONYMS

A-D	Anderson Darling
C-S	Chi-Square
DLC	Duration of Load Curtailment
FLC	Frequency of Load Curtailment
FMEA	Failure Mode and Effect Analysis
GIC	Geomagnetically Induced Current
HV	High Voltage
IEEE	Institute of Electrical and Electronic Engineers
K-S	Kolmogorov-Smirnov
MCS	Monte Carlo Simulation
NERC	National American Electric Reliability Corporation
PDF	Probability Density Function
PLC	Probability of Load Curtailment
$\mathbf{T_{pt}}$	Time window
TDPA	Time-Dependent Probabilistic Approach
TTF	Time-to-Failure
TTR	Time-to-Repair
SAWS	South African Weather Service
SDM	State Duration Method
SEM	State Enumeration Method
SSM	State Sampling Method
RBTS	Roy Billinton Test System

1. INTRODUCTION

1.1 BACKGROUND

The Swedish royal war-ship, the Vasa, is one of history's great marvels [Borgenstam & Sandstroem, 1995]. Its capsizing in 1628 is however one of the great examples of poor design The Vasa capsized on its maiden voyage after travelling only 1300 m. Several reasons have been put forward to explain why the ship sank [HMS website]. One underlying aspect of the Vasa catastrophe, more than 3 centuries ago, still affects us today: Basing critical decisions on unreliable information and data. Such data is usually as a result of applying wrong or poor methodologies. The construction plan set out in the beginning was for a small ship but the builders of the Vasa were unsuccessful in changing the method appropriately when the Swedish King required the Vasa to be bigger and bigger.

Reliability planning is based on the long-term state of a power network; a year, five years or longer. Planning is performed in the context of modifications required to the existing system so as to meet future power supply and demand contingencies. Network operation however looks to manage contingencies that affect the current state of the network. Operation involves power system security monitoring, fast simulation and implementation of emergency control and restoration protocols [Bebic, 2008; Schlabasch & Rofalski, 2008; Henderson et al, 2009]. Medium to short-term time windows lasting hours, days or months are usually applied in network operational studies.

According to Li [2013], there are fundamental differences between reliability assessments for operation and long-term system planning. One expects the reliability requirements for network planning and operation to be different. Further, the influence of network conditions such as loading, generation and external factors should be modelled according to either a network's planning or operational states. It may even be necessary in some cases to modify a component's failure model from a planning state to an operational one [NERC report, 2012].

However, conventionally the same reliability methodology is applied to networks irrespective of whether the reliability results are required for a network planning or operation decision. Since network planning models do not cater for short-term changes in network parameters a situation similar to that faced by the builders of the Vasa is created; network operators not able to adjust the network models so as to cater for variable operating conditions. The operating decisions would thus be based on unrealistic and inaccurate reliability results which could lead to catastrophic results.

Cost-risk analysis is a major component of reliability evaluation for network planning and operation. Planners aim to achieve a balance between network reliability and investment in the network, such that an increase in investments, targeting improved service reliability, has to be justified. Planners thus weigh the cost of investing to improve reliability with the losses that could occur (equipment damage, customer interruption costs and lost power sales) as a result of network unreliability. Network operators on the other hand are not only concerned with network risks that lead to network failure but also the cost attached to respective network failures. To ensure effective decision making at both planning and operation levels, the reliability models applied should not only represent network component parameters realistically but also ensure that the outputs are in a form that can be interpreted usefully by both planners and operators.

This thesis explores the use of different reliability criteria for planning and operation purposes. A new reliability evaluation method will be applied. It will also be shown how the same approach can be consistently applied to either planning or operational reliability analyses and how the results yielded are more beneficial than those derived from conventional reliability approaches.

1.2 NETWORK PLANNING AND OPERATION CHALLENGES

It is widely accepted that the provision of continuous electricity-on-demand is neither technically nor economically feasible.
Instead, the basic function of a power system is to supply power that satisfies the system load and energy requirements economically at acceptable levels of continuity and quality. However there exists a range of factors that directly and indirectly influence a network's ability to perform its core function.

Member countries of the United Nations Framework Convention on Climate Change (UNFCCC) are called upon to ensure that their Green House Gas emissions do not exceed specified levels [UNFCCC website]. In the United Kingdom, so as to conform to a European Union directive to close the most polluting oil and coal fired power stations, 12 GW of generating capacity is expected to be lost. This, combined with the decommissioning of ageing nuclear reactors, means that prolonged power cuts in the United Kingdom are imminent [Fells Associates, 2008; Kinver, 2008]. The South African electricity consumption growth for the next 20 years is forecast at an average rate of 3%. To ensure adequate reserve margins, 20 GW of additional generation capacity is required by 2020 and 40 GW by 2030 [IRP, 2010]. Such expansions, requiring significant capital investment while maintaining adequate power delivery, should be carefully included in the long term planning of a network. Renewable energy sources are one of the 'green' solutions to meeting the ever increasing demand for electricity. The emergence of such power sources and their increasing penetration levels impact on network planning and operation. With such variable supply included, planners have to be careful before approximating base generation to constant levels while operators have to probabilistically assess the available supply before load scheduling.

New concepts and practices have also led to operating conditions not previously observed, that significantly impact on network reliability and its evaluation [Borges et al, 2001]. Deregulation has increased competition so that bulk power sales have grown.

As a result the number and level of power transfers between systems have increased pushing network components closer to their maximum ratings. In addition, interconnection of national grids and the strong reliance of critical infrastructures on each other significantly influence planning and operation. The increased complexity of networks may turn a local disturbance in one system or sub-grid into a blackout via cascading events with catastrophic effects [Mili & Qiu, 2004]. According to Lee [2009], measures used to quantify the failure of current networks to supply power must be able to compute the probability and impact of different failure stages.

A key limitation to the availability and quality of electricity supply is the unpredictability of network operating conditions. Energy markets, transmission open access and restructuring of the electric utility sector have introduced unprecedented uncertainty in transmission planning and operation practices [Marakov & Hardiman, 2003]. One of the major sources of uncertainty in operating conditions is the sporadic behaviour of a network's environment. In particular, the risk posed by external network threats such as adverse weather. This has not only increased the significance of reliability analysis to the planning, design and operation of power systems, but also facilitated changes in the methodologies applied. New methods being developed for reliability analysis need to incorporate probabilistic multi-scenario assessment [Marakov & Hardiman, 2003].

The above issues indicate that networks face a problem with several dimensions. The network risks faced by planners and operators are similar. The models, decisions and approaches applied to network planning could manifest themselves as constraints to operation. A probabilistic approach ensures flexibility in reliability assessment (hazard and risk). Such an approach might be useful and replace conventional contingency approaches and even develop a consistent basis extending from planning to operation.

1.3 REVIEW OF WORLD WIDE ENVIRONMENT INDUCED NETWORK OUTAGES

Literature defining and analyzing network risks is available from many authors. A key aspect in the definition of network risks is the impact of their occurrence. According to Koonce et al [2008], the event that occurs, the likelihood of it occurring and the assessment of its consequences are what constitute a risk.

Falcao and Bollen [2009] term network risks as 'exceptional' or 'force majeure' if they resulted from events that were not only sufficiently rare, but also with an effective cause beyond control of the network operator. Lee [2009] also categorized failure events in terms of their likelihood of occurrence and the acceptability levels of their consequences. It is also stated that the different categories of events that constitute network risks vary greatly in terms of their nature and degree [Lee, 2009]. Network risks lead to power interruptions which have negative social, financial and environmental impacts. The many causes of power interruptions can be categorized into component degradation, environmental factors, utility maintenance, human error and unknown factors. However, component degradation and environmental factors contribute most to power interruptions.

1.3.1 Component degradation

Component failures are usually deemed a result of different types of deterioration. For mechanical components the different failure mechanisms can be grouped into four main categories: corrosion, erosion, overload and fatigue. Component failures can be further categorized as either chance or non-chance failures [Li, 2005]. Chance failures relate to sudden component failures while non-chance failures consider planned outages and component ageing. Component life-cycles take on different shapes. The bathtub curve shown in Figure 1.1 is commonly used to represent the life-cycle of component/ equipment and system failures. Chance failures occur during the useful life portion while ageing failures occur during the end of life portion of the curve.

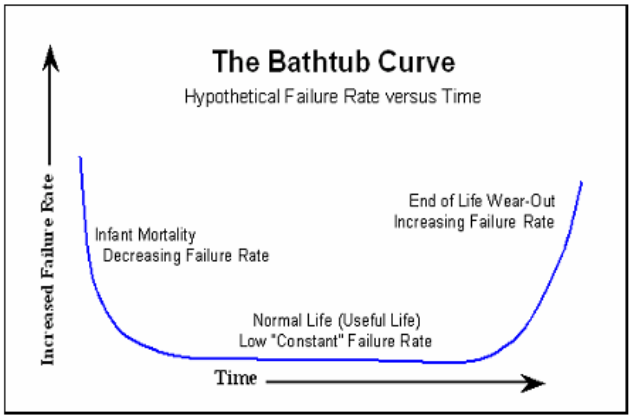

Figure 1.1: Variation of component failure rate with time [Wilkins, 2002]

While the bathtub curve could be applied to electronic components, real transformer failure data does not follow the same trend [Jagers et al, 2007]. Chance failures are random fatal events independent of the age of a component. Such failures are usually modelled such that the component failure rate is deemed constant [Li, 2005]. The failure models presented in this research can be developed for any region of a component's lifecycle.

1.3.2 Environmental factors

Power networks are exposed to a range of external threats that lead to outages. The occurrence and severity of external threats are quite variable. It is for this reason that the use of constant values to represent component failure parameters in the useful life-section of the bath-tub curve is questionable. Compared to other environmental factors such as animals, tree contact and motor vehicle accidents, adverse weather conditions contribute most to failures and faults in bulk networks [Chowdhury & Koval, 2008]. Adverse weather elements such as lightning, strong winds and conductor icing are the commonly known elements that cause power outages because their occurrence leads to immediate component failure, particularly to transmission lines. While it is clear how adverse weather affects transmission lines, power generation has also been significantly influenced by change in weather patterns. The gradual drop in hydropower generation in East Africa was linked back to dropping levels of liquid precipitation [Mason et al, 2006].

Wind and solar based power generation is also sensitive to wind speeds and irradiation levels respectively. Research on other adverse space conditions patterns such as geomagnetically induced currents (GICs) that do not lead to immediate component failure is ongoing.

Some of the major world-wide power outages in recent years are summarized in Table 1.1. Some outages were catastrophic while others led to rolling black outs. It should be stated that Table 1.1 is not exhaustive.

Table 1.1: Summary of some significant power outages around the world

Location	Date	Scale (population or GW or duration)
Brazil [Filho et al, 2000]	11/03/1999	>90M customers 25 GW, 5 hours
East Africa [USGAO, 2005; Mason et al, 2006]	2000-2005	1.5M customers, 0.12-0.3 GW
North America [POSTS, 2004]	14/08/2003	50M customers, 62 GW, > 1 hour
Italy [UCTE report, 2004]	28/09/2003	57M customers, 27.7 GW, 27 minutes
Indonesia [Jakarta Post]	18/08/2005	>100M customers, >7hours
Western Cape-South Africa [Eskom report, 2006]	19/02/2006	9 GW, > 1 week
Kosovo [KOST, 2007]	24/07/2007	Albania, Macedonia, Serbia and Montenegro, >1 hour 30 minutes
France, Spain [BBC news; RTE, 2010]	23/01/2009	>1.7M customers, >12 minutes
Brazil, Paraguay [Fox news, 2009]	10/11/2009	60M customers, >20GW, 4 hours
Texas-US [Reuters-US, 2011; Reuters-Africa, 2011]	03/02/2011	>5M customers, 3-7 GW, >5 hours

Brazil, 11th March 1999

A lightning bolt struck the Bauru 440 kV bus bar causing a phase-to-ground fault. All five 440 kV lines connected to the sub-station opened and the power system began to collapse starting with the disconnection of T.Irmãos-I.Soteira 440 kV. A sequence of tripping of a number of power plants in the São Paulo area and loss of both the HVDC and 750 kV AC links from Itiapu finally led to the separation of the whole system. A loss of 24.7 GW load for up to 5 hours was caused by this disturbance [Filho et al, 2000; Chen, 2004]

East Africa, 2000-2005

Droughts in East Africa in 1999-2004 had a serious impact on the hydroelectric facilities in the East African region. Stager et al [2007] and Mason [2008] correlated drops in river flow rates to sun spots. In Uganda the hydro power generation of the Nalubaale power station dropped by more than 50% (300MW–120MW) between 2000 and 2005 leading to rolling blackouts. Neighbouring countries, Kenya particularly that imports electricity from Uganda also suffered severe power shortages [USGAO, 2005; Mason et al, 2006].

Western Cape Province, South Africa, 18-19 February 2006

High pollution levels and misty conditions caused several lines into the Western Cape (South Africa) to trip, resulting in a full blackout on the 18th and 19th February 2006 [Eskom, 2006].

Kosovo, 24th July 2007

On 24 July 2007 at 15:59 hrs a power blackout of Kosovo power system occurred. The black out was attributed to the 2007 European heat wave. The blackout affected Albania and Macedonia, with a partial blackout in Monte Negro and Serbia [KOST, 2007].

France and Spain, 23rd January 2009

Hurricane-force winds in south-western France and northern Spain left more than a million homes without electricity. Outage lasted 12 minutes and 19 seconds [BBC news-13/10/09].

Brazil and Paraguay, 10th November 2009

Heavy rain, lightning and strong winds caused three transformers on a vital high-voltage transmission line to short circuit. Two other lines went down as part of the automatic safety mechanism. The massive Itaipu dam on the border with Paraguay, the world's second-largest hydroelectric power producer, was completely shut down during the blackout. The blackout cut electricity to 18 of Brazil's 26 states and left them without power for up to four hours. All of Paraguay briefly lost power [Fox News-11/11/2009].

Texas-US, 02nd February 2011

More than 50 generating units, capable of producing 7 GW of power, shut down due to extreme cold, forcing the Electric Reliability Council of Texas (ERCOT), the grid operator, to impose rolling blackouts [Reuters US-03/02/11; Reuters Africa-10/02/11].

Herman and Gaunt [2008; 2010] distinguish between power failures based on the frequency and likelihood of their occurrence. Three types of network interruptions were identified; momentary, sporadic and chronic interruptions.

- Momentary Interruptions are characterized by flicker, dips and sags caused by switching actions such as auto-reclosers. Such operations mainly affect transmission and distribution networks. LaCommare and Eto [2004] state that momentary interruptions in some cases constitute over 60 % of a network's total outages and consequently significantly affect power delivery systems. They are due to temporary faults, lasting for short durations dependent on the time-delay settings of the auto-recloser (less than 30 seconds), and are thus usually ignored in broader reliability assessments.
- Sporadic interruptions are common to networks with robust power delivery systems such as those in developed countries. In most cases such interruptions are caused by adverse weather conditions and mainly affect transmission and distribution systems. Sporadic interruptions usually occur when reclosing systems lock-out due to sustained faults [Yun et al, 2003]. According to several utilities, sporadic interruptions last more than 1 minute long [Bevers & Saint, 2006].

- Chronic interruptions occur regularly and affect the generation, transmission and transmission facilities of a network. Such interruptions are generally due to load shedding necessitated by a shortfall in generation, age induced equipment failure, a lack of maintenance and compromise of the capacity carrying ability of delivery systems. This type of interruption is typical of developing nations where the load growth outstrips the supply and network reinforcement requires substantial investment. In developed countries, loss of critical generation units could lead to chronic interruptions.

1.4 HYPOTHESIS AND RESEARCH QUESTIONS

The effects of external threats can be categorized based on the short- and long-term states of a network. As such, reliability methodologies should model, analyze and quantify network risks in the respective categories. The use of different reliability parameters for network planning and operating reliability studies is however uncommon.

A reliability approach that has sufficient flexibility is required to take into account the influence of variable network risks on either network planning or operation. It appears that a probabilistic technique could be more useful than the present approaches of contingency analysis.
Thus the hypothesis that this research is based on is that:
Incorporation of continuous probability distributions in reliability analyses to account for network interruptions caused by adverse external conditions contributes to effective network planning and operation decisions.

The research questions required to test the validity of the hypothesis include:
Qn.1: How is network reliability evaluated and how are the results represented?
The concept of network reliability is not new. The risks to which networks are exposed have however evolved. It is thus important to determine how the evaluation of bulk network reliability has changed and the techniques developed thus far. The different indices computed as reliability outputs and how they are presented in literature will also be investigated.

Qn.2: How applicable are continuous probability distributions in network reliability analyses?

External threats such as adverse weather elements are stochastic such that the conventional use of average values to describe and model them may not be sufficient [Billinton & Allan, 1992]. The use of an average value assumes that the parameter being described will not change throughout the analysis period. Network risks such as those posed by adverse weather elements change per climatic season and occur for short periods of time.

It has been shown that the impact of variation in reliability parameters (due to intermittent operating conditions) on reliability indices can be clearly presented using probability distributions. This question aims at identifying the distributions commonly applied in reliability analyses. A reliability analysis that considers network risks whose intensity is dependent on the season and time-of-day, requires a probability distribution that can exhibit any level of skewness (right or left) and also represent data that falls within a finite range. Literature will be analyzed to determine which probability distributions are suitable for this purpose.

Qn.3: What block of a power network is required for this analysis?

It is important to identify in literature the section of the power network (generation, transmission or distribution) that is significantly affected by stochastic network threats.

Qn.4: What is the effect of external threats on bulk networks and what contingency approaches have been developed for modelling vulnerability of network components to external threats?

The causes of power interruptions include both internal degradation and external threats like inclement and even extreme weather, and these are necessary inputs to any model of reliability. External threats are however characterized by intermittency and therefore create uncertainty in the performance of bulk networks. It is thus important to analyze the effect of variable external threats on network components. Literature will be reviewed to analyze the approaches developed thus far and applicable modelling component reliability parameters (failure rate and restoration time) when exposed to external network threats.

This research posits that variability in network risks impact network planning and operation differently. The modelling approaches applied in the thesis should thus be able to take into account the different requirements of planning and operation reliability analyses.

Qn.5: How significantly do seasonal and time-of-day variations impact on component reliability parameters?

The stochasticity in network component parameters is both inherent and induced. The most significant source of variability in reliability parameters is the external environment of a network which changes with season and time-of-day. A review of how seasonal and time-of-day variations influence network parameters is required. Reliability analysis for planning purposes is on a long term basis and annual time lines are usually considered. For network operation, a more dynamic approach is required for the analysis. The potential of an approach that analyzes reliability parameters and the network risks that affect them according to the season and time of occurrence will be investigated. A season could represent any given period such as an hour, a week or months for operation and a year or longer for planning. A season could also be based on the climatic seasons in a year.

Qn.6: How can continuous probability distributions be incorporated in either planning or operational reliability analyses?

This question will help determine the reliability technique that is most suitable for the type of analysis proposed in the thesis. The technique should be able to incorporate the probability distribution(s) selected for use in the thesis. A number of software packages have been developed for reliability studies. Most of them however use single deterministic values as reliability inputs and outputs. The technique selected should be able to use reliability inputs based on probability distributions for both short- and long-term reliability analyses.

Qn.7: Does the use of probability distributions in either network planning or operation studies yield more useful results for each scenario?

Realistic and accurate reliability analyses are critical to network planning and operation decision making. The outputs of the reliability model applied in this research must be in a form that can be interpreted usefully by both planners and operators. More information could be derived from a reliability analysis when probability distributions are used to describe its outcomes compared with using the average values.

The level of skewness of the distribution of an index is quite important when interpreting the index. Instead of computing single deterministic values, reliability indices should also be represented as PDFs to allow for a range of values per index. This way the impact of risk-based decision making on planning and operation practices can be investigated.

Qn.8: Can PDFs be applied in linking planning and operational failure models?

Network planning and operation reliability studies require different inputs. Network planning studies are based on long-term periods while operation considers short-term periods. The threats investigated in each analysis are however the same. Variability and severity of network threats are also distinct in the network operation scenario. One could thus regard operational failure models as planning failure models modified so as to account for an increase or decrease in the probability of failure of the network components.

1.5 OUTLINE OF THE THESIS

Chapters two and three present the literature reviewed that relates to some of the research questions posed in Section 1.4. Chapter two discusses the concept of reliability. It highlights the need for reliability evaluation, the techniques applied and the factors that hinder effective reliability evaluation. Chapter two also discusses the probability distributions proposed in literature for use in reliability studies. Chapter three discusses the effect of a network's external environment on its generation and transmission facilities.

The chapter then provides an in-depth discussion on the component vulnerability modelling approaches proposed in literature. The models highlighted relate component failure to intermittent failure causes. The shortcomings and limitations of the modelling approaches are presented. The chapter also assesses the correlation between network failures and seasonal and time-of-day variations.

Chapter four analyzes the areas identified in literature that require improvement so as to validate the thesis hypothesis. The chapter considers the probability distribution, reliability simulation method and network failure modelling approach required. The suitability of the Beta PDF which thus far has had limited application in reliability studies is analyzed. A comparative study is performed with the commonly applied PDFs. The time-dependent probabilistic approach (TDPA) for reliability analysis that is applied in this research is also developed in Chapter four. The component vulnerability model applied that incorporates probability distributions is described. The chapter further discusses the methodology applied when deriving probabilistic models for both network planning and operation cases.
The performance of the TDPA is tested on a published test network and compared with one of the conventional reliability evaluation methods.

Chapter five applies the TDPA to a real power network. The South African power grid and local weather threats typical of the region are considered. The chapter presents the input failure models applied in the planning and operation case studies performed on the network. The case studies performed on the real network aim at investigating the impact the input failure models have on the perception of a network's reliability. The planning case studies aim at showing the importance of using the right input failure models in a reliability analysis. The operational study highlights the need to use different failure modelling approaches in planning and operational reliability analyses.

Chapter six presents and discusses the results of the planning and operational TDPA simulations. The chapter discusses the implications of representing reliability inputs as PDFs. The importance of the selecting the correct failure model and applying it appropriately is also discussed. The improvement PDFs make to index interpretation is discussed. The chapter emphasizes the impact of risk-based decision making i.e. the significance of attaching a risk or confidence level to index values is presented.

Chapter seven uses the TDPA to analyze the effect of network threats whose occurrence has both immediate and deferred effects on the network. The chapter specifically analyses global space weather threats on the reliability of a network already predisposed to local weather threats. While the GIC threat can be considered a planning issue, it significantly affects the operation of a network. The chapter thus shows how planning PDF models can be modified to account for elevation in component risk of failure due to such threats. Thus, translating long-term failure models for use in operational analyses. The implications of the results computed with the GIC threat considered are also discussed in the chapter.

Chapter eight presents the conclusions drawn from the research. A review of the answers to the research questions is presented and the validity of the hypothesis assessed. Some implications of the thesis research are also presented.

1.6 PUBLICATIONS SUBMITTED DURING COMPLETION OF THESIS

(I) Journal Papers

- R. Okou, E. Niwagaba, O. Kyahingwa, M. Edimu, A. B. Sebitosi, *Considerations for renewable energy mini-grid systems for isolated areas in Uganda,* Submitted to Journal of Engineering, Built Environment and Technology for review, August 2013
- M. Edimu, K. Awodele, C. T. Gaunt, R. Herman, *Appropriate protocol for applying Beta probability distribution functions to reliability data-sets*, submitted to IEEE Transactions on Reliability, in progress

- M. Edimu, K. Alvehag, C.T. Gaunt, R. Herman, *Performance of a time-dependent probabilistic approach for bulk network reliability assessment*, Accepted for publication in Electric Power Systems Research Journal, Available online:http://www.sciencedirect.com/science/article/pii/S0378779613001661
- M. Edimu, C. T. Gaunt, R. Herman, *Using probability distribution functions in reliability analyses,* Electric Power Systems Research Journal, Vol. 81, 915-921, June 2011

(II) Conference Papers

- R. Okou, S. Kirya, W. Semazzi, M. Edimu, A. B. Sebitosi, *Potential impact of hybrid battery/supercapacitor controllers in solar home systems,* SIDA Regional Collaboration and Annual General Meeting, Bagamoyo, Tanzania, July/August 2013
- M. Edimu, R. Herman, C.T. Gaunt, *Effect of transmission line failure models on the perception of its reliability,* 21st Southern African Universities Power Engineering Conference, South Africa, January 2013
- M. Edimu, R. Herman, C.T. Gaunt, *Probabilistic modelling of the effects of external network threats on transmission reliability assessment,* Probabilistic Methods Applied to Power Systems, Istanbul, Turkey, 2012
- Edimu M, Gaunt C T, Herman R, A*pplying probability density functions when modelling failures due to adverse weather,* presented at: Power Systems Computation Conference, Stockholm, Sweden, August 2011
- Herman R, Gaunt C T, Edimu M, *Procedure for investigating the planned and operational reliability of transmission networks with GICs*, IASTED, Gaborone, 2011
- Herman R, Gaunt C T, Edimu M, Dzobo O, *The development of a probabilistic reliability assessment process for decision-making in South Africa using CIC surveys,* 19th Southern African Universities Power Engineering Conference, Johannesburg, 28th–29th January 2010

2. ESTIMATING BULK NETWORK RELIABILITY

2.1 INTRODUCTION

Reliability of power networks is not a new concept. Engineers and network operators in the past used only experience to help determine and predict power system performance. The power industry has however evolved since the early 1890s and with this, the network risks to which power networks are exposed. Developments in the power industry such as energy markets, transmission open access, interconnection of national grids and, networking of electricity systems to other critical infrastructures have directly or indirectly changed the way utilities are planned and operated [Borges et al, 2001]. Utilities are less sufficient and more dependent on their neighbours for imported power. Financial and environmental constraints in the last decade or so have worsened the situation. The mode of operation of power networks around the world is now different from what was initially planned; with increased power interchanges occurring. The management of reliability is even more critical today to network planners and operators. Improvements, not only in the evaluation techniques used but also in the way analysis results are presented and interpreted, are required.

2.2 RELIABILITY OF A POWER NETWORK

The International Organization of Standardization (ISO) defines reliability of a component or system as its ability to perform the functions required of it under given operational and environmental conditions, for a stated period of time [ISO, 1994]. Network reliability is also described in terms of two main aspects, network adequacy and network security [Billinton & Allan, 1992].

Network adequacy is the ability of a network to not only generate, but also supply the electrical demand and energy required by consumers.

'Adequacy' is concerned with continuity of supply i.e. the facilities necessary to generate sufficient energy and the associated transmitting facilities required to supply all load under performance requirements [Leite da Silva et al, 1993; CEER report, 2005]. Network security on the other hand relates to ability of the network to respond to dynamic or transient disturbances occurring in the network [Billinton & Li, 1994]. Security thus considers the quality of supply and the ability of the system to respond to the various perturbations to which it is subjected [Fong & Grigg, 1994]. Billinton and Li [1994] state that these perturbations include conditions associated with local and widespread disturbances and the abrupt loss of major generation and/or transmission facilities which can lead to transient, dynamic or voltage instability of the network.

Reliability analyses on a power network are carried out separately in the functional zones of a power system; generation, transmission and distribution. Generation system reliability evaluation examines the total generation capacity to determine its adequacy to meet the total system load requirement [Billinton & Allan, 1996]. Distribution system reliability evaluation focuses on the impact of distribution element failures on individual consumer load points. Distribution systems are usually localized to one geographical location such that all the components are always exposed to the same weather elements.

The work presented in this thesis was carried out on a composite or bulk power system. This is a system consisting of only the generation and transmission facilities of a power network [Billinton & Allan, 1988; Zhang & Billinton, 1998]. While reliability analysis of composite systems is a complex task, the impact of interruptions at this level makes the analysis a vital component of power system planning and operation. Not only are the number of electricity customers affected always high, but significant resources are usually required to restore power supply to the customers [Solver & Amelin, 2006].

2.3 MEASURING NETWORK RELIABILITY

This section aims at identifying and describing the main techniques developed in literature for reliability evaluation. The representation of reliability outputs is also discussed.

Measurement of reliability performance has become and continues to be more established in the power industry. In fact, several guidelines and codes have been revised to ensure more realistic reliability specifications of engineering design. A Federal Energy Regulatory Commission (FERC) ruling in USA called for the development of new reliability standards to address power network risks previously disregarded [FERC, 2013]. Haldar and Mahadevan [2000] mention the American Institute of Steel Construction Load and Resistance Factor design specifications and the European and Canadian structural design specifications as having been reviewed to include the probabilistic nature of reliability. Reliability performance measurement provides feedback to utility planners on the results of executed plans and to operations personnel on the reliability effects of operating and maintenance practices [Fong & Grigg 1994]. Reliability evaluation however does not benefit planners and operators alone. According to Fong and Grigg [1994], information on actual reliability "*can be helpful to customers planning to locate in the utility's service area. Through measurement, it is also possible to determine the difference in reliability performance between operating districts within a utility*."

2.3.1 Reliability Indices

While it helps to know what events lead to unreliability in a system, it is of added importance to know the probability of occurrence and severity of these events, hence the need for reliability or unreliability indices [Fong & Grigg, 1994]. Reliability indices are determined for a given system or component and it is the interpretation of these indices that sheds light on how reliable the system or component is.

Network reliability indices can be regarded as either past performance indices or predictive indices.

This categorization depends on whether the indices computed are to provide information relating to future system performance or show actual performance of the system [Endrenyi, 1978]. It is common for network planners to base their decisions on past performance indices. Predictive indices are however more applicable to operational purposes.
Indices can be calculated so as to provide information on the reliability of either the overall system reliability or at individual load buses.

Load point and overall system indices complement each other. Load point indices are very useful in system design and in comparing alternative network configurations, while system indices indicate the ability of a composite system to meet its total load demands [Billinton & Kumar, 1990]. Several reliability indices can be identified. According to Billinton & Kumar [1990] "*it should be noted however, that the selection and definition of these indices are very dependent upon the intent behind the studies and the methodologies used*." The most appropriate indices are dependent on a given system and its requirements [Fong & Grigg, 1994]. The Institute of Electrical and Electronic Engineers (IEEE) proposed indices for use in reliability studies. These are described in Appendix A. Most indices identified for use in power system evaluation can generally fit into four categories: Probabilities, Frequencies, Durations and Expectations [Billinton & Kumar, 1990]. After determining the probability, frequency and duration of failure of a given network outage, one can go on to evaluate most of the other indices required for an analysis [Endrenyi, 1978].

Billinton and Wangdee [2006] state that system reliability performance based on average interruption information may not be sufficient. Such average values are valuable information but provide only a single customer risk dimension without underlying probability distributions. Random events affecting power networks like the occurrence of a fault or the time to restore the service after a fault are represented by using random variables. As such, reliability indices built on the basis of these random variables would also become random variables [Carpaneto & Chicco, 2004]. The performance indices of a power system should be considered as stochastic values with inherent variability.

Wangdee & Billinton [2005] state that indices vary from year to year and should therefore be regarded as random variables that are dependent on the system topology, operating philosophy and external conditions. More information could be derived from the outputs of a reliability analysis if probability distributions were used to describe them, compared to using average values [Billinton & Huang, 2005]. The level of skewness of the distribution of an index is important when interpreting the index [Billinton & Allan, 1996]. For example, the likelihood of occurrence of extreme events can be investigated using the tails of a distribution.

Histograms have previously been used to determine the probability distribution that fits a given reliability index. Probability density functions (PDFs) are characterized by shape and range parameters [Walpole, 2007; Papoulis, 1991]. One could thus infer on the shape of an index probability distribution without having to plot a histogram of the index data set.

2.3.2 Network reliability measurement techniques

The techniques identified for use in reliability evaluation can be designated as either deterministic or probabilistic. Deterministic techniques have traditionally been used by system planners who attempt to predict a network's operational status using past experience [Billinton & Allan, 1992]. Some of the drawbacks identified with deterministic techniques include [Song et al, 2006]:

- Variability in input data and uncertainty in operating conditions is ignored
- Contingencies considered neglect unlikely events such as cascading failures
- No indication is provided on the severity of risks falling beyond the deterministic security boundary
- Plans that satisfy the traditional criteria are assumed free of failure risk which is misleading

Probabilistic techniques complement deterministic techniques. The two techniques are usually combined. Probabilistic techniques overcome the fact that deterministic techniques cannot account for the stochastic behaviour of power networks [Billinton & Allan, 1992].

They consider the likelihood of possible outages occurring by capturing the increased risk due to multiple scenarios and uncertainty in future operating conditions [Song et al, 2006].

Most of the probabilistic techniques identified in literature can be categorized as either analytical methods or simulation ones [Singh & Mitra, 1997].

2.3.2.1 Analytical Methods

The use of analytical methods involves the development of mathematical models to represent the network and derive reliability indices through numerical computation [Fong & Grigg, 1994; Billinton & Huang, 2005]. Several books and research papers have been published on the concepts, models, algorithms software and application of analytical methods [Billinton & Allan, 1992; Beshir et al, 1996; Li, 2005]. A key component of analytical methods is network reduction. Billinton and Allan [1992] and Beshir et al [1996] describe in detail how some reduction methods can be applied to a network.

Many analytical methods have been developed such as Markov methods, application of conditional probability, fault and event tree method and the cut set approach [Billinton & Allan, 1992]. The most significant analytical method, with regard to bulk networks, is the State Enumeration Method (SEM). This method analytically evaluates all possible system states up to a specified maximum contingency level or probability threshold According to Li [2005], evaluation of system reliability using SEM is based on the expansion of (2.1) to (2.3).

$$P(S) = \prod_{i=1}^{f} Q_i \prod_{i=1}^{N-f} P_i \quad (2.1)$$

$$F(S) = P(S) \sum_{i=1}^{N} \lambda_i \quad (2.2)$$

$$D(S) = \frac{1}{\sum_{i=1}^{N} \lambda_i} \quad (2.3)$$

P(*S*), F(*S*) and D(*S*): probability, frequency and mean duration of a system state (*S*) occurring

P_i and Q_i: success and failure probabilities of the i^{th} component

N: total number of components in the system

F and N-*f*: number of failed and non-failed components in system state *S* respectively

λ_i: departure rate (either failure or repair rate) of the i^{th} component from state *S*

According to Solver and Amelin [2006], "*analyzing risks using numerical reliability methods is rather complicated even for small systems, and the altitude level of the complexity grows rather quickly to cumbersome proportions as the system grows larger*." This can be explained by the fact that power networks are complex systems, highly integrated and almost always with a great number of components. The failure of these networks is not only dependent on other network components but also on the environment in which the network operates [Haroonabadi & Haghifam, 2009]. Given (2.1) to (2.4) and that the number of system states increases exponentially with the number of system components, it is clear that application of SEM to large real networks makes the analysis a cumbersome task [Billinton & Allan, 1996; Yongji et al, 1999].

So as to reduce the number of failure states enumerated in an analysis a maximum contingency level (fault level) is selected or a minimum system state probability threshold is set. Some system states are thus deemed negligible [Zhang & Billinton, 1998]. A contingency level is determined by the number of components in a given system outage state. The first contingency level involves only single component outages. The second and third contingency levels consider up to two and three simultaneous component outages respectively [Billinton & Allan, 1992]. It is usually assumed that higher contingency levels are unlikely to occur i.e. they have very low probabilities of occurrences such that system states with probabilities lower than the specified threshold are neglected. The likelihood of occurrence of extreme events such as the 25th/01/ 2009 widespread power outage in Northern France and Southern Spain [BBC news, 13th /10/2009] or the Italian black-out on 28th /09/ 2003 [UCTE report, 2004] may be low. When such events do occur, the impact is very severe. With analytical methods, such events or system states are neglected. As a network gets larger more assumptions are required such that the final network model developed could be unrealistic [Endrenyi, 1978; Billinton & Allan, 1992].

Analytical methods are thus more suitable when an overview of a system's reliability is required. This makes such methods more applicable to planning studies which are based on the average performance of a network.

Analytical techniques could provide snapshots of the operational state of a network. Network operation is however so variable that corresponding reliability studies require more dynamic techniques.

2.3.2.2 Monte Carlo Simulation methods

Monte Carlo simulation consists of randomly sampling system states, testing them for acceptability, and aggregating the contribution of loss of load states to the reliability indices till the coefficients of variation of these indices drop below pre-specified tolerances [Singh & Mitra, 1996].

Simulation methods, through random sampling, simulate the actual performance of a network [Haroonabadi & Haghifam, 2009]. One significant difference between analytical methods, SEM in particular, and Monte Carlo Simulation (MCS) methods, is the way system states are chosen and analyzed. With SEM, the system states are chosen from a predefined list [Rei et al, 2006]. One key SEM assumption, for application of (2.1), is that system states are mutually exclusive such that the failure of a given component is never dependent on, or as a result of, failure of another component [Li, 2005]. This is not a realistic condition since cascading network failures are usually due to operational dependencies [Chen, 2004; Lee, 2008].

The most common simulation method used is Monte Carlo Simulation (MCS). With MCS, the stochastic nature of power networks is taken into account and system states are generated randomly. It is usually necessary to evaluate not only simultaneous outages of a number of system components, but also dependent failure system states due to the severity of their impact [Rei & Schilling, 2008].

According to the Blackout White Paper compiled by IEEE PES Power System Dynamic Performance Committee [PSDPC, 2004]:

"*On August 14th 2003, a cascading outage of transmission and generation facilities in the North American Eastern Interconnection resulted in a blackout of most of New York state as well as parts of Pennsylvania, Ohio, Michigan and Ontario Canada.*

On September 23rd 2003, nearly four million customers lost power in eastern Denmark and southern Sweden following a cascading outage that struck Scandinavia. Days later, a cascading outage between Italy and the rest of central Europe left most of Italy in darkness on September 28th."

Apart from consideration of all system states, MCS methods treat the input parameters of a reliability analysis as random variables and let them take on values according to specified probability distribution functions (PDFs) [Alvehag, 2008]. If the system components are statistically independent, system states are determined by sampling from PDFs of each component [Rei et al, 2006]. Also, through repetition, a whole set of values can be computed from a given reliability analysis. Index data sets can thus be derived that are not estimates of the average index value. The underlying probability distributions can be determined from these data sets [Miranda et al, 2009]. The derivation of statistical parameters from reliability data sets and the use of PDFs to model component failure rates and present reliability indices will be discussed later.

Two main MCS methods have been identified in literature:

- Non-Sequential MCS: State Sampling Method (SSM)
- Sequential MCS: State Duration Method (SDM)

Non-Sequential MCS: State Sampling Method (SSM)

This MCS method samples all states of the components without considering the chronology of time-dependent events. The concept is based on the fact that a system state is a combination of component states and each component state can be determined by sampling the probability of the component appearing in that state [Li, 2003; Li, 2005].

Random numbers are generated and compared to the failure probabilities of the components. The range of a given random number determines the state of the component (available/up, de-rated or failure/down).

The steps below describe the procedure for using non-sequential MCS:

1) For each component, generate a random number U_i. It is assumed that the behaviour of each component can be categorized by a uniform distribution (0, 1)
2) Compare the random number generated with the respective component's forced outage rate (FOR). Probability of component outage is determined based on comparison with the FOR i.e. if U_i is less than the corresponding FOR, the component is deemed to be in a failed state, otherwise, it is in service (up-state)
3) Outage of a component can directly lead to load curtailment at a load point. Otherwise, a DC load flow could be applied to evaluate any resulting load curtailments
4) Steps 1 and 3 are repeated for all the components
5) The load curtailment states are accumulated and the adequacy indices computed for different load points and the overall system

The flow chart in Figure 2.1 shows how steps 1–5 are implemented for an SSM analysis. The only network parameter input required by SSM for the sampling process is each component's FOR. It then becomes easy to simulate component and network unavailability due to different factors like ageing and weather. The results of SEM are always estimates of the network reliability or unreliability on an annual basis. This is not always the case with SSM. Simulations can be easily performed over any length of time; short term weekly, monthly, or seasonal) or long term (yearly, every 10 years etc) [Li, 2005].

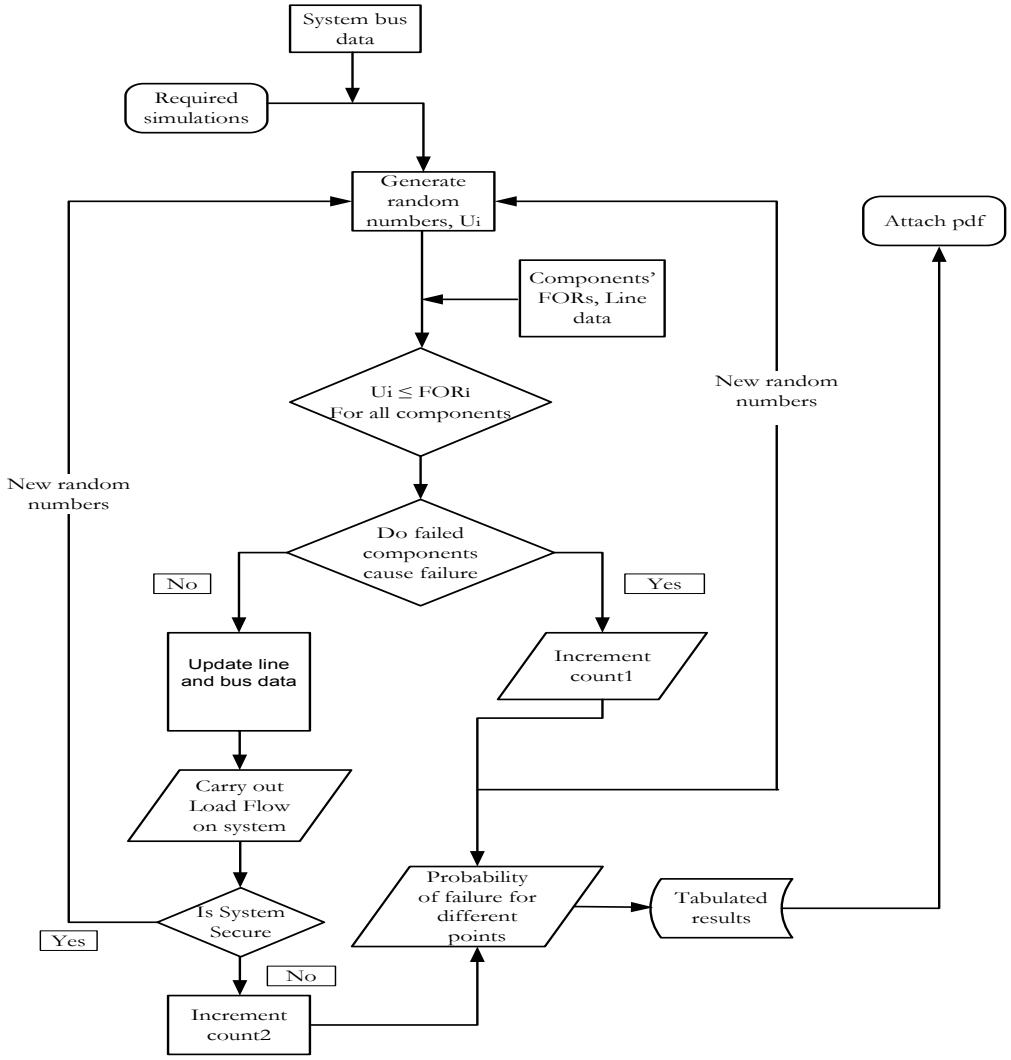

Figure 2.1: Data Flow for applying State Sampling Method [Edimu, 2009]

The SSM does not allow for variable inputs and is thus suitable for analyzing states with static conditions. Also, the inability of SSM to allow for chronology of time-dependent events means that realistic failure frequency and duration cannot be evaluated. From SSM, the frequency of the given state occurring can be determined. The inverse of this provides the maximum expected duration of lying in the state. Thus, SSM does not provide a well rounded impression of the reliability/unreliability of the network.

Sequential MCS: State Duration Method (SDM)

SDM is applied when dealing with chronological events such that the probability of occurrence of different states, frequency and duration can be evaluated [Billinton & Li, 1994]. Random numbers generated are converted into state durations using the component state distribution functions. The system state transition cycle is then obtained by combining the probabilistically generated up-and-down component cycles [Fong & Grigg, 1994; Billinton & Tang, 2004]. The steps below describe the basic procedure when using the conventional sequential MCS:

1) Assume the initial states of the system components in the analysis period. A component can either be in or out of service
2) For a given component, generate two uniformly distributed random numbers, U_i and R_i
3) Use the random numbers to compute the component time-to-failure (TTF) and time-to-repair (TTR). Component TTFs and TTRs can be described by any distribution. The reliability data dictates the distribution used i.e. the distribution that best fits the data is selected. Goel [2000] illustrated how different distributions can be applied in a sequential MCS. For any distribution, an inverse translation function is derived so that time random numbers generated are changed in time-to-failure and time-to-repair quantities. The exponential distribution has a simple inverse translation as shown in (2.4) and (2.5). This could explain why it has had extensive use in reliability studies.

$$T_{up} = \frac{1}{\lambda}\ln(U_i) \tag{2.4}$$

$$T_{dn} = \frac{1}{\mu}\ln(R_i) \tag{2.5}$$

λ: failure rate

μ: repair rate

T_{up}: time to component failure

T_{dn}: time to component repair

4) Repeat steps 2 and 3 to create a chronological state transition cycle for the component in the time span required

5) Repeat steps 2-4 for all components
6) Combine the component cycles to generate the chronological system state transition cycle
7) Analyze system cycle and compute: load point indices, based on failure states that occur, and system indices
8) Simulation runs until coefficient of variation in duration index is less than specified threshold

Figure 2.2 shows a flow diagram for carrying out SDM. SSM and SDM MCS techniques were applied to a bulk test network and the results compared for different load models [Billinton & Sankarakrishnan, 1995].

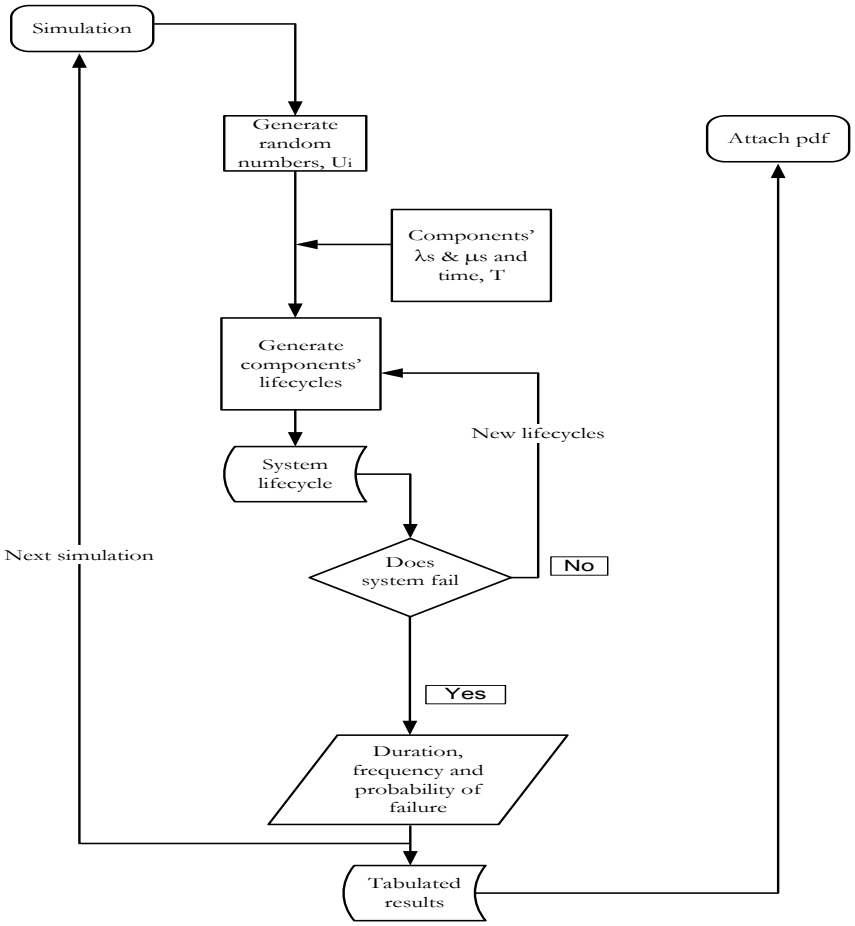

Figure 2.2: Data Flow Diagram for applying State Duration Method [Edimu, 2009]

One key advantage of SDM over SSM is the inclusion of component repair rates so that, unlike SEM and SSM, simulations over a long period of time in which many failures and repairs have occurred can be carried out. Frequency and duration indices can also be computed. Thus, SDM not only has a high reality potential, it is flexible in terms of modelling repair state duration distributions and provides a well rounded impression of the reliability of a given network [Goel, 2000; Li, 2005].

While SDM based algorithms are more powerful when complex systems have to be analyzed, the computation effort required is significantly higher than SSM [van Casteren & Bollen, 2000]. The computation times have however been reduced significantly through the development of fast computer processors and new computation time reduction techniques [He et al, 2010]. Methods such as state space pruning [Singh & Mitra, 1996] and outage screening [Yongji et al, 1999] aimed at screening the states simulated. Extensions to conventional SDM such as the sequential cross-entropy [Gonzalez & Leite da Silva, 2011] and pseudo-chronological [Leite da Silva et al, 2000] MCS have been proposed. These methods aimed at only reducing the computation effort by either identifying the most significant component transition rates [Gonzalez & Leite da Silva, 2011] or determining the most likely state transitions [Leite da Silvaet al, 2000]. The methods assumed that a system is exposed to a non-changing environment so that a component's transition rate between any two states is constant.

Annual time lines have been predominantly applied in SDM analyses. All network risks were assumed to be dominant over the whole analysis period. This research will show that such an assumption is valid only for network planning where each network risk can be regarded on an average scale. Sequential MCS has also been applied to studies with a time span shorter than one year. Network operational analyses however also consider short-term periods such as a couple hours during a given day. Unlike planning analyses, the major challenges in system operation reliability assessment include probabilistic simulations of various operational measures, remedial actions, and system dynamics at different timescales, as well as special requirements in input data and computing speed [Li, 2013].

Further, identifying chronology for operational reliability assessments could be an issue with SDM. In fact, collecting, representing and modelling the data required for a complete time-simulation is the main problem when implementing a sequential MCS.

Simulation methods, particularly SDM are easy to apply and offer great versatility in modelling and analyzing complex systems. Mettas and Sawa [2001] indicate however that there are some limitations to their effectiveness. For example, if the number of simulations performed is not large enough, these methods can be error prone. In addition, performing a large number of simulations can be extremely time-consuming. This thesis will present a new reliability evaluation approach that is based on the SDM. The modification to the SDM will aim at making the approach less dependent on the number of simulations and improving its computational efficiency.

2.4 USING PROBABILITY DENSITY FUNCTIONS (PDFs) IN RELIABILITY ANALYSIS

Non-parametric statistical procedures can be regarded as those procedures that do not require an assumption about the shape or form of the probability distribution from which a sample data set has been derived [Sheskin, 2011]. However, the 'truth' about the population from which the sample dataset has been drawn is what is usually sought. As such, parametric methods that rely on estimates of the parameters of the population are usually employed. Such estimates are particularly significant in reliability studies where the underlying distribution of reliability datasets could impact on the results and decisions made based on the computed results. The use of deterministic values for the input failure parameters in a reliability analysis may yield unrealistic outputs. The expected values of reliability indices are also sometimes computed. These are estimates of the mean values of the indices in question. Only considering the average of a given index provides network planners and operators with very little information on which to base decisions regarding the system performance, costs, planning and operation decisions.

Current work on reliability is taking a probabilistic approach. Haldar and Mahedavan [2000] suggested the use of probability-based methodologies whilst developing a risk-based model that can account for both cognitive and non-cognitive sources of uncertainty. Suntanto et al [2002] apply a probabilistic approach to power generation cost and reliability calculations. The authors derive equivalent generating capacity PDfs using the Z-transform method and operate them on the system demand. Krahl et al [2009] investigate the impact of using the distributions of reliability indices when evaluating the effect of different electricity quality regulation mechanisms on network operators.

External network conditions contribute to variability in component reliability parameters. The use of average values disregards any uncertainty in reliability parameters and so insufficient descriptions of reliability inputs and outputs are derived. Instead of using single deterministic values, a range of values can be developed to describe reliability parameters and conversely, the computed reliability indices. The issue then is which value best represents a given reliability parameter or what level of confidence can be attached to a given index value? So as to quantify the uncertainty in a reliability data set, Haldar and Mahadevan [2000] proposed the use of probability density functions (PDFs).

The probability density function f_y (Y) is a mathematical function that provides a model for the probability that a value of a continuous random variable lies within a particular interval. It is a mathematical model for the population histogram containing relative frequencies which must be greater than or equal to zero, and must sum up to unity [Nelson, 1982]. When represented graphically this probability is the area between the grapgh of the function and the x-axis, bounded by the particular interval. A probability density f_y (Y) is a function of *y* with the properties.

a) $f_y\,(\mathrm{Y}) \geq 0$; for all *y* in the range φ

b) $\int_{\varphi} f_y\,(\mathrm{Y})dy = 1$; where the integral runs over the range φ

'Density' relates to the height of the graph. At places on the x-axis of the PDF graph where values of the random variable are closely packed, the height is greater than at places where the values are sparse.

2.4.1 Commonly used probability distributions in reliability related studies

The choice to use a specific family of distributions is justified by the goodness of fit of that given distribution to the data. Most times this is not known and as such distributions with versatile characteristics are applied. Several distributions have been proposed for use in reliability analysis. Some common distributions are described in Table 2.1. They include the negative exponential, Gaussian, lognormal, gamma and Weibull PDFs. This section will describe their characteristics and application thus far in reliability analyses.

Table 2.1: Characteristics of some probability distributions [Papoulis, 1991; Leon-Garcia, 1994; Walpole, 2007]

Distribution	f(x)	Range	Parameters
Negative exponential	$k\exp(-xk)$	$x \geq 0$	k
Gaussian	$\frac{1}{\sigma\sqrt{2\pi}} exp\left[-\frac{1}{2}\left(\frac{x-\mu}{\sigma}\right)^2\right]$	$-\infty < x < \infty$	μ, σ
Lognormal	$\frac{1}{\sigma_x x\sqrt{2\pi}} exp\left[-\frac{1}{2}\left(\frac{\ln(x)-\mu_x}{\sigma_x}\right)^2\right]$	$0 \leq x < \infty$	σ_x, μ_x
Gamma	$\frac{\lambda(\lambda x)^{\alpha-1}exp(-\lambda x)}{\Gamma(\alpha)}$ $\Gamma(z) = \int_0^\infty x^{z-1}e^{-x}\,dx$	$0 < x < \infty$ $z > 0$	λ, α
Two-parameter Weibull	$\frac{\beta}{\eta}\left(\frac{x}{\eta}\right)^{\beta-1} exp-\left(\frac{x}{\eta}\right)^{\beta}$	$x \geq 0$	η, β

The negative exponential has been applied extensively in reliability analyses. This is due to the assumption that a component's failure rate is constant during its useful life period. The negative exponential was described by van Catesteran et al [2000] as being mathematically elegant because its PDF is simple and easily manipulated in analytical studies.

Analytical calculations, with distributions other than the negative exponential, are cumbersome and almost impossible [Li, 2002]. In addition, reliability approaches such as the sequential MCS described in Section 2.3.2.2 are hinged on the use of the negative exponential PDF because of the simplicity of its corresponding inverse time transformation[1] [Billinton & Allan, 1992; 1996]. Bollen et al [2008] defined network operational reliability assessment as one that investigates its reliability in very short periods of time of the ranging between 1 to 5 hours. To demonstrate the concept, the failure rates were modelled using the negative exponential PDF. The justification lies in the assumption that because of the short periods being investigated, a component's failure rate does not change.

The Gaussian distribution is symmetric about the mean. The mean, median, and modal values are identical and can be estimated directly form the data being described [Haldar and Mahadevan, 2000]. As such, it is mainly used in the analysis of manufactured items and their ability to meet specifications. The Distribution is also used to model failures that are a result of component ageing or wear and tear [Li, 2002]. The negative exponential and Gaussian distributions exhibit specific shapes so that they can only be applied to specific data sets. The decision to use these two PDFs for modelling purposes is thus based usually on experience.

The lognormal, gamma and Weibull distributions can take on more than one shape. A random variable has a lognormal distribution when its natural logarithm has a Gaussian distribution. Its distribution can only be skewed to the right which limits the shapes it can match. Similar to the Gaussian, the lognormal distribution is used to model physical fatigue of components. Gray and Schucany [1969] show the suitability of the lognormal distribution for modelling repair rates. The authors however neglect the influence of other time-dependent factors, such as availability of labour, on repair. Secui et al [2009] probabilistically characterized the operational behaviour of 110 kV power equipment. The results showed that the lognormal distribution function provided the highest quality of fitting to the empirical function representing the time to equipment corrective maintenance.

[1] Key MCS requirement for changing randomly generated numbers into time to failure or time to repair values

The gamma and Weibull distribution each have a shape parameter that allows them to be either left or right skewed. They are more versatile and can represent or approximate a wide range of distributions [Sahinoğlu et al, 1983]. The Weibull distribution has been extensively used in modelling and mapping wind speed data. The improved data fitting method proposed by Deaves and Lines [1997] indicated that the two-parameter Weibull distribution can be fitted to the complete range of wind speeds. Lun and Lam [2000] also applied the two-parameter Weibull distribution to numerical estimations of the wind speed frequency distribution function of a given set of wind data. The Weibull distribution was also used to show that the occurrence interval of strong wind speeds is a random variable with a certain probability distribution [Xiao et al, 2006]. For reliability purposes, a Weibull-Markov model for stochastic durations was proposed to allow for analytical computations [van Casteren et al, 2000]. The model produced only bell shaped duration distributions that could be used in non-sequential reliability assessment methods.

Wang et al [1991] verified that the failure mode of power capacitors can be represented by Weibull distributions. Using data from operating records, Xianhe et al [1999] verified that the Weibull distribution could also be used to represent the random failure mode of distribution transformers. Table 2.1 shows the range of the different distributions. The lognormal, gamma and Weibull distribution functions are not suitable for data sets bound by finite positive ranges [Herman & Gaunt, 2008].

Goel [2000] investigated the use of different PDFs in a distribution network reliability analysis to represent component times-to-repair. The data-fitting capability of a range of PDFs was analyzed on different reliability parameter data sets was investigated by Cross et al [2006]. The authors included the Beta PDF which has had limited use in reliability studies thus far.

2.5 THE BETA PDF

Section 2.4 described the PDFs commonly applied in reliability studies. Two key limitations of the PDFs presented with regard to representing historical data were identified: Some of the PDFs like the exponential and Gaussian exhibit specific shapes while others like the gamma and Weibull have infinite ranges. The Beta PDF describes the distribution of a random variable that lies within the interval (0, 1) and is defined by (2.6) and (2.7). Similar to the gamma and Weibull distributions, the Beta PDF can also be used to represent left or right skewed data. This is first accomplished by varying the values of its two shape parameters, α and β [Gupta & Nadarajah, 2004; Cross et al, 2006].

$$f(x) = \frac{x^{\alpha-1}(1-x)^{\beta-1}}{\mathcal{B}(\alpha\beta)} \tag{2.6}$$

for $0 \leq x \leq 1$, $\alpha > 0$ and $\beta > 0$

where

$$\mathcal{B}(\alpha\beta) = \int_0^1 A^{\alpha-1}(1-A)^{\beta-1}du \tag{2.7}$$

Marantes and Pais da Silva [2009] used PDFs to stress how quantifying the probability of networks performing within certain boundaries or not beyond specific thresholds is important to assessment of system reliability performance. Unlike other PDFs, the Beta also has a scaling parameter that allows the Beta PDF to be scaled to a finite range. A Beta random variable Y, defined in the interval [0,1], can thus be rescaled or shifted to obtain a Beta random variable Z in the interval [a, C] of the same shape by using (2.7) and (2.8).

$$Z = a + (C-a)Y \tag{2.7}$$

$$f_y(Z) = \frac{1}{\mathcal{B}(\alpha\beta)}\left(\frac{(Z-a)^{\alpha-1}(C-Z)^{\beta-1}}{(C-a)^{\alpha+\beta-1}}\right) \tag{2.8}$$

where $a \leq Z \leq b$; $\alpha > 0$; $\beta > 0$

a: lower bound; C: upper bound (scaling factor)

The scaling factor of Beta PDFs must be equal to or greater than the maximum value recorded in the data set being described. For example, failure statistics are usually based on historical records. Planning studies that cover more than 10 years have to include unlikely events that may have very low probabilities of occurring but are associated with catastrophic effects. For such extreme events, emphasis is on the tails of the distributions. The tails can be thus extended by adopting a scaling factor based on extreme value theorem [Smith, 2003].

Most reliability analyses in operation and annual planning studies, such as those carried out in this research, are however more concerned with the most likely event from a fixed possible set. These can be predicted based on the historical performance of a network and its components. For such studies future extreme events may not be modelled. The range of the Beta PDF would thus be dependent on the maximum value of a given historical data set.

The shape of a given Beta PDF is thus described by α, β, and a scaling value, C. The shape parameters can be computed using (2.9) and (2.10) from the mean, variance, and scaling factor of measured or computed data.

$$\alpha = \frac{(C\mu - \mu^2 - \sigma^2)}{C\sigma^2} \tag{2.9}$$

$$\beta = \frac{(C-\mu)(C\mu - \mu^2 - \sigma^2)}{C\sigma^2} \tag{2.10}$$

μ: mean of data; σ^2: variance; C: scaling factor

The Beta PDF is very versatile in the shapes it can exhibit. Figure 2.3 illustrates some shapes of the Beta PDF. Both symmetrical and asymmetrical shapes are displayed. All the Beta PDFs presented in Figure 2.3 have the same scaling factor (C=100). The values of α and β are however varied to yield a different shape. For example, to achieve a Bell shaped PDF, α and β should both be equal to or less than 0.5.

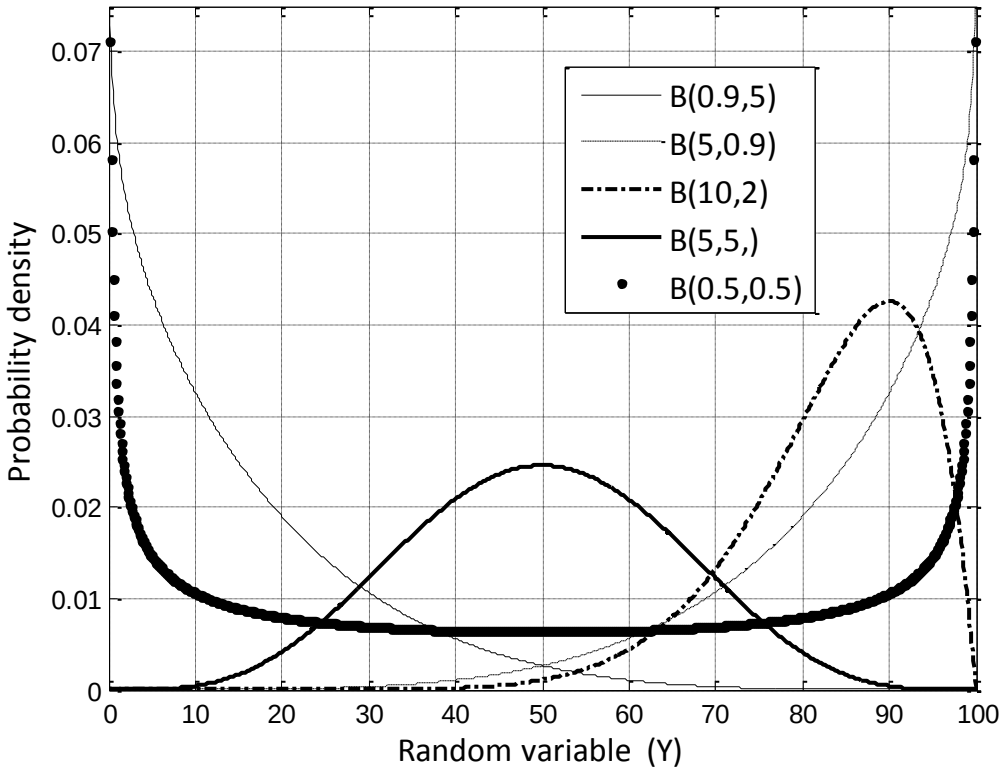

Figure 2.3: Different shapes exhibited by the Beta PDF by varying α and β for C=100

The mean, variance and moment of a Beta PDF can be equally computed from given Beta shape parameters using (2.11), (2.12) and (2.13).

$$\mu = \frac{\alpha C}{(\alpha+\beta)} \tag{2.11}$$

$$\sigma^2 = \frac{\alpha\beta C^2}{(\alpha+\beta)^2(\alpha+\beta+1)} \tag{2.12}$$

$$\mu_r = \frac{\alpha^{[r]}}{(\alpha+\beta)^{[r]}} \tag{2.13}$$

r: an integer; μ_r: r^{th} moment about the origin; y^r = y(y+1)……..(y+r-1)

Extensive research has been carried out, using the Beta PDF, to perform voltage drop calculations along distribution feeders. It is now the prescribed method for residential LV-feeder analysis in South Africa [SANS 507; Herman & Heunis, 1998].

As far as reliability analyses are concerned, Pham and Turkkan [1994] assumed Beta-distributed component life-cycles in the reliability analysis of a standby system. Nadarajah and Kotz in [2006] present a generalized distribution called the Beta-exponential distribution. However, just like the conventional negative-exponential, the Beta-exponential is also limited to applications that consider constant failure rates. It has however been shown that the Beta PDF can be applied in a sequential MCS reliability analysis to capture variability in failure parameters and represent the influence of such variability on the indices computed [Edimu et al, 2011(1); Edimu et al, 2011(2)]. A comparison of the Beta PDF with other commonly used ones will be presented in Chapter 4.

2.6 SUMMARY

The review of the concept of reliability, particularly its measurement and representation, provides some answers to the research questions developed in Chapter 1.

Qn.1: How is bulk network reliability evaluated and how are the results represented?

A review of the main approaches developed for bulk network reliability evaluation was presented. The sequential MCS is useful to this research because it is applicable to chronological events and can produce the PDFs that describe the computed indices. A number of probability distributions can be used in conjunction with the sequential MCS. One should however be able to derive the inverse translation function for each choice of distribution. Thus far this is not possible for the Beta distribution and as such can not be used in the conventional sequential MCS. An approach that is not hinged on deriving the prerequisite inverse translation would be required.

Qn.2: How applicable are continuous probability distributions in network reliability analyses?

A number of PDFs have been proposed for use in reliability studies with the exponential extensively applied.

Seasonal and time-of-day variations in external conditions induce variability in component outages so that the PDFs that describe failure parameters will exhibit a range of shapes. To capture the different shapes, the Weibull and gamma PDFs are used. However, failure parameters are usually derived from historical data which is defined by a specific range. The Beta PDF can also exhibit a variety of shapes but unlike the Weibull and gamma, it can be rescaled to another finite range. The Beta PDF appears to be the most suitable PDF for reliability studies that apply distinct failure data sets. It has however been seldom applied in reliability studies. It may thus be necessary to investigate the suitability of the Beta PDF compared to others for reliability analyses.

2.5.1 Onward

The next chapter will analyze the different models proposed thus far in literature for component failure parameters. The chapter will focus on identifying those modelling approaches that consider variability in failure parameters.

3. MODELLING EFFECTS OF EXTERNAL THREATS ON NETWORK COMPONENTS

3.1 INTRODUCTION

Several factors influencing reliability as a whole have been identified in the literature. The network's configuration, loading and component characteristics are some of the generally known factors. Extensive investigative work has thus been carried out in these fields.

- Network configuration: Mili and Qiu [2004] conclude that interconnection of various critical infrastructures has increased the vulnerability of networks to outages and thus contributed to the depreciation of bulk network reliability. Zhu [2007] also analyzed the impact of altering the design and configurations of power networks on their reliability

- Network loading: Cheng et al [2009] use a graph trace based analysis technique to evaluate the reliability of a power network with time varying loads. The relationship between reliability indices and the daily load curve is also investigated on a real network by Jadrijev et al [2009]

- Network components: Kolowrocki and Kwiatuszewska-Sarnecka [2008] apply limit reliability functions, particularly the asymptotic approach, to a multi-state network with ageing components. Koonce et al [2008] also rank infrastructure components according to the impact of their failure to operate on the network's reliability

Blake et al [2009] however, state that there are other drivers tending to increase the level of risk to continuity of electricity supply. One of these is external threats such as adverse weather. Local weather elements, according to Koval et al [2006], are primary contributors to network interruptions. The weather elements create variability in the inputs of reliability analyses such as component failure and repair rates.

3.2 VULNERABILITY OF BULK NETWORKS TO EXTERNAL THREATS

This section provides an overview of the contribution of external elements to network outages. The section will also detail the influence of external (local and global) threats on bulk network facilities. Emphasis is put on threats common to South African conditions.

Bulk networks cover vast areas, in particular the transmission lines that traverse several geographical regions. Distribution networks on the other hand are usually confined to small specific geographical regions such that at any given time all the distribution network components are exposed to similar external conditions. Different geographical regions are associated with different external conditions so that the external threats to which a distribution network is exposed are region dependent. Thus, analysis of component failures within a utility's distribution systems provides an insight to the different elements that could also influence bulk network reliability. Pahwa et al [2007] investigated the contribution of external network threats to outages in distribution networks in South Africa and USA. The results are indicative of network risks in the different geographical areas that South African transmission lines traverse.

The IEEE data analysis task force [1994] developed codes aimed at capturing different aspects of USA and Canadian overhead transmission outages at 230 kVA and above. The aspects considered ranged from type and cause of transmission circuit faults, to circuit restoration and effect of outage events. The categories of outage causes developed included foreign interference, human element, defective line equipment, environmental factors, network condition and unknown causes. The task force also presented the sub- causes under each category. A causal and seasonal contribution to forced outages of bulk transmission lines was analyzed for the Mid-Continent Area Power Pool (MAPP) in North America [Chowdhury & Koval, 2008]. Figure 3.1 shows the 230 and 365 kV lines' outage data based on the IEEE outage cause categories.

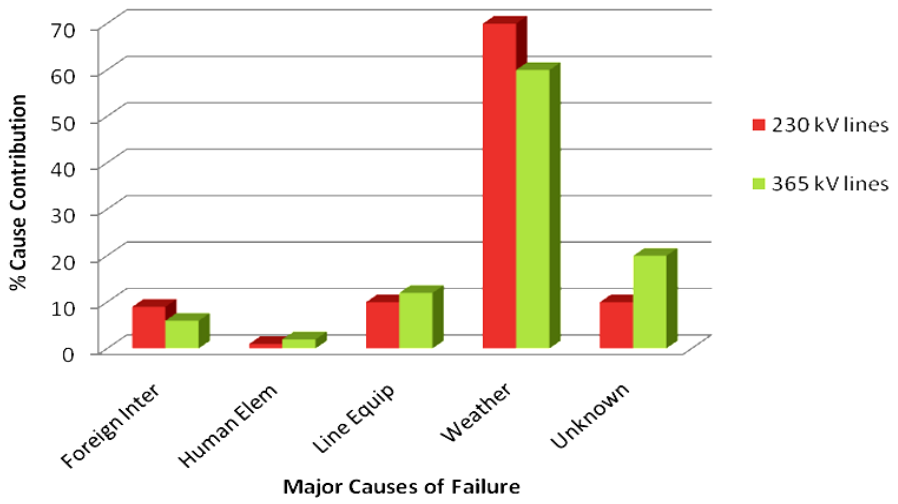

Figure 3.1: Cause contribution to line-related sustained outages [Chowdhury & Koval, 2008]

Environmental factors, particularly weather contributed significantly to line outages. Koval et al [2006] indicate that the major adverse weather elements contributing to Alberta Power Limited's transmission line outages are lightning, precipitation and wind. Literature discussing outage data from different power networks around the world also indicates the significant contribution by adverse weather to power outages [Makkonen, 1998; Lundstedt, 2005; Zhou et al, 2006; Almeida et al, 2009; Gu et al, 2010]. In 2004 a list of primary fault causes and sub-categories was introduced by the South African utility, Eskom, to provide analysis that could trace the root cause of faults [Vosloo, 2005]. The primary causes and some sub-categories are presented in Table 3.1.

Table 3.1: Causes of South African transmission outages [Sukhnandan & Hoch, 2002; Vosloo, 2005; Jandrell et al, 2009; Vosloo et al, 2009]

	Primary Categories				
	Birds	Lightning	Pollution	Fire	Others
Sub-categories	• Streamer • Pollution • Electrocution • Nest	• Direct stroke • Indirect stroke	• Industrial • Marine • Bird pollution • Fog • Rain	• Veld • Cane • Reed • Fynbos • Refuse	• Theft • Vandalism • Human element • Foreign objects • Wind

An extensive analysis of fault records for South African transmission lines was carried out to identify the major causes of the faults and their characteristics [Minnaar et al, 2012]. The four most significant individual causes of faults were identified as: Birds, Lightning, Fire and Pollution. Together the four external conditions contributed 89 % of all transmission outages as shown in Figure 3.2.

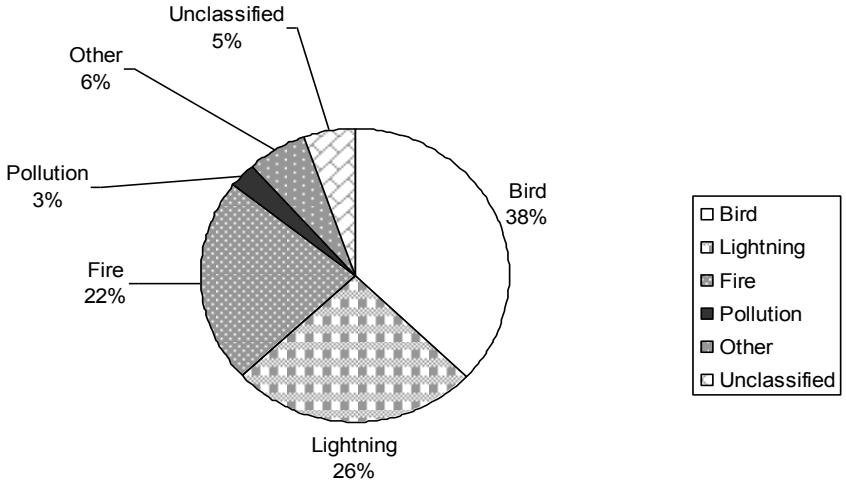

Figure 3.2: Fault causes for 132 kV to 765 kV transmission lines [Minnaar et al, 2012]

3.2.1 Effect of local weather threats on power generation

Local weather threats are specific to utilities i.e. the threats vary from one utility to another and are thus dependent on the local geographic conditions to which the network (or portion of the network) is exposed.

A significant push towards implementation of renewable energy technologies is on-going worldwide. Several proposals incorporating renewable energy have been put forward so as to develop an optimum mix between different sources of energy. The "*Global Energy Scenario"* predicts that half of the worldwide primary energy demand will be supplied by renewable energy sources by 2050 [EREC, 2007]. In a South African context, a "*progressive renewable scenario"* in which renewable energy plays a moderate role in power generation forecasts 15 % to 20 % contribution by 2020 and up to 70 % by 2050 [Banks & Schäffer, 2005].

While renewable energy sources such as wind, solar and oceanic waves, provide a means for 'clean[2]' electricity generation, they are vulnerable to environmental conditions [Ozgener & Ozgener, 2007]. Breslow and Sailor [2002] also agree that productivity and efficiency of most renewable energy sources is dependent on environmental conditions. The significant drop in hydro power generation levels, in East Africa, between 2000 and 2006, is attributed to long droughts [USGAO, 2005; Mason et al, 2006].

Wind turbines are designed to 'cut off' when wind speeds fall below or above specified thresholds. However, variability still exists within the operational range of wind speeds, thus impacting on the quality of power generated and, particularly, leading to supply voltage and frequency fluctuations [Heier, 2006]. The wind speed models developed by Breslow and Sailor [2002] showing variations in projected wind speeds due to global warming indicate potential reduction in continental United States wind power generation of the order 30 % to 40 %. Solar energy, whether from solar thermal energy conversion or photovoltaic (PV) energy generation, is vulnerable to variations in cloud cover and atmospheric turbidity [Patel, 1999]. PV generation has variable output characteristics dependent on irradiation and ambient temperature [Park et al, 1999]. Cha et al [2004] show the necessity to include weather effects when investigating impact of PV systems on reliability of a given network.

3.2.2 Effect of local weather threats on transmission facilities

The key transmission line reliability inputs affected by variability in the network environment and thus sensitive to adverse external conditions are component failure rates and restoration times.

Transmission line failure rates

Globally, adverse weather contributes most to network failures compared to other external factors. The physical stresses on the network components are higher in adverse weather conditions than those encountered under normal weather conditions [Billinton & Wu, 2001].

[2] No green house gas emissions during power generation

The increased stress causes network component failure rates, which are otherwise low for most the year, to increase significantly for short periods when adverse weather is prevalent. Some adverse weather elements include lightning, adverse wind, ice storms, fog and rain.

Lightning strokes cause direct and induced flash-overs in a network as shown in Figure 3.3(a). Direct flash-overs occur when a lightning stroke strikes a phase conductor(s) leading to phase-to-phase, phase-to-neutral or phase-to-ground flash-overs. Induced flash-overs are due to surges occurring due to lightning striking the ground near a line structure. Also, back-flash-overs can occur when a shield wire, struck by lightning, fails and allows the lightning to reach the phase conductor [Balijepalli et al, 2005]. Transformers have also been known to fail due to lightning strikes.

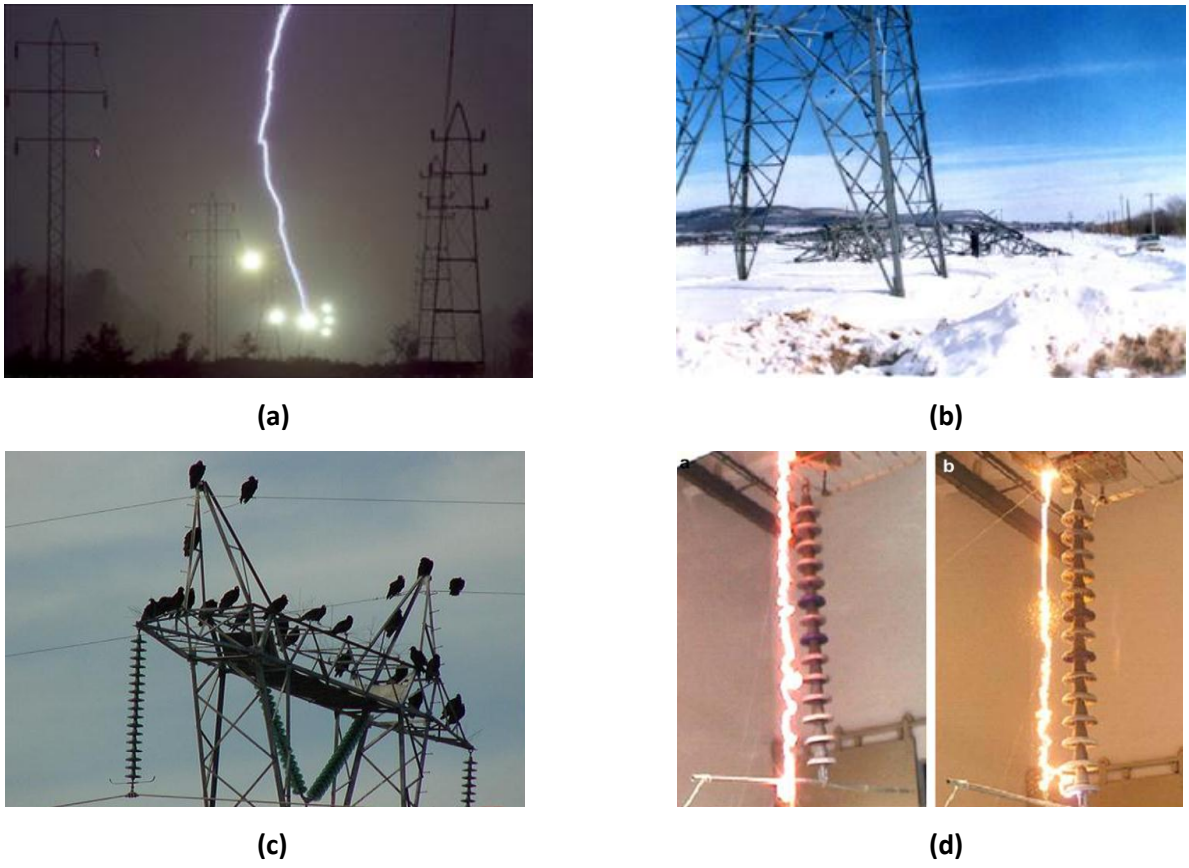

(a) **(b)**

(c) **(d)**

Figure 3.3: (a) Consecutive line flash-overs due to lightning strike [Staco website] (b) Collapse of Hydro-Québec pylon during the 1998 Ice Storm [Vancouver Island Powerline website] (c) Birds on transmission lines in Mexico [Tena et al, 2010] (d) Insulator flash-over experiments [Zhou et al, 2009]

Alvehag and Söder [2011] cited wind as a significant cause of overhead line failures in Sweden. Adverse winds usually cause line to line faults and contribute to flash-overs but have also been known to bring down transmission line structures [Brostrom et al, 2007]. Transmission structures are designed to withstand wind and ice loads up to specific thresholds. Loredo-Souza and Davenport [1998] through aeroelastic tunnel tests investigated possible explanations for transmission line failures in adverse winds. The authors confirmed the importance of turbulent wind characteristics to a conductor's dynamic response to wind. Loredo-Souza and Davenport [1998] also determined that the aerodynamic damping plays a key role in conductor motion of overhead lines under adverse wind conditions. Thus, the quasi static action in response to slowly varying wind loads and the resonant response are the main contributors to a conductor's fluctuating response under adverse winds.

High voltage outdoor insulators are exposed to pollution because of salt in regions near the sea and dust and chemical residues in industrial regions. There are mainly two types of flash-overs due to pollution. The first type occurs when ionisable materials drift between line conductors so that the line-line clearance and effective air-insulation is compromised. The second type is due to pollutants deposited on insulation discs [Looms, 1988]. Pollution deposited on the insulator surface becomes a conductive electrolyte when the insulator surface is wetted by rain or fog or under humid conditions [Gençoğlu & Cebeci, 2008]. Line insulators are normally designed to withstand about twice the operating voltage [Habib & Khalifa, 1986]. The development of partial discharges on an insulator's surface and propagation of these discharges over a period of time allows the leakage currents to increase over the surface. The electrical withstand voltage of the insulator thus decreases so that a flash-over and possible power outage may result [Aydogmus & Cebeci, 2004].

Birds contribute to line failures in three ways; bird streamers, electrocution and bird contamination [Sundararajan et al, 2004]. Bird droppings are a mix of urine and excrement passed out when birds perched on transmission structures take flight.

Bird streamers were first determined as one of the contributors to 'unknown' transmission line faults in the 1920s [Michener, 1928]. Bird streamer flash-overs occur when large birds release long continuous emission of conductive fluid droppings which partially or totally short the air gap between the line structure and conductor [Burnham, 1995, Naidoo et al, 2006]. Streamer outages in Florida, Nevada, California and South Africa have been found to exhibit similar characteristics. These include [Burnham, 1995, Taylor et al, 1998, Sundararajan et al, 2004]:

- Unknown cause, neither lightning, switching surge, contamination or any known cause.
- The presence of large bodied birds, such as eagles, hawks, ospreys, vultures, and herons.
- Outages that occur between the hours of 2300 to 0600 giving the suspicion that it may be a contamination flash-over.
- The lack of natural roosts, such as trees in the area of the outages.
- The abundant availability of food, agricultural land, sugar cane field and ponds.
- Outages involving typically the central phase.
- Seasonal pattern related to the presence of birds or their feeding habits.
- Instantaneous relay actions with successful reclosure, typically not more than two in the same area.
- Flashed insulators, hardware, or structures, possibly evidencing burn spots on the upper bridge of metallic structures.
- The presence of dead or injured birds or burnt feathers near the structure after an outage.

It was believed that bird streamers caused flash-overs generally at lower voltage levels such as 110 kV and 220 kV due to shorter insulation gaps as compared to 500 kV lines. However, in recent years bird streamer flash-overs in 500 kV lines have been reported [Zhou et al, 2009].
Bird contamination flash-overs occur due to the accumulation of bird droppings. This is mainly due to birds building nests in the gaps and on the structures in substations as shown in Figure 3.3(C).

The highly conductive droppings and the wetness of bird excrement on insulators reduce the surface resistance to an extent that the nominal line voltage easily establishes an arc across the insulators [Sundararajan et al, 2004]. Bird contamination develops from overnight or long-term accumulation of faecal contamination at sites that attract birds. Long-term contamination creates conductive paths during wet external conditions such as rain storms. Flash-overs due to electrocution and collision occur when birds come into direct contact with conductors. Many collisions with power lines occur during daily flights within a daily use area [IEEE task force, 1994]. According to van Rooyen et al [2003], bird electrocution mainly occurs below voltages of 132 kV where clearances are smaller. Other line flash-overs occur due birds nesting on line structures. Nest building could lead to bird contact in tight places where the energized equipment is close to grounded surfaces. Nesting materials dropped by birds lead to short circuits while the presence of nests also attracts predators and increases the risk of outages due to animal electrocution.

Lanoie and Mercure [1989] concluded that a correlation exists between proximity of fires and line faults. Bush fires, either due to clearing of vegetation, sugar cane harvesting, natural sparking during extreme temperature conditions or human error, cause transient earth faults on transmission lines. This usually occurs for short periods of time particularly when the fires are in the vicinity of the transmission lines. Sometimes the flames are large enough to engulf the conductors as depicted in Figure 3.4.

Figure 3.4: Sugar cane fire and smoke engulfing transmission line conductors [Sukhnandan, 2004]

A major part of the air-gap is filled with the flame leaving a small gap between the flame-tip and the conductor. This gap is often filled with smoke and particles so that flash-overs are either induced through the conductive flame or due to a reduction of the air gap between conductors [Sukhnandan & Hoch, 2002]. The presence of the flame reportedly causes phase to phase and phase to earth flash-overs. This not only causes damage to transmission line hardware but also causes voltage dips due to the large fault currents. According to Sukhnandan [2004] this type of fault is more serious than other transient faults because the line often re-trips and locks out.

Transmission line repair rates

The restoration time of a failed network component is a variable parameter dependent on a range of factors such as the utility response to create repair orders, waiting time to serve a repair order and transportation time of the repair crew [Zapata et al, 2008]. Other key influencing factors include the time the failure occurs and the cause of the failure. Generally, outages that occur at night have longer restoration times than in the day-time. This is attributed to unavailability of sufficient work force at night [Cha et al, 2004]. Restoration times increase as the magnitude of a fault increases. Repair on a network, especially on transmission lines, usually commence only after adverse weather subsides. For example, unless strong winds subside, repairs cannot commence on any fallen transmission lines. This increases the duration of the outage. Billinton and Singh [2002] make a case for the relative reduction in outage duration with repairs carried out in normal and adverse weather conditions.

3.2.3 Effect of global space weather threats on power networks

Space weather refers to conditions on the sun, in the solar wind, the magnetosphere and the ionosphere that can influence space and ground man-made technologies (Pulkkinen, 2003). The space weather chain starts at the surface of the sun in the form of either solar flares or corona mass ejections and culminates as geomagnetically induced currents (GICs) on the surface of the earth [Kappenman et al, 2000].

GICs are typically driven to or from various power system electrical ground points as shown in Figure 3.5 by the voltages induced in the transmission lines [Ngwira, 2011].

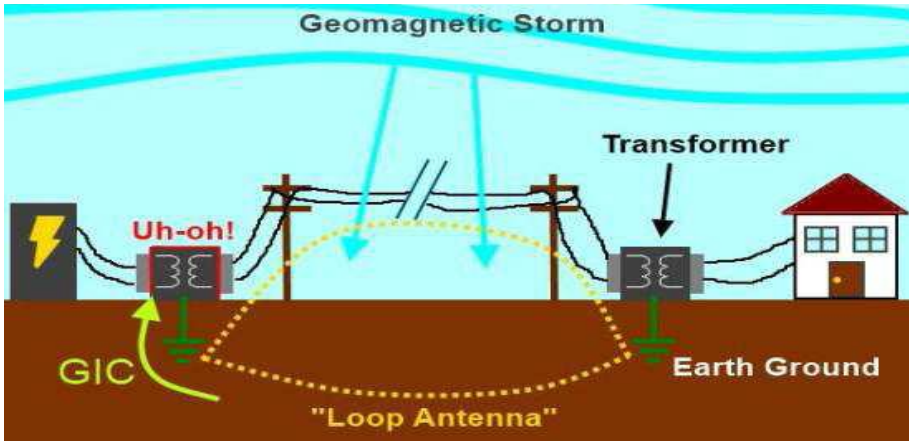

Figure 3.5: Induced voltage drives GIC to and from neutral ground points of power transformers [Ngwira, 2011]

Unlike local weather threats, space weather elements create large-scale problems because a storm's footprint can extend across a continent. According to Kappenman et al [2000], power networks in the upper latitudes of the Northern hemisphere are at increased risk because aurora activity. Gaunt and Coetzee [2007] presented findings that testify to GICs contributing significantly to transformer failures in Southern Africa (mid and low latitude countries). Exposure of power transformers to GICs leads to the phenomenon called '*half-cycle saturation*' [NERC report, 2012].

Most external threats to network reliability directly lead to immediate component outages. Saturation of power transformers and reactors is known to have short and long-term effects on network reliability. In the short-term, exposure of a network to GICs results in harmonic currents which could cause protection relays to trip required equipment [Boteler et al, 1989; NERC report, 2012]. GICs exposure would also increase internal reactive power losses (Vars consumption) in transformers. This ultimately impacts on network vulnerability by increasing its reactive power supply requirements, components' loading and voltage dips [Koen & Gaunt, 2001].

Loss of reactive power support could thus lead to voltage instability and power system collapse. Internationally, the best known example of the devastating effects of GICs on network reliability occurred during the 13th March 1989 super storm. The complete blackout of the Hydro Quebec power grid was attributed to the GIC events associated with the super storm. The power outage occurred because of widespread transformer saturation and the network's failure to compensate for reactive power due to tripping of its shunt capacitors [Kappenman & Albertson, 1990].

GICs generate fringing magnetic flux i.e. flux that flows outside the core. Gaunt and Coetzee [2007] state that, "*without adequate control of the flux under saturation conditions, local heating in parts of the transformer may not be cooled effectively, leading to rapid temperature increase. The intensity of overheating depends on the saturation flux paths, cooling flow and the thermal condition or loading of the transformer. Overheating causes the breakdown of oil and paper insulation*." Development of hotspots within the transformer puts stress to the winding insulation. If the stress surpasses the design withstand level, the transformer could fail. Damage to insulation could also be the root cause of failure of transformers exposed to future stresses. Inspections of failed generation step-up transformers in Tutuka and Matimba sub-stations (South Africa) identified heat damage, mostly to paper insulation, in various parts of the transformers, as illustrated in Figure 3.6.

(a) **(b)**

Figure 3.6: (a) Overheating LV terminal one of the Tutuka transformers (b) Failure of HV windings in Matimba transformer [Gaunt & Coetzee, 2007]

Six modern transformers failed 7 months after the geomagnetic storm –the "*Halloween storm*" of November 2003 [Gaunt & Coetzee, 2007].

The NERC report [2012] presents more detail on the thermal effects of GICs on transformers and also presents an overview of reported instances where transformers have been reported to be affected by GICs. Lundstedt [2006] also provides a historical description of disturbances in the Swedish electrical system, up to November 2004, related to occurrence of adverse space weather. The report showed that GICs are induced at different frequencies. Network component's that operate at higher frequencies could thus also be affected by space weather effects.

3.3 APPROACHES APPLIED TO MODELLING NETWORK COMPONENT FAILURES

Network failure events are associated with uncertainty. The uncertainty arises either from the random nature of the phenomenon that cause network failure or, from the lack of knowledge of the events themselves [Kim & Singh, 2002]. Representation of the former type of uncertainty has been attempted by a number of authors through fuzzy methods [Zhou, 2005; Li et al, 2009; Liu & Singh, 2011]. The scope of the work presented in the thesis is however limited to uncertainty induced in network failures due to variability in the root-cause phenomenon.

This section will present the modelling approaches developed to capture the vulnerability of network facilities to failure. The models can be categorized, based on the relationships derived between a component failure event and the time-of-occurrence of the event, into:

- Time-independent failure modelling approaches
- Time-dependent failure modelling approaches

Literature indicates that of all external network threats, local external threats are the most common contributors to transmission outages, world wide. As such, most of the literature identified on reliability modelling in the network operational paradigm has been limited to local weather, particularly adverse weather.

3.3.1 Time-independent failure modelling approaches

Time-independent approaches do not consider the influence time-of-occurrence has on the failure rates of components. The bath tub curve is a common model of component vulnerability: the failure rate initially decreases, stays constant and then increases with time.

Most literature on reliability considers the period when component failures are deemed constant so that network reliability parameters are represented as single deterministic values, usually an average. This is the criterion commonly followed when reliability models are developed for planning purposes. An 'average year' is derived such that the 'average' failure and repair rates computed are based on several years that cover many operational states and all kinds of external factors [Bollen et al, 2008].

Several authors however agree that while this may suffice for an overview of a network's reliability, the use of single average values to represent failure and repair rates of components is most times unrealistic and could provide misleading results [Billinton & Allan, 1996; Bollen, 2001; Billinton & Singh, 2006; Carer & Briend, 2008].

Alvehag [2008] states that "*using average values may, therefore, be misleading since the 'average year' never occurs. In the majority of years a small number of interruptions occur, and during extreme years with for example a major storm, many interruptions can occur. Average indices are based on all years, but a year that produces these average indices may never have occurred*." Reliability parameters have inherent uncertainty dependent on a network's configuration, component location and inter-relationship with other components and, the network's environment. Operational reliability analysis considers a network's performance in short periods of time ranging from hours to a couple of months. External factors have a significant influence on reliability parameters during such short periods. Using reliability parameters derived from long-term observations may not be sufficient when reliability models for operational purposes are required.

The time-independent modelling approaches identified in literature can be grouped into :

- Discrete (N-n) adverse state modelling approaches
- Stochastic adverse state modelling approaches

3.3.1.1 Discrete (N-n) adverse state modelling approaches

This approach develops deterministic states, for adverse external conditions, capturing various levels of severity. The main model used when considering stochastic causes of outages is the two weather state representation. This can be regarded as the conventional model applied when considering adverse weather in reliability analysis. The modelling approach is illustrated in Figure 3.7. A normal-weather state and an adverse-weather state are defined [Billinton & Allan, 1996]. A_i and N_i represent the duration of the i^{th} adverse and normal weather periods respectively. λ_a represents the average failure rate in adverse weather conditions.

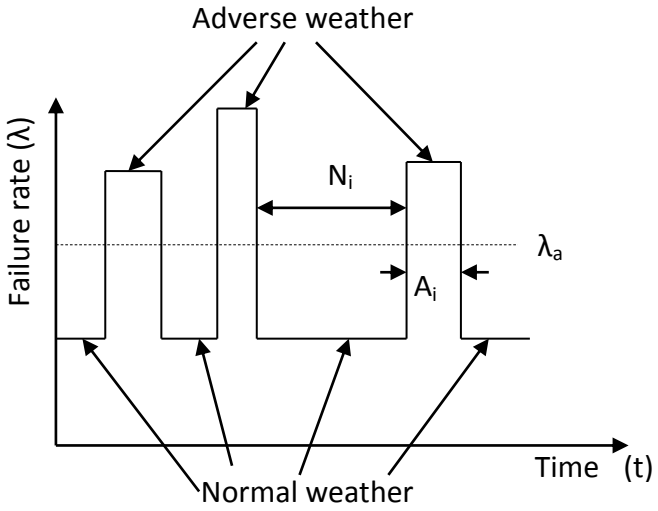

Figure 3.7: Random failure rate history [Billinton et al, 2002]

According to Billinton and Allan [1996] the decision to categorize a type of weather as either normal or adverse depends on the impact on failure rates during the exposure period. Those weather conditions having little or no effect on the failure rate should be classified as normal and those having a large effect, classed as adverse. Component failure rates are derived from failure data collated for the two weather states and are expressed as average number of failures per year of the given weather condition.

A component's failure rate is assumed constant during normal weather conditions. Different constant failure rates that apply for the duration of adverse weather conditions are used to compute the average failure rate for adverse weather. This allows for the probability distributions associated with the failure and duration parameters to be negatively exponential. Billinton and Allan [1996] detail the two weather state model further, together with numerical examples.

Extensive reliability-related work has been carried out using this conventional model. Bollen [2001] showed that the two weather state model is applicable to simple analytical reliability calculations involving non-constant failure rates due to adverse weather. Using the weather model it was deduced that adverse weather needs to be included in the reliability analysis when parallel components are involved. Billinton & Wu [2001] developed a Markov state space diagram and corresponding steady state probabilities for a two component redundant system exposed to normal and adverse weather conditions. The analysis showed that the failure rate increased as the percentage of failures occurring in adverse weather increased. By differentiating weather as normal and adverse, Sannino and Bollen [2003] showed that the load-tripping frequency of a static transfer switch increases when the percentage feeder outages is higher in adverse weather. The tripping frequency however decreased with reduction in duration of adverse weather exposure.

A two weather state model is not sufficient to capture the variability in local weather conditions [Lecomte et al, 1998; Billinton et al, 2002]. Makkonnen [1998] states that the data sets used to develop previous weather models, in particular for freezing precipitation, seldom include extreme situations. The IEEE Standard 859-1987 proposed the division of a network's weather environment into three categories: normal, adverse and major adverse weather [IEEE Standard, 1988]. Thus, the two weather state model provides a framework for adding other weather state conditions [Billinton & Singh, 2002]. The three weather state model, incorporating major adverse weather is illustrated in Figure 3.8.

In which a, m and n are transition rates between adverse, major adverse and normal weather states. Failures occurring in major adverse weather are not combined together with adverse weather failures but rather considered separately.

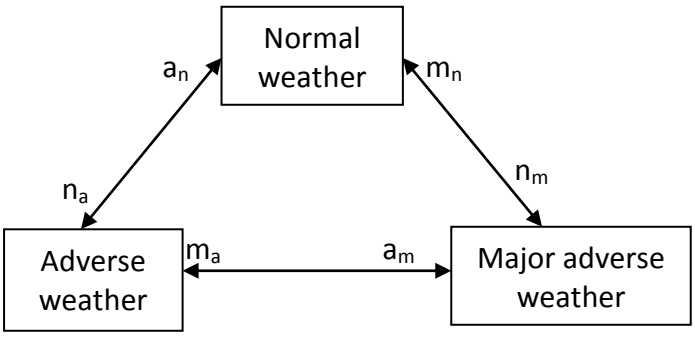

Figure 3.8: Three weather state model [Billinton & Singh, 2006]

Billinton and Singh [2006] illustrate the impact of dividing bad weather into adverse and major adverse weather. A significant difference in the reliability indices computed was noted when major adverse weather failures were also considered. The authors also use the model to illustrate the reduction in outage duration when repairs are carried out during adverse weather conditions as opposed to after the conditions subside [Billinton & Singh, 2002]. Billinton and Acharya [2005] extended the three weather state model to include additional adverse weather severity levels. Using the Markov approach, they showed that the three state weather model is inadequate as far as showing a wide range of weather conditions is concerned. A multi-state weather model was thus proposed to account for continuously varying levels of stress due to weather.

Zhou et al [2005] apply the multi-state weather modelling approach. Numerous combinations of the wind gust speeds and the lightning stroke currents were categorized into 15 weather states and the probabilistic relationship between each weather state and failure level investigated.

Section 3.2.1 described the effect of changing weather conditions on renewable sources of energy such as solar and wind. Literature shows that the failure rate function of wind turbines is a negative exponential curve [Ozgener &Ozgener, 2007]. The multi-state weather approach is commonly used to model such fluctuating primary energy sources. Various capacity states are evaluated from the level of the weather parameter being considered.

Singh and Lago-Gonzales [1985] grouped unconventional power units (renewable) into different subsystems with varying capacity levels. Cha et al [2004] use the radiation intensity to develop PV generation models for a distribution network reliability study. Wen et al [2009] investigated the effect varying wind speeds, within three categories, on the reliability of a network incorporating wind turbines. Discrete power outputs were determined for each wind speed considered. The three wind speed categories considered included the cut-in, rated and cut-off wind speed. Figure 3.9 shows typical power output models for a solar cell generation unit and a wind turbine. A relationship between power output and weather parameters, wind velocity and solar radiation, is presented.

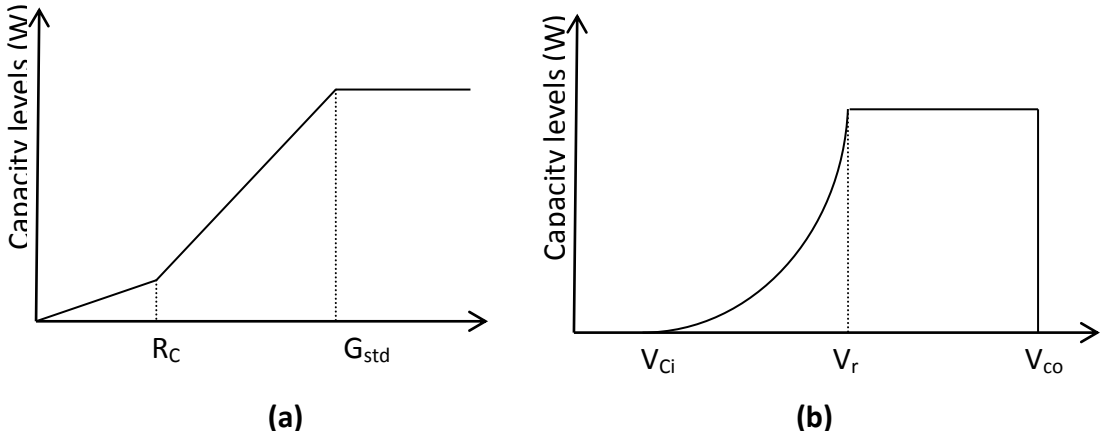

(a) **(b)**

Figure 3.9: (a) Power output model of a solar cell generating unit [Park et al, 1999] (b) Wind turbine power out characteristic [Deshmukh & Deshmukh, 2008]

R_c: radiation point

G_{std}: solar radiation in a standard environment

V_{ci}, V_r and V_{co}: cut-in, rated and cut-off wind speed

Discrete models are usually developed on an annual basis. The reliability parameters are computed as average values over a year of the given weather state conditions. Failure rates, repair rates and capacity levels are thus assumed constant for a particular weather state. However, weather patterns are intermittent in nature such that using constant values neglects variability of network component reliability parameters within each specified weather state.

Furthermore, weather patterns and other external factors such as presence of birds vary according to seasonal changes in a given year such that the network risk posed occurs only for short periods during a given year. Bollen et al [2008] state that the failure rate of, especially, overhead lines increases several orders of magnitude with intensity of adverse weather conditions. The probability of having various levels of adverse weather within short periods is no longer negligible so that discrete (N-n) models are no longer sufficient, particularly for reliability assessments that relate to external conditions.

3.3.1.2 Stochastic adverse state models

Stochastic adverse state models are based on a random parameter of the adverse phenomenon being investigated. The random parameter could be an integral part of the external factor(s). For adverse weather, the random parameter describes the severity of the weather element such as wind speed for wind related outages or ground flash density and the magnitude of the lightning crest for lightning strokes. The parameter could also be as a result of the occurrence of the external factor(s) such as the electric field on the surface of an insulator due to deposited pollutants. Stochastic adverse state modelling is more commonly applied in network operation reliability studies. The network state is determined based on prevailing conditions.

Haghifam and Omidvar [2006] derive stochastic output electric power of a wind farm based on historical wind velocities. Using recorded speeds for daily, monthly and seasonal periods, wind velocity profiles were developed. The corresponding wind turbine power output model is constant for wind speeds within the rated and cut-out values, a normal distribution between rated and cut-in values, and zero for all other wind speed values.

The model developed is not generic as the wind velocity data used in the modelling was obtained for a specific location and not tested with other locations. Also, the authors state that the binomial distribution was assumed and fitted to the data collected.

Brown et al [1997] derived quadratic functions of the wind speed to model the expected number and duration of faults due to a potential storm event. For overhead line failures, each line was characterized by a base storm failure rate, λ_{base}, at a base storm wind speed, S_{base}. The storm failure rate of the overhead line at wind speed, S, was then described as shown in (3.1).

$$\lambda(s) = \lambda_{base}\left(\frac{S}{S_{base}}\right)^2 \tag{3.1}$$

The quadratic function was based on the fact that the pressure exerted on trees and poles is proportional to the wind speed squared. The model was used to formulate criteria to determine whether a potential storm threat could actually develop into a storm event. The model was however applied to a single location and not verified against storm related failure data. Brostrom et al [2007] developed a weather impact model such that the risk of a transmission outage is connected to the specific weather conditions. The authors modelled ice storm severity levels through exponential functions of the ice and wind load factors. The latter computed as an integral factor. For a given component outage however, weather was regarded as deterministic and the component's vulnerability, stochastic. Thus, discrete storm severity levels were considered so that component vulnerability could also be regarded in discrete levels.

Carer and Briend [2008] also considered a localized area when modelling failure rates of MV electrical network components exposed to adverse wind. A critical wind speed was specified such that for wind speeds below this threshold, component failure rates were deemed constant. Failures were assumed to grow exponentially for wind speeds above the threshold. Only one year's failure data was used such that only a partial model was developed.

Alvehag and SÖder [2008] propose a stochastic weather dependent reliability model to investigate the effect of variable failure and restoration times of a radial distribution network, due to adverse wind, on the interruption cost. The model is based on the stochasticity of adverse weather severity and duration. The model proposed by Brown et al [1997] is adopted by the authors such that a quadratic function is achieved as shown in (3.2). The model applies only for wind speeds greater than the critical wind speed (w_c).

$$\lambda_a(w(t)) = \left(1 + k\left(\frac{w(t)^2}{w_c^2} - 1\right)\right)\lambda_n \quad (3.2)$$

λ_n, λ_a: constant normal weather and adverse wind failure rates

k: scaling parameter

w(t): wind speed at a given time t

Alvehag and SÖder [2011] compare the quadratic model in (3.2) and an exponential model. The quadratic model regarded wind speeds below w_c as normal weather such that the failure rate was deemed constant. However, the data presented indicated that the range of wind speeds, $w(t) < w_c$, contributed almost 40 % of the recorded wind–caused overhead line failures. To model varying restoration times due to adverse weather, an approach similar to Wang and Billinton [2002] was adopted. Weight factors were used to account for variation in restoration times due to availability of a repair crew and duration of adverse winds conditions. The failure rate model was tested using data from only one location. Further, the application of weight factors varies from one utility to another. Utilities have different restoration protocols such that factors influencing the restoration time in two utilities could differ.

Network failures due to lightning are usually modelled using the ground flash density (N_g). Balijepalli et al [2005] defined the N_g as the average number of lightning strokes per unit area per unit time at a given location. The lightning line flash-over rate was then modelled linearly using N_g for both direct and induced over head line flash-overs. Further, the repair rate for lightning failures was modelled as an exponential distribution. The two models developed were based on data collected from a single utility.

Alvehag and SÖder [2011] also applied a linear relationship between overhead line outages due to lightning and the ground flash density as shown in (3.3).

$$\lambda_l(N_g(t)) = \lambda_n(1 + \gamma N_g(t)) \tag{3.3}$$

λ_n, λ_l : failure rate in normal weather and lightning conditions

γ : scaling parameter

A constant failure rate was assumed for normal weather. This model was applied, together with a wind vulnerability model previously estimated by the authors [Alvehag & SÖder, 2008] to a distribution network that experienced both adverse wind and lightning conditions. The validation however did not consider scenarios when components concurrently experienced adverse wind and lightning conditions. Furthermore, the model only investigated a discrete set of lightning storm levels and corresponding failure rates.

Experimental and analytical tests have been developed to assess the flash-over performance of polluted HV insulators. Experimental tests usually require the insulators to be separate from the power network and are set in special sites for measuring the degree of pollution [Habib & Khalifa, 1986]. Analytical tests on the other hand use mathematical models to compute the flash-over voltage of polluted insulators [Gençoğlu & Cebeci, 2008]. The most common mathematical model is the dynamic model that allows the prediction of discharge activity leading to a flash-over on a polluted surface. The stochastic parameter modelled by the dynamic model is the discharge arc. A relationship exists between the propagation of the discharge arc, and subsequent flash-over voltage, and variations of pollution film conductivity, temperature and peak leakage current [Streubel, 1983; Amer, 1987]. The dynamic model accounts for the instantaneous changes of the arc parameters [Aydogmus & Cebeci, 2004].

Stochastic modelling approaches are particularly important to network planning that considers periods that are longer than 10 years. The patterns and intensities of external threats such as adverse weather could change significantly over such periods due to climate change.

By linking a component's failure parameters to specific weather parameters, stochastic models are able to reflect the effect of future changes in the weather element on the component's performance. The stochastic models proposed thus far are however applicable to specific weather parameters. With such modelling, significant effort must also be put into modelling not only the weather conditions but also how component failure parameters relate to each weather element. The modelling approaches relate component failures to time-varying weather parameters.

3.3.2 Time-dependent component failure modelling approaches

The timing of an outage has a significant bearing on the consequences a utility and its customers face. According to Alvehag and SÖder [2008], severe weather intensity changes with time-of-day so that component failure rates are time-dependent. The failure rates of some components such as some underground cables, protection equipment and indoor substations are independent of external factors. However, overhead lines, transformers and outdoor substations are strongly exposed to external risk factors and so experience strongly time-dependent failure rates [Bollen, 2008]. In South Africa, the power network faces its highest loading during the winter season during which outages impact greatly on the reliability of an already strained network. This suggests the need to include the time when interruptions may occur.

Wang and Billinton [2002] recognized the importance of the time-of-occurrence of fault events and introduced time-varying weight factors. The weights represent the effects of weather and available (time-dependent) restoration resources on component failure and repair rates. The 'normal' weather component failure rate, λ_n, is weighted by a time-varying weight factor, w(t), to obtain the time-varying failure rate in (3.4). In (3.5) the authors represented the effect of available restoration resources on the restoration time using weekly, daily and hourly weight factors as shown.

$$\lambda(t) = \lambda_n * w(t) \quad (3.4)$$

$$r(t) = (w_w(t) * w_d(t) * w_h(t)) * r \quad (3.5)$$

r(t), r: time varying and normal weather restoration times

w_w, w_d, w_h: weekly, daily and hourly weight factors

In the text the authors however did not show how the different weights can be computed. Thus it is not clear whether the time varying weight factor for component failure rate is a function of the component's characteristics or the fault causing weather element. Further, the use of weight factors component restoration is utility specific. Utilities have different restoration protocols and resources so that a vast array of influencing factors would need to be weighted. Also the weight assigned to a given factor would have to change from one utility to another.

Wangdee and Billinton [2004] characterized a feeder using a time-dependent feeder cost priority index (FCP). The FCP is divided into two categories, a day time high cost priority index and a night time low cost priority index. In determining the curtailment priority of the feeders in a network, feeders are assigned either a low or high FCP depending on the time an outage occurs. This however does not take into account the cause of faults such that for a given feeder the same interruption cost is assigned to all faults occurring during the day. Similarly, it is assumed that all faults at night have the same cost impact. Faults that occur during peak hours of consumer demand usually have a more significant impact than faults recorded outside peak hour intervals.

Kjolle and Holen [1998] applied a different approach and develop component statistics based on all types of failures caused by weather or by technical and human aspects. The data was grouped into monthly, weekly and hourly periods and conditional probabilities extracted from the data sets.

The probability of failure occurrence (qλ) in a particular hour (h), on a particular day (d) and in a particular month (m) was then determined using (3.6) while assuming independence between the three factors.

$$q\lambda_{(h,d,m)} = q\lambda_h * q\lambda_d * q\lambda_m = \frac{\lambda_h}{\lambda_{av}} * \frac{\lambda_d}{\lambda_{av}} * \frac{\lambda_m}{\lambda_{av}} \quad (3.6)$$

λ_h, λ_{av} : hourly based failure rate and average annual failure rate of a component

$\frac{\lambda_h}{\lambda_{av}}$: conditional probability of failure in a particular hour

Using (3.6) a component's failure was time tagged by month, day and hour so that it's time-dependent failure rate pattern can be regenerated. The authors stated that by developing conditional probabilities, a random sampling of time of failure occurrence can be performed while still keeping track of the particular month, day and hour. A weather model is thus not required because the effect of the weather on failure is embedded in the conditional probabilities. The failure statistics are an aggregated result of all failure causes.

From a planning point of view, the approach provides a better approximation of the overall vulnerability of network components to outages compared to the use of deterministic average values. However, the data sets developed do not allow the vulnerability to specific threats to be evaluated. Applying the models to operation scenarios would provide misleading results. The analysis periods are quite short and yet the conditional probabilities are based on annual data sets. As described in Section 3.2.2, specific threats are prevalent in distinct periods in a year. The modelling approach described assigns the same likelihood of occurrence to all failure causes.

Herman and Gaunt [2010] also considered the segmentation of failure data. They proposed a time-dependent characterization of interruptions so that duration and frequency of interruptions could be associated with seasonal and time-of-day intervals as shown by the 4X4 matrix in Table 3.2.

The matrix vulnerability model in Table 3.2 shows four seasons and four time-of-day intervals. Each cell or time window represents a specific season and time-of-day interval.

Table 3.2: Time windows for frequency or duration of interruptions [Herman & Gaunt, 2010]

Season (S)	Time Period (P)			
	P1	P2	P3	P4
S1	μ_{11} , σ_{11}	μ_{12} , σ_{12}	μ_{13} , σ_{13}	μ_{14} , σ_{14}
S2	μ_{21} , σ_{21}	μ_{22} , σ_{22}	μ_{23} , σ_{23}	μ_{24} , σ_{24}
S3	μ_{31} , σ_{31}	μ_{32} , σ_{32}	μ_{33} , σ_{33}	μ_{34} , σ_{34}
S4	μ_{41} , σ_{41}	μ_{42} , σ_{42}	μ_{43} , σ_{43}	μ_{44} , σ_{44}

μ_{ij}, σ_{ij} : mean and standard deviation of failure data in season i and time slot j (cell ij)

The authors state that the seasons need not coincide with annual climatic seasons, calendar months or be of equal duration. Rather, categorization should be based on the periods in the year when components are vulnerable to interruptions. The time-of-day intervals could also be variable and dependent on the more likely period of vulnerability. Such a vulnerability model can be consistently applied to both long-term and short-term reliability analyses. For long-term, the length of the season in Table 3.2 is increased to a year or longer. Short-term studies could consider climatic seasons in a year, a calendar month, week or a couple of hours.

A matrix is developed for a component. Similar to Kjolle and Holen [1998], the components historical failure data is distributed into each of the cells, or time window, and failure parameter statistics (mean and standard deviation) derived. Each time window takes into account those threats that occurred during the selected window. The data in each cell can thus be analyzed further so that failure statistics can be derived for each network threat or the cumulative effect of all the threats that occur during the same time window.

Unlike the conventional approach that only uses average values to represent interruptions and component parameters, the modelling approach proposed by the authors includes the standard deviation to account for variability within different time intervals. The standard deviation however only describes the degree of dispersion about the mean value. Component parameters are influenced by stochastic external elements so that fitted probability distributions could exhibit any shape. The model, as is, would thus provide no indication to the shape or the level of skewness of a parameter's underlying distribution. This model is discussed further in Chapter four. It is extended so that more realistic failure data distributions can be achieved.

3.4 ANALYZING SEASONAL AND TIME-DEPENDENCY OF NETWORK FAILURES

This section analyzes the impact of seasonal and time-of-day variations on network failures. External network threats are stochastic [Habib & Khalifa, 1986]. They vary for different lengths of time and also have a range of severity levels. External threats mostly occur within specific seasons of the year such that a pattern can be attached to their occurrence. Also, some interruptions have specific time-dependence. Burnham [1995] described a time-of-day approach to investigating the cause of unknown faults. The investigation on Florida Power and Light (FPL) company transmission lines showed that outages due to lightning storms predominantly occurred during summer months particularly in the afternoon as shown in Figure 3.10.

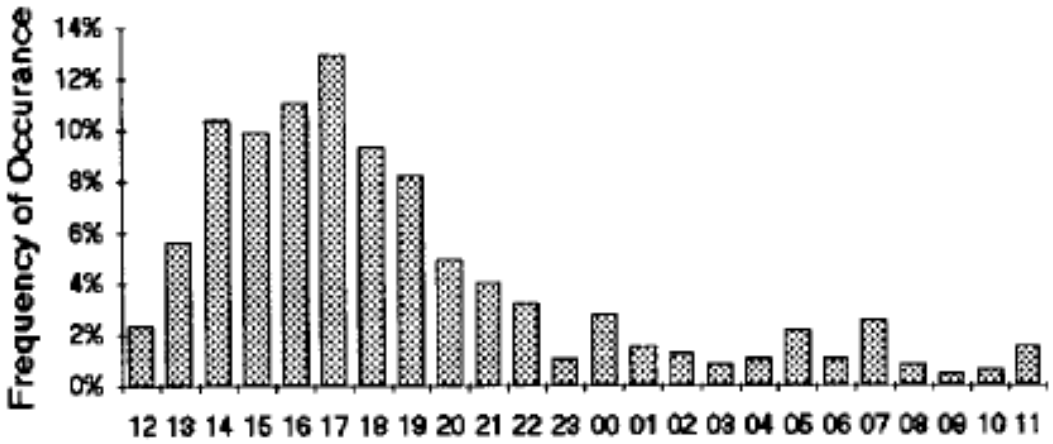

Figure 3.10: Hour of day of lightning caused outages on FPL transmission lines [Burnham, 1995]

Weather data from the South African Weather Service (SAWS) also indicates a high likelihood of lightning activity during summer afternoons [SAWS, 2010]. Summer rainfall in South Africa is generally associated with summer thunderstorms and lightning [Jandrell et al, 2009]. The lightning flash density maps for South Africa are presented in Appendix B.

According to Naidoo et al [2006], faults due to pollution and to bird streamers occur at similar times during the day. Pollution related flash-overs due to insulator contamination mainly occur in drier non-summer periods. The number of outages increases at night when humidity levels rise and reach a peak just before the sun rises. A review of transmission outages on the South African 200 and 400 kV network showed that pollution related failures occurred mainly between 2200 hrs and 0600 hrs as shown in Figure 3.11 [Bekker et al, 1999].

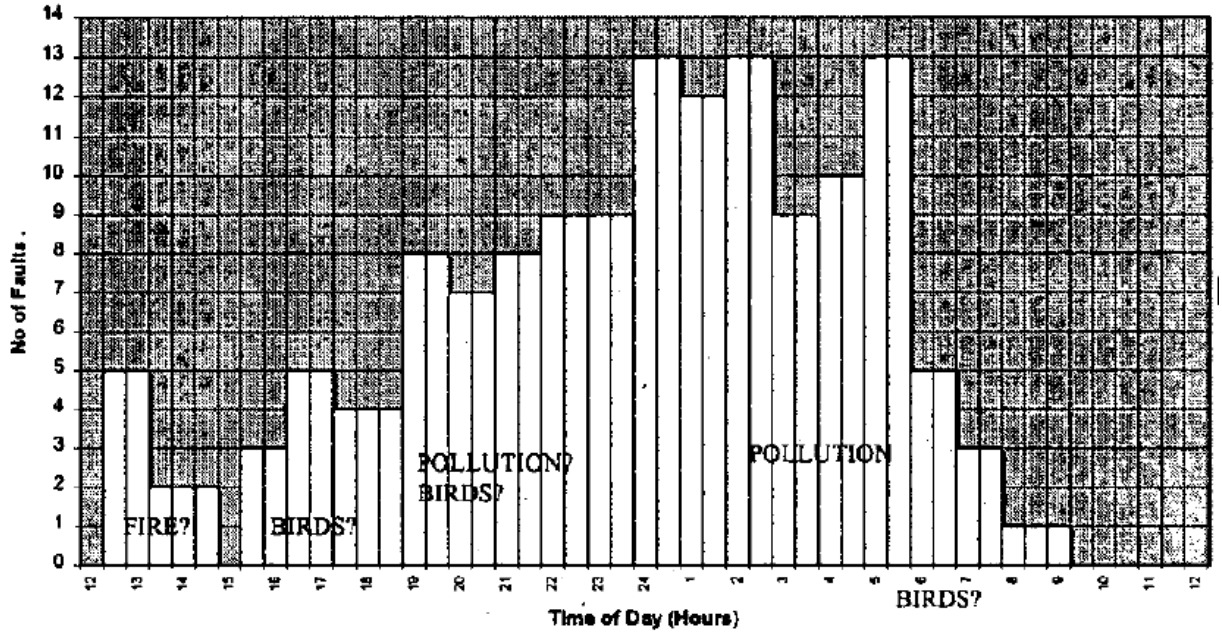

Figure 3.11: Histogram for fault times of South Africa's rogue transmission lines [Bekker et al, 1999]

Burnham [1995] indicated that recorded bird related outages occurred during the same time of day interval. The author deduced that the peak, in bird related outages, at 23:00 hrs occurred due to birds processing the last large meal of the day. The peak at 06:00 hrs was due to by birds not eliminating when asleep and eliminating large volumes upon waking.

3.4.1 Time-dependent characterization of South African transmission line failures

Minnaar et al [2012] performed an extensive analysis of fault records to identify the major causes of faults on the South African transmission network and their characteristics. Failure events occurring between 1993 and 2009 were considered and the failure data analyzed.

South Africa can be divided geographically into two areas indicating the dominant nature of rainfall activity that is present i.e. frontal and thunderstorm rainfall activity regions. More rainfall falls in the thunderstorm region. The South African power network is composed of transmission lines operated at voltage levels of 220 kV, 275 kV, 400 kV and 765 kV. However, lines operated at 400 kV comprise the bulk of the South African transmission system that is extensively exposed to both frontal and thunderstorm activity.

The failure data analyzed with respect to the geographical regions is shown in Table 3.3. The average fault frequency values depicted in Table 3.3 shows that lines within the summer rainfall area (thunderstorm region) have a higher fault frequency than those in the frontal region.

Table 3.3: Fault frequency statistics based on geographical regions [Minnaar et al, 2012]

Rainfall activity	Total line Length (km)	Average fault frequency (faults/100km/year	Standard Deviation
Thunderstorm	18,416	2.9	0.649
Frontal	7,906	1.6	0.265
Whole country	266,322	2.5	0.451

Figure 3.12 also illustrates the higher fault frequency, particularly for lines rated at 400 kV, in the thunderstorm region. Analysis of the data also showed that the network is mainly influenced by four external threats which include lightning, bush fires, pollution and birds.

Figure 3.13 depicts the fault frequency of 400 kV lines based on the identified failure causes and on the geographical regions. It is noted that bird streamers contribute most to line failures in both regions.

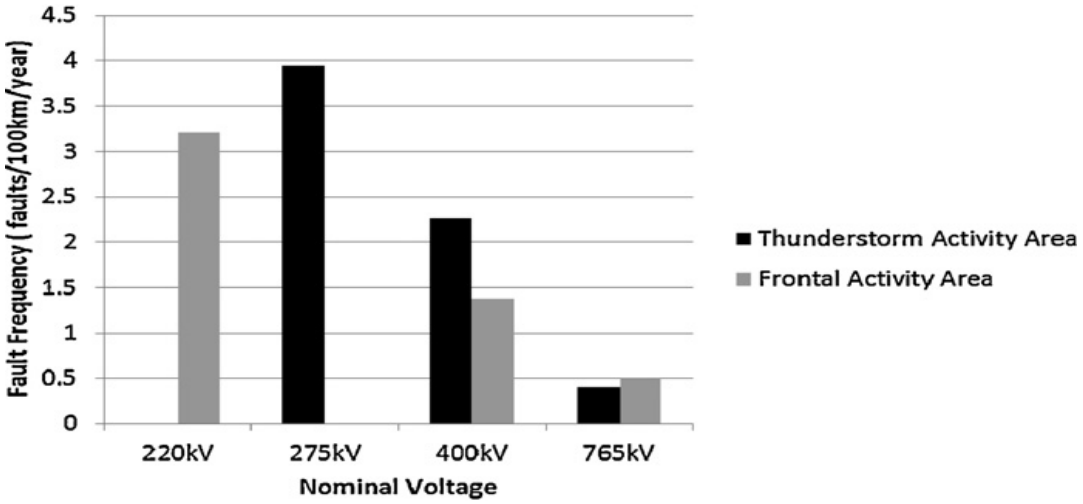

Figure 3.12: Average fault frequency per 100 km per year per rainfall activity area [Minnaar et al, 2012]

The fault frequency due to bird streamers in both regions is however high. Thus, the difference in rainfall patterns between the two regions does not significantly influence the likelihood of bird streamer line faults. The fault frequency statistics for other failure causes are however significantly different in each geographical region.

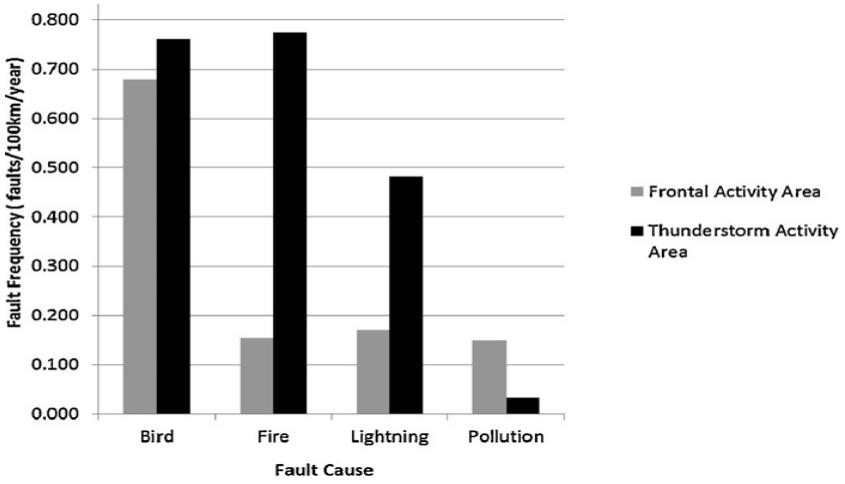

Figure 3.13: Average 400 kV line fault frequency by fault cause and geographical region [Minnaar et al, 2012]

To analyze the seasonal and time-of-day patterns associated with fault events due to each failure cause, the data collected was distributed into the 4X4 matrix proposed by Herman and Gaunt [2010]. Figure 3.14 provides a visual inspection of the frequency of line failure statistics for bird streamer faults. Quarter years and six hour intervals were considered by the authors.

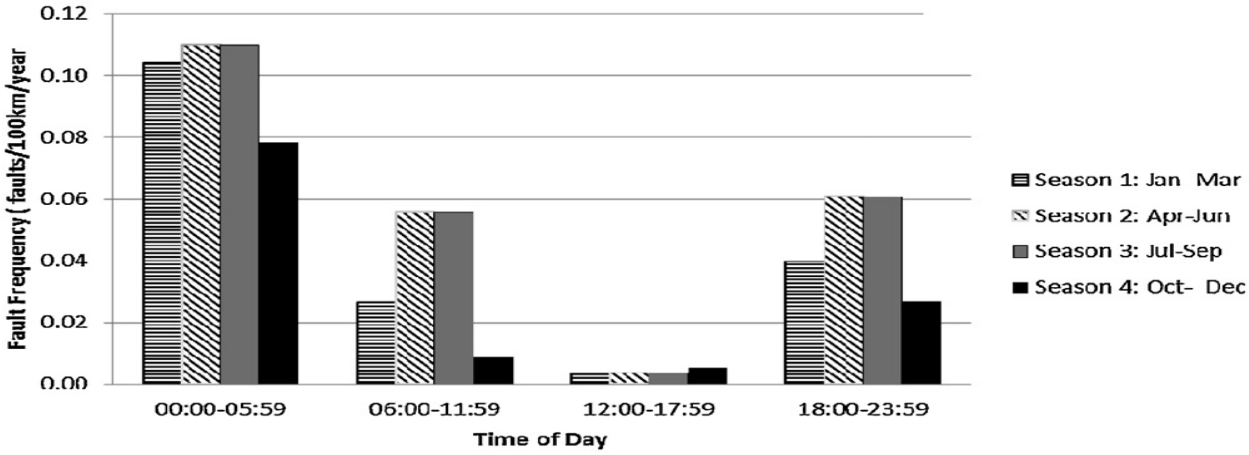

Figure 3.14: Seasonal and time-dependent frequency of bird streamer faults on South African 400kV lines [Minnaar et al, 2012]

3.5 SUMMARY

This chapter was able to answer some of the research questions. However, there is need to develop some aspects in literature further so that the hypothesis can be validated. The research questions addressed in the chapter include:

Qn.3: What block of a power network is required for this analysis?

Most of the literature encompassing reliability and adverse weather is limited to distribution power networks. Such networks are usually confined to one geographic area such that all network components are exposed to the same adverse weather element. The thesis will consider the effect of different adverse weather elements affecting the same component. Transmission lines traverse different geographical regions and as such are exposed to threats different adverse environment. A bulk power network will be considered for this thesis. The thesis will aim to adapt those reliability techniques developed that only apply when the effect of an external threat is localized.

Qn.4: What is the effect of external threats on bulk networks and what contingency approaches have been developed for modelling vulnerability of network components to external threats?

The chapter discussed the impact of exposure to adverse local and global space weather on bulk network facilities. The failure rate of components is a variable parameter. The local weather threats discussed result from different factors so that their occurrence and severity of impact within a given analysis period could also be variable. While different approaches have been proposed to model vulnerability of network component to external threats, time-independent approaches do not consider the time-of-occurrence of fault events. Failure parameters are modelled as time-varying quantities. The time-dependent models discussed in the chapter were mainly suited for network planning studies. Applying them to operational scenarios could yield misleading results. As far as the author is concerned, no modelling approach has been developed to capture threats geomagnetically induced currents (GICs).

Such threats could have either immediate or deferred effects on a component's failure. A flexible modelling approach, applicable to both planning and operational studies, is thus necessary. The matrix vulnerability model proposed by Herman and Gaunt [2010] has great potential in this regard. It however needs to be extended so that component parameters derived from historical data can be represented more realistically i.e. accounting for both dispersion and skewness in the failure parameter distributions.

Qn.5: How significantly do seasonal and time-of-day variations impact on component reliability parameters?

Different authors indicated that local weather threats have specific time-dependence and predominantly occur in certain seasons and times-of-day during the year. Minnaar et al [2012] showed that South African transmission line failures have a high season and time-dependency. The failure statistics (mean and variance) for the threats considered changed during the year. The use of PDFs to represent the statistics presented could highlight the variation in the failure statistics due to change in season and time-of-day.

3.5.1 Onward

The next chapter will develop a time-dependent probabilistic technique required for the analyses performed in this research. The chapter will:

- Extend the Herman and Gaunt [2010] vulnerability matrix model so that a more versatile PDF can be incorporated
- Investigate the suitability of the Beta PDF over the commonly used ones, for representing reliability data in the PDF-based matrix model.
- Present the methodology applied by the new techniques when developing PDF-based models for failure parameters
- Develop a new sequential MCS technique that will be used to apply the PDF-based matrix model.
- Test and analyze the performance of the time-dependent probabilistic technique using a published test network

4. DEVELOPING A TIME-DEPENDENT PROBABILISTIC APPROACH FOR RELIABILITY ANALYSIS

4.1 INTRODUCTION

Overhead lines, transformers and outdoor substations are strongly exposed to external risk factors so that they experience strongly seasonal and time-dependent failure rates [Bollen et al, 2008]. The reliability evaluation techniques identified in literature are however unable to realistically capture the induced variability in component failure rates. A time-dependent probabilistic approach (TDPA) is developed in this chapter. Unlike previous approaches, the approach will be able to:

- Simultaneously account for the effect of seasonal and time-of-day variations when developing network failure models.
- Realistically model historical data such that both the skewness and dispersion of their underlying distributions are considered at the input stage of a reliability analysis. The finite ranges that characterize such failure data should also be considered.
- Apply any distribution in the simulation process. The limiting requirement to develop the inverse transform for each distribution applied should be overcome. The approach should be able to apply the Beta distribution as input failure models.
- Perform similarly to or preferably better that the conventional sequential MCS. The potential of the approach for high computational efficiency should be high.

4.2 SUITABILITY OF THE BETA PROBABILITY DENSITY FUNCTION FOR RELIABILITY STUDIES

It is important to investigate how suitable the Beta PDF is for reliability analyses compared to other PDFs. Goodness-of-fit tests are carried out for this purpose. These tests match empirical frequencies to theoretical models and consist of absolute and relative measures. A graphical technique for evaluating goodness of fit is drawing a histogram and a PDF curve together.
Goodness-of-fit tests are thus used to determine whether a random sample comes from a particular distribution.

Three goodness-of-fit test methods are available: Chi-square (C-S), Kolmogorov-Smirnov (K-S) and Anderson-darling (A-D) tests [O'Connor, 2002]. Each test has different advantages and disadvantages and as such, used in specific applications; some are more suitable to large samples and others to small samples. The dispersion or distance tests are either based on the probability density functions or the cumulative distribution functions. The power of the tests to reject the null hypothesis, that a sample fits a certain distribution, varies with the number and type of data available, and the assumption being tested [O'Connor, 2002].

Preliminary work was carried out by Cross et al [2006] to investigate the possibility of using the Beta PDF to describe various parameters in the reliability analysis of power systems. The Kologomorov-Smirnov (K-S) method was used to compare the 'goodness-of-fit' achieved by several distributions, including the Beta distribution, when fitted to reliability data sets. The results showed that the Beta PDF is one of the best fits generally for reliability data sets. Cross et al [2006] also noted that the Beta PDF fitted better in cases where the tail of the distribution was in the direction of the minimum value of the data set. The K-S test is however suitable for analyzing the tails of distributions. The A-D test is a modification of the K-S and is thus also suitable for analyzing the tails of distributions. The C-S test however is dependent on the number of bins and thus provides a better analysis of the goodness-of-fit around the mean value of a given data set. A summary of the differences between the three tests is presented in Table 4.1.

Table 4.1: Summary of the characteristics of the Goodness of fit test

Characteristic	Kolmogorov Smirnov	Anderson Darling	Chi-Squared
Binning of data	No	No	Yes
Sample size	Small	Small	Large
Distribution specific	No	Yes	No
Considers tail of the distribution	No	Yes	No

To get a more rounded impression of how the Beta PDF compares to other commonly used ones, an analysis similar to that presented by Cross et al [2006] was carried.

Table 4.2 shows some typical inputs to a reliability analysis and the probability distributions commonly used to describe them.

Table 4.2: Probability distributions usually considered for reliability inputs

Parameter	Probability Distribution
Failure rate	Exponential
Restoration rate	Exponential, Lognormal, Weibull
Switching time	Uniform, Gaussian, Gamma, Lognormal, Poisson
Time to failure (TTF)	Exponential, Gamma, Gaussian, Lognormal, Poisson
Time to repair (TTR)	Exponential, Gamma, Gaussian, Lognormal, Poisson

Goel [2000] investigated the use of different PDFs in a distribution system reliability analysis. A component's TTF was assumed to be exponentially distributed while the TTR was described by exponential, lognormal, normal, and gamma distributions. This thesis proposes the use of the Beta in reliability analyses. The exponential PDF is however the most commonly applied function. The Beta PDF should thus be able to represent the same data sets as the exponential. Also, the results computed using either the exponential or the Beta PDF for reliability inputs should be comparable.

A key step in the conventional sequential MCS is the translation of randomly generated numbers into time variables. Given the Beta shape parameters and scaling factor of a component's TTF or TTR distribution, the Beta PDF-based TTF or TTR is generated in the MATLAB software package using (4.1).

$$T_j = betarnd(\alpha_j, \beta_j) * C_j \tag{4.1}$$

T_j : either TTF or TTR

C_j: scaling factor of either TTF or TTR data sets

betarnd(α,β): random number generator (0,1) from Beta PDF with shape parameters (α, β)

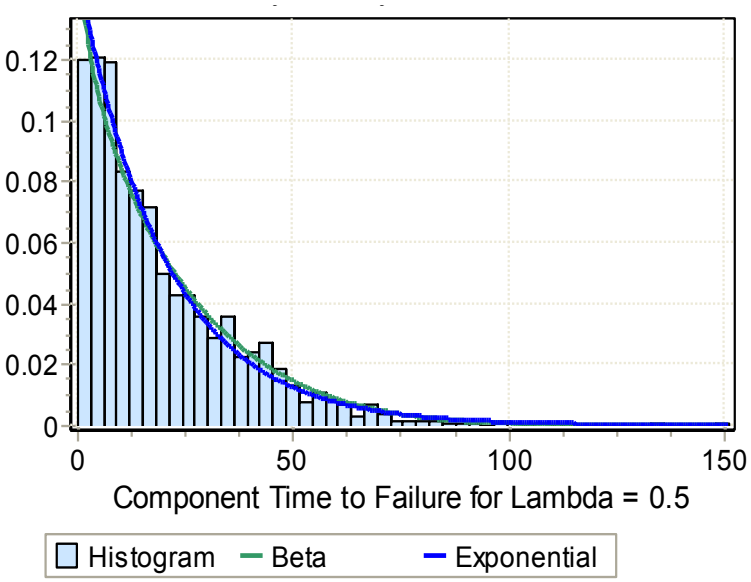

Figure 4.1: TTF data set fitted with exponential and Beta PDFs [Awodele et al, 2012]

Figure 4.1 shows a Beta PDF fitted to an exponentially distributed TTF data set using EasyFit software. The three Goodness of fit test were applied. Table 4.3 presents the results of the goodness-of-fit tests.

Table 4.3: Goodness-of-fit tests on distributions fitted to histogram of TTF data [Awodele et al, 2012]

PDF	Kolmogorov Smirnov		Anderson Darling		Chi-Squared	
	Statistic	Rank	Statistic	Rank	Statistic	Rank
Exponential	0.034	1	1.49	1	16.80	1
Beta	0.035	2	3.45	2	16.90	2

As expected the exponential PDF is ranked higher than the Beta PDF. It is however important to note that test statistics of the exponential and Beta PDFs, from the K-S and Chi-square tests, are very close. The difference in the test statistics derived from the A-D test could have resulted from the differences in the respective tail regions.

To validate the use of Beta PDF based TTFs and TTRs, Awodele et al [2012] performed a comparative analysis between results obtained using exponential and equivalent Beta PDFs to represent component failure parameters.

Component TTFs and TTRs were thus derived, in the MCS performed, using either the exponential inverse translations shown in (2.4) and (2.5) or the MATLAB function in (4.1). Figure 4.2 shows a comparison of one of the indices computed the different TTF PDF inputs. The index PDFs have the same range and almost overlap which indicated that the Beta PDF could be used in place of the exponential to represent component TTFs. Similar observations were made from other the load point indices computed.

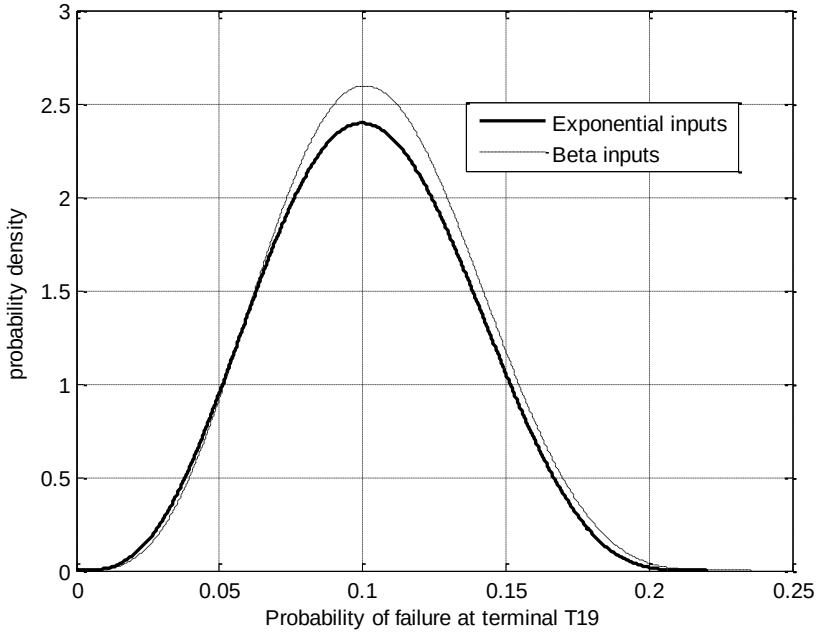

Figure 4.2: Probability of failure at load point for exponential and Beta represented reliability inputs [Awodele et al, 2012]

Awodele et al [2012] also checked the goodness of fit of the Beta PDF for the reliability index data sets computed. Figure 4.3 shows a histogram developed by Awodele et al [2012] from the frequency of failure data set computed for a load point and the Beta, gamma, lognormal and Weibull PDFs fitted. The results of the goodness-of-fit tests are presented in Table 4.4.

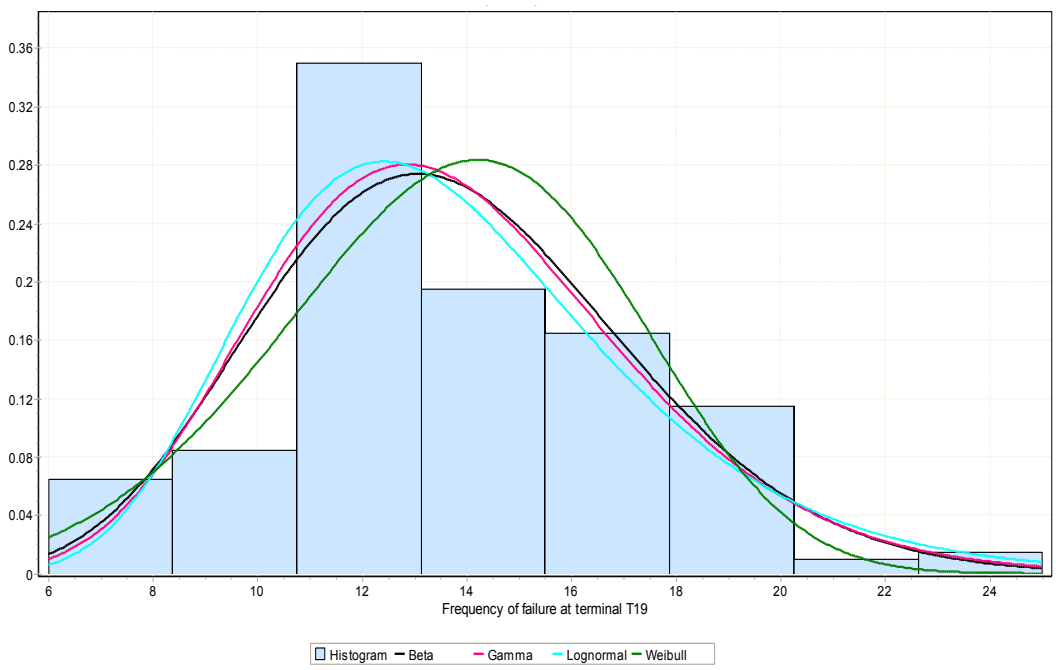

Figure 4.3: Histogram of Frequency of failure at a load terminal with fitted PDFs [Awodele et al, 2012]

Table 4.4: Goodness of fit tests on histogram of Frequency of failure at a load terminal

Distribution	Kolmogorov Smirnov		Anderson Darling		Chi-Squared	
	Statistic	Rank	Statistic	Rank	Statistic	Rank
Beta	0.07	1	0.59	1	10.18	1
Gamma	0.07	1	0.80	2	12.64	3
Lognormal	0.08	3	1.05	3	12.73	4
Weibull	0.10	4	1.37	4	10.91	2

With finitely ranged TTF and TTR inputs, the Beta PDF was ranked as the best fit of the frequency of failure index of the selected load point. The results also showed a high ranking attached to the Beta PDF for other load points and system indices computed.

4.3 METHODOLOGY APPLIED BY THE TDPA

This section will describe the methodology applied by the TDPA and identifies the key differences with the conventional sequential MCS.

Even though many adverse conditions are stochastic, with variable severity and duration, a season- and time-dependent pattern can be associated with their occurrence and the outages they cause [Minnaar et al, 2012]. In contrast to the conventional sequential MCS, the TDPA samples from PDF models of component failure data that simultaneously account for seasonal- and time-dependency. The TDPA simulates when and for how long component failures affect a network by randomly sampling from frequency and duration PDFs that characterize component failure events in a selected time window. These failure events define the chronological cycle for each component. During the rest of the time the component is in the up state.

4.3.1 Analysis of network failure data in terms of time windows

The Herman and Gaunt [2010] matrix model described in Section 3.3.2.1 is extended in this section. The model previously used the mean and standard deviation to represent component reliability parameters. Parameters representing the stochastic reliability (outage frequency or duration) of a component are expressed probabilistically in each cell using Beta PDFs. A scaling factor is thus introduced for this research. The scaling factor describes the range of a given component parameter data set in each matrix cell. Extreme events are not considered in the work presented here. As such, a given cell's scaling factor was determined as the maximum parameter value recorded in the cell. The matrix dimensions applied by Minnaar et al [2012] are considered here. The matrix is thus characterized by quarter-year seasons and daily variation over six-hour intervals as shown in Table 4.5.

The matrix model allows one to analyze historical failure data for different purposes. A matrix can be built with regard to a specific component, the whole network, a specific threat and/or geographical region. However each matrix relates to a specific reliability parameter such as frequency or duration of failure.

Table 4.5: TDPA 4X4 matrix model with Beta PDF shape parameters

Season (S)	Period (P)			
	0000-0559 hrs	**0600-1159 hrs**	**1200-1759 hrs**	**1800-2359 hrs**
January - March	$\alpha_{11}\ \beta_{11}\ C_{11}$	$\alpha_{12}\ \beta_{12}\ C_{12}$	$\alpha_{13}\ \beta_{13}\ C_{13}$	$\alpha_{14}\ \beta_{14}\ C_{14}$
April – June	$\alpha_{21}\ \beta_{21}\ C_{21}$	$\alpha_{22}\ \beta_{22}\ C_{22}$	$\alpha_{23}\ \beta_{23}\ C_{23}$	$\alpha_{24}\ \beta_{24}\ C_{24}$
July - September	$\alpha_{31}\ \beta_{31}\ C_{31}$	$\alpha_{32}\ \beta_{32}\ C_{32}$	$\alpha_{33}\ \beta_{33}\ C_{33}$	$\alpha_{34}\ \beta_{34}\ C_{34}$
October – December	$\alpha_{41}\ \beta_{41}\ C_{41}$	$\alpha_{42}\ \beta_{42}\ C_{42}$	$\alpha_{43}\ \beta_{43}\ C_{43}$	$\alpha_{44}\ \beta_{44}\ C_{44}$

α_{ij}, β_{ij}, C_{ij} : Beta PDF describing a component parameter in season i and time slot j

The dimensions of each matrix cell are dependent on the type of analysis i.e. either planning or operation. The component's failure data for a parameter is distributed into the different time windows. The failure data in a given time window (T_{pt}) is then categorized according to the failure causes that occurred in the T_{pt}. It is important to note that in practice, irrespective of the type of analysis, the dimension of a T_{pt} is limited by the availability of failure data required to populate the T_{pt}. The statistical parameters, mean and standard deviation are computed for each failure cause data set.

It may be necessary in some analyses to aggregate the data sets corresponding to each identified failure cause. Aggregated results can be regarded as the composite of the contributing failure data or sub-data sets. Composite data sets are required in planning analyses where two or more operational cells may need to be combined. Aggregation across the matrix enables the derivation of planning failure data sets from matrices describing operational failure data. For example, four quarter-year operational cells can be aggregated, along a matrix column, to yield an annual planning T_{pt}. The time slot is retained. With this type of aggregation the same reliability approach can be applied consistently to network planning and operation scenarios by evaluating different periods (e.g. 6 hours or a year) and even changing the component parameters to reflect their discrete adverse conditions.

Aggregation can also be performed within a given cell. The sub-data sets corresponding to the failure cause categories can be aggregated to yield a composite cell data set. This is applicable to cases where a given component is exposed to more than one of the failure causes occurring in the given cell. For example a transmission line may be exposed to more than one external threat simultaneously.

A new mean, standard deviation and maximum value is computed for the composite data sets. When developing aggregated data sets for long-term periods, the covariance between different external threats could be relevant; occurring due to the presence or absence of similar conditions [Minnaar et al, 2012]. The failure statistics (mean, standard deviation and scaling factor) of the composite data set are derived by aggregating the mean, standard deviation and maximum value of each sub-data set using (4.2), (4.3) and (4.4) [Papoulis, 1991; Leon-Garcia, 1994].

$$C_{composite} = \sum_{i=1}^{N}[M_i] \tag{4.2}$$

$$\sigma_{composite} = \sqrt{\left(\sum_{i=1}^{N} VAR[x_i] + \sum_{i=1}^{N}\sum_{j=\mathrm{i}+1}^{N} COV[\,x_i, x_j]\right)} \tag{4.3}$$

$$\mu_{composite} = \sum_{i=1}^{N} E[x_i] \tag{4.4}$$

$\mu_{composite}$, $\sigma_{composite}$: mean and standard deviation of composite data set

$C_{composite}$: scaling factor of composite data

M_i: maximum value of sub-data set i; ($i \in$ N)

COV [x_i, x_j]: covariance of variables x_i and x_j

Over long-term periods, the covariance between different failure causes could be relevant, due to the presence or absence of similar external conditions. Mostly, external failure causes such as birds, lightning and fires are unrelated and even occur predominantly in different seasons, so the failure events can be considered as independent.

The work presented in this thesis considers South African external conditions. South African weather conditions and patterns are geographically based [Minnaar et al, 2012]. As such, each external threat has a unique seasonal and time-of-day dependency such that they can be regarded as independent of each other. The use of the matrix model strengthens the independence between different threats, particularly in operational analyses. The second term in (4.3) can thus be disregarded to yield (4.5).

$$\sigma_{composite} = \sqrt{(\sum_{i=1}^{N} VAR[x_i])} \tag{4.5}$$

Discrete and stochastic modelling approaches evaluate failure rates for different seasons to cater for the effects of weather on a network. Seasonal variation is just one dimension of component failure dependency. The matrix model ensures that the independent effects of seasonal and time-of-day variations on network failures can be analyzed concurrently without extensive modelling. Further, the vulnerability models described in Section 3.3 were developed for specific applications i.e. either planning or operational studies. While the reliability data sets used in either analysis are the same, the methodologies required tend to be different. The matrix model applied in the TDPA ensures that a multi-dimensional approach can be applied to the analysis of component parameter data sets. By varying the dimensions of the TDPA matrix model, the same vulnerability modelling approach can be applied to either a planning or operational analysis. The failure data sets are however manipulated so as to take into account the dissimilar adverse conditions in planning and operation studies.

4.3.2 Deriving PDF models from failure data sets

With the network failure data distributed in the different windows of the matrix model, the statistical parameters (mean, standard deviation and maximum value) of each window are determined. These are then applied in the expressions (2.9) and (2.10) to derive the shape parameters of the required Beta PDF models.

For each component, a Beta PDF model is derived per failure parameter from a single or composite failure data set. The TDPA focuses on component down states and as such considers the frequency and duration of component failure. Frequency and duration of failure Beta PDFs are thus derived for each component in every T_{pt}. The Beta PDFs are derived from component failure data sets corresponding to the parameter being modelled.

The number of times a component fails in a T_{pt} during each TDPA simulation run is randomly selected from the component's Beta PDF frequency-of-failure model. The Beta PDF will represent the component's vulnerability to either a single failure cause or combination of multiple failure causes. The duration of each failure is randomly selected from a component's duration of failure Beta PDF. The duration-of-failure PDF model is derived for each time window in the same way as the frequency-of-failure model. This research is concerned with the most likely component reliability parameter values and corresponding reliability index values. The Beta PDF describing a given data set is thus scaled using the maximum value of the data set.

4.3.2.1 Network planning considerations when deriving TDPA failure models

Extensive historical data regarding network component outages, the root cause of each outage, time of outage occurrence and outage duration is usually required when developing models for planning purposes. For the TDPA, more sets of data are required. These could relate to:

Extensive historical data regarding network component outages, the root cause of each outage, time of outage occurrence and outage duration is required in developing models for long term or planning purposes. For the TDPA, more sets of data are required. These could relate to:

- Network configuration; such that components are assigned to geographical locations and specific network risk factors.
- Space and weather data; such that network outages are correlated with seasonal variations in space and weather.

- Restoration protocols; such that variation in restoration times are associated with time-dependent factors such as day of the week.
- Maintenance protocols; to capture network vulnerability and response to scheduled maintenance activities

The vulnerability of a given component to any external threat, on any given day is thus represented by the single composite PDF. In planning, data is collated over many years such that the PDF model derived would represent the 'average' vulnerability model for the analysis period i.e. the vulnerability model on a day with 'normal' external network conditions. Using the TDPA planning the same network threat PDF model is applied on every day of the time window. Each day of the time window thus has the same model for likelihood of failure assigned.

Using deterministic average values to describe a parameter infers that that the parameter will take on that value 100 % of the time. A PDF model however not only shows the range of values that a given parameter can take on, but also attaches a degree of confidence (or risk) to each value: The confidence that the actual parameter value will not exceed (or the risk that it will exceed) the value selected from the PDF. Deterministic average values are single risk values that allow for a 50-50 chance of exceedance. PDF models on the other hand allow selection of parameter values at various levels of confidence. Selecting the 50 percentile of a distribution is equivalent to selecting the value with 50 % level of confidence attached. For a Gaussian distribution, this value also corresponds to the average of the data set described by the PDF. When the distribution is skewed however, selecting the 50 percentile value yields the median of the distribution. Attaching confidence levels to values provides a means of quantifying the uncertainty in that value. To obtain the most likely value of a parameter, one would have to select values from a PDF at higher levels of confidence. A comparative analysis between the use of deterministic average values and PDFs for inputs in a planning reliability analysis will be presented later in the thesis.

4.3.2.2 Network Operation considerations when deriving TDPA failure models

The planning PDFs derived using the TDPA are to be regarded as the 'average' model for a given network threat. Reliability analysis for network operation is on a short-term basis i.e. months, days or hours. In a planning analysis, an overview of the network's reliability is required so that using 'average' vulnerability models and values may suffice. Intermittent network risks like adverse weather however vary considerably in short periods such that the single network risk models applied in planning may not be adequate for short-term time windows. The severity at which a given external threat is forecasted is thus very significant when modelling vulnerability of exposed network components.

It is well known that the impact of external threats on network components varies with geographical location. Adverse weather may not affect the entire transmission network simultaneously so that different transmission lines may experience different weather conditions. Billinton and Li [1991] developed a weather model that divides the network coverage area into geographical divisions. With the model, different sections of a single line may also be exposed to different weather conditions. The model however neglects the fact that different sections of a single line may be exposed to the same weather conditions but at varying levels of severity.

A case can be made for the analysis of network threats in terms of their level of severity. A number of factors that influence the likelihood and impact of lightning flashes have been identified. Some of these include the type of tower, location of transmission towers, type of lightning, and tower footing resistance. Procedures for calculating the risk of outages, based on these and other factors, due to lightning have been published [IEEE Guide, 1997]. Almeida et al [2009] however showed how variations in these factors impact on the lightning withstand performance of over-head lines in different sections of the Portuguese power system.

- Location of transmission tower: Each geographical area is characterized by specific weather conditions which directly relate to occurrence of lightning. No lightning, no risk of lightning over-current flash-overs. The higher the number of lightning flashes and ground flash density, the higher the likelihood of lightning related outages
- Type of lightning: The negative downward lightning strokes represent the majority of the lightning that affects the Portuguese transmission system [Almeida et al, 2009]
- Type of transmission tower: The heights of towers vary with the terrain geography. South African failure data shows that transmission lines at lower voltage levels are more predisposed to lightning flashes [Minnaar et al, 2012]. However, within the same overhead lines, several tower types can occur so that the risk of exposure is different
- Tower footing resistance: Measurement depends on, amongst other variables, the soil resistivity. While this varies from location to location due to geographical characteristics like soil type, during a year weather conditions like precipitation causes the soil resistivity and thus tower footing resistance, of a specific location, to vary climatically

The location of transmission lines and the activity in the areas through which the lines traverse can be used to categorize the severity of pollution related outages. Gençoğlu and Cebeci [2008] identify four levels of pollution severity; light, medium, heavy and very heavy pollution. The authors tabulated different levels of pollution and provided a description of some typical environments for each severity level. A similar table could be developed for other network threats. The table did not include the effect of time-of-day on the severity levels.
A correlation could be made with the daily activity pattern of say mining and the flash-over pattern of power lines within the mine's vicinity.

The concept of varying severity levels of external threats is not limited to local weather threats. The levels of GICs are significantly higher in networks located in the high-latitude regions such as Canada and Sweden. The values of GICs have also been known to vary in the different sections of a power network particularly due to change in the transmission line orientation and earth's resistivity [Molinsky, 2002].

The IEEE working group on Geomagnetic disturbances and Power system effects [1993] reported that "*there is also an important coastal effect resulting from induced ocean currents that must be continuous as they impinge on land masses where the resistivity is much higher; this effect will produce high values of earth-surface potential and GICs in power systems located in low conductivity regions that are close to some coastal areas.*"

Since operational risk assessment deals more with dynamic events, the models used should be as realistic as possible. The likelihood of external threats occurring at different levels of severity should be considered. The predominance of specific network threats in different time windows becomes evident under operational conditions. Table 4.6 shows the dominant network threat affecting operational time windows developed for the South African Transmission network. Table 4.6 is developed from collated failure data [Minnaar et al, 2012]. The failure patterns due to the threats presented in Table 4.6 are as described in Section 3.2.

Table 4.6: Dominant network threats affecting operational time windows

Season	Period			
	00:00–06:00 hrs	00:06–12:00 hrs	12:00–18:00 hrs	18:00–24:00 hrs
January-March	Birds	Pollution	Lightning	Lightning
April-June	Birds	Birds	Fire	Birds
July-September	Birds	Birds	Fire	Birds
October-December	Birds	Birds	Lightning	Lightning

Bhuiyan and Allan [1994] state that the behaviour of weather elements, occurrence and duration, impacts on the stress level each element imposes on the failure and repair processes of exposed components. Bhuiyan and Allan [1994] extended the weather model developed by Billinton and Li [1991] to transmission lines and computed the proportion of failures, of a given line, that occurred in different geographical regions. The fraction of a line exposed to a given set of conditions could thus be identified. A similar approach is applied by TDPA to derive operational vulnerability models.

The severity of a given external threat can be categorized based on a random parameter of the threat being investigated; wind speed and ground flash density for wind and lightning related failures. Each level of severity causes different levels of stress on an exposed line so that the number of failures is different. Appendix B shows the template developed by the IEEE data analysis task force [1994] for use in capturing overhead transmission line outage causes. While a significant range of outage cause categories were identified, no provision was made for variation in the severity of the stochastic outage causes. Correlation of metrological data and failure data would yield operational sub-failure data sets corresponding to each severity level. The correlation would show that the number of failures increased with the severity level of the external threat. One thus has to allow for say low and high extremes in the component vulnerability models developed for operational reliability analysis; Beta PDFs are derived for each severity level sub-data set.

To predict the severity level of an imminent threat, forecasts are carried out by monitoring and measuring specific parameters of the given external threat. A network threat will be predicted at a range of severity levels over the course of a day. Variations in daily weather forecasts or predictions of occurrence of storms testify to this. Not only do day-to-day recorded values change, daily forecasts also predict high and low readings per weather parameter. In practice, a threshold can be set. Depending on the severity level, sub-data sets can then be identified in the historical data.

The severity threat-level is thus identified depending on the margin by which the parameter of the threat being investigated exceeds the threshold value. The corresponding severity level Beta PDF is then assigned to components exposed to the threat. A composite network threat model can also be derived in operational analysis. However unlike in planning where aggregation was carried out along different cells, in operation the severity level sub-data sets are aggregated within a single cell. The corresponding composite cell PDF describes the expected (average) performance of a given line when exposed to the given external threat i.e. vulnerability on a normal day.

Three severity level models were defined for each external threat in this research; average, high and low severity level. Analysis of collected failure data, for an operational reliability analysis, would yield component failure models for low and high severity level failures. High severity levels are characterized by high frequency of interruptions and longer repairs. Low frequency of interruptions and short component repairs correspond to low severity level failure models. Low and high severity level models are aggregated to derive average severity level failure models. For such models the frequency and duration of interruptions are within the expected mean range. Table 4.6 showed that in the first quarter of the year between noon and 06:00 pm, lightning is the dominant threat.

In the planning approach, the same single PDF models will be applied on every day of the analysis period. Given the variability in short-term periods, operational analyses have to consider the duration of exposure of a component to a given threat or more importantly, to each severity level of the threat. Consider the first quarter of the year between noon and 06:00 pm. The same time window can be expanded, as shown in Table 4.7, to include each of the 91 days. The external threats occurring within the cell vary over the 91 days so that the severity of each threat and corresponding failures could be high or low on certain days within the time window; high number of failures on days when the severity level of a given threat is determined as high and vice versa.

Table 4.7: Expanded time window for period of 91 days between 12:00am and 06:00 pm

	12:00 – 18:00 hours																		
Season (91 days)	Day 1	Day 2	⋯															Day 90	Day 91

The duration of each severity level of a given threat can be determined by analyzing metrological data. According to the weather data collected from the South African Weather Service (SAWS), variation in weather parameters, in a specific location, is captured by recording the weather parameter values thrice a day [SAWS, 2010]. It is expected that the severity of a given weather parameter will have changed by the next reading. A given reading thus predicts

30 % of the day's weather. It was thus assumed for this research that for days, in the time window, with high severity level forecasts, the dominant threat is at high and low severity levels for 60 % and 30 % of the given day respectively. On other days, all external threats are simulated either at a low severity level or 'average' level for the whole day.

The portion of a component, particularly the length of a transmission line, exposed to each severity level on a given day within the time window should also be assessed. Distribution lines are confined to small geographical areas and one could apply a given risk model to their full lengths. Transmission lines traverse various regions and this was considered by Bhuiyan and Allan [1994]. The severity of a given external threat however also varies from location to location within a specific region. Instead of considering only the proportion of line failures in each geographical region, this analysis also considers the portion of the line exposed to each severity level of a threat. Figure 4.4 shows the section of a line (100 km) in a specific region and the portions of the line exposed to different severity levels of a given threat.

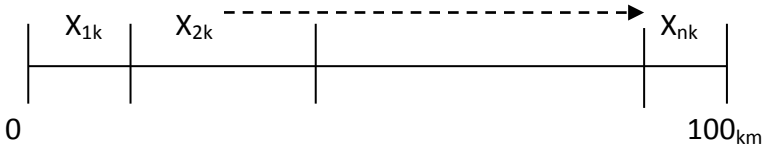

Figure 4.4: 100 km of a line exposed to a different severity levels of a given threat

X_{nk}: portion on line exposed to threat k at n^{th} severity level

For simplicity, the section of a line in a specific region was divided into four equal portions. The severity level models developed would thus be applied to the sections of line exposed to the specific threat affecting that portion of line. Depending on the storm, the portion of line exposed to a given severity level can change. For this research the quarter sections were maintained throughout the operational analysis. It was however assumed that the high severity level PDF model would always be applied to a quarter of the affected line on simulated days with the threat at high level of severity. On such days a uniform random number generator is used to apply either a low or average severity model to the rest of the line.

With the line fraction model proposed by Bhuiyan and Allan [1994], each line was regarded as a combination of series elements. Each element corresponded to a geographical region. The same principle is applied here. The total number of line failures is computed as the sum of the failures due to each severity level of a network threat. Figure 4.5 shows three severity level PDF for lightning related failures as applied to the entire network.

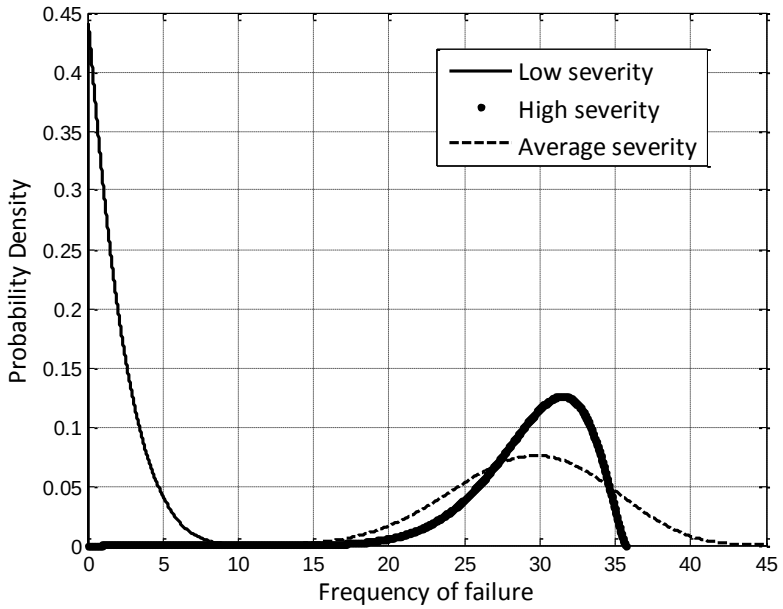

Figure 4.5: Severity-based Beta PDF models for lightning frequency of failure

The effect of the severity level PDFs on the likely maximum number of failures on different days is shown in Table 4.8 for lightning related failure. It is clear that the use of severity models, as opposed to the single risk models used in planning could yield higher failure frequencies.

Table 4.8: Maximum number of lightning related failures on different types of days

Type of day	Number of failures	
	Maximum (failures/severity level)	Total Maximum (failures/day)
High severity	35.7	(35.7X1) + (13X3) = 74.7
Low severity	13.0	(35.7X0) + (13X4) = 52
"Average" severity	48.7	48.7

The collated data used to develop planning reliability models is also used for operational reliability analysis. The data only has to be refined to include:

- Network risk severity classification; Historical data such as storm data needs to be categorized according to levels of severity e.g. low, medium and high storm level
- Forecasts for operational purposes, usually based on monitoring storm parameters, should be complemented with a likelihood of occurrence and duration index.

  A network operator thus knows the likelihood of a potential storm occurring and the expected duration. This would help categorize the storm and the relevant severity model can be applied to the affected components
- Network risk vulnerability; It is necessary to reclassify outage data according to the risk severity classes. This captures the network's response to variation in the risk severity levels such that the operational Beta PDF models developed are also risk-severity based
- Length of transmission lines; Transmission lines traverse great distances such that different portions of one line are exposed either to different network risks or, to different severity levels of a given risk. The failure data should be represented in per exposure length to ensure more accurate application of the vulnerability models

4.3.3 Simulation steps required by the TDPA

Section 2.3.2 presented the different techniques available for evaluating bulk network reliability. Sequential MCS is the most commonly applied technique. The prerequisite inverse translation limits the application of the method when distributions like the Beta PDF have to be used.

Also, the significant computation time associated with the approach makes the approach in its conventional form unsuitable for operational studies. This section presents a new simulation technique based on sequential MCS that can apply Beta PDF-based failure models. By contrast with the conventional sequential MCS, the TDPA samples from frequency and duration of failure PDFs and not the time-to failure and time-to-repair PDFs. No inverse translation is thus required.

A prerequisite to any network reliability analysis is the determination of the failure states of the network and its load points and, the combination of components whose outages contribute each state. A Failure Mode and Effect Analysis (FMEA) is usually incorporated in the reliability simulation for this purpose. A network power flow is one of the FMEA techniques available and was applied in the analyses performed. The power flow was however decoupled from the reliability analysis. This ensured that the computation time was only dependent on the reliability simulations. The network planning and operation simulation was thus performed in two parts: A network power flow and reliability simulation. This section describes how each simulation was performed.

4.3.3.1 Power flow analysis simulations

A power flow analysis is one of the methods commonly used to carry out adequacy analysis on a network. DIGSILENT software package was used for this purpose. The procedure included:

1) Build network in DIGSILENT and run power flow to ensure network is stable.
2) Run a Failure Mode and Effect analysis (FMEA) on the network. This analysis was used to determine the components in the network whose outage affects a particular load point. A component outage was simulated by taking it out of service.
3) The power flow was re-run to determine affected load points. Any failure state was recorded including the components and load points involved. A failure state was regarded as one that met the following conditions:
    - Capacity deficiency in the system due to component outage
    - Isolation of load points due to overloading of other network components
    - Voltage collapse at any system bus
    - MVAr limit violations detected
    - Failure of load flow to converge due to voltage and power limits
4) Reconnect component. Repeat steps 1-3 for all components.

4.3.3.2 TDPA reliability analysis simulation procedure

The MATLAB software package was used to develop the TDPA simulation technique. The simulation procedure is represented by 12 steps shown in the Figure 4.6 and described below:

1) Assume all components are in service i.e. up state. Simulation begins with an array of "ones" representing an only up-state life-cycle of a component. The approach only simulates component failure events (down states)
2) Select a component and a time window (T_{pt}). The dimension of each matrix cell depends on the type of analysis i.e. either planning or operation and represents a selected period (days, months, a year or longer or a climatic season) and the time/s of day.
3) Select the adverse conditions (C_i-C_N) that affect the component. Each time window takes into account only those failure causes a component is exposed to within the time window.
4) Aggregate the component frequency-of-failure data corresponding to each identified failure cause.

   4a. In planning studies, component failures may be affected by more than one failure cause, in which case the failure parameters for each cause are aggregated. A component's planning failure data set is derived either for a single failure cause e.g. FC_{ip} (μ_{ip}, σ_{ip}) or FC_{jp} (μ_{ip}, σ_{ip}) for failure causes i and j respectively or for multiple failure causes, FC_{ijp} (μ_{ijp}, σ_{ijp}).

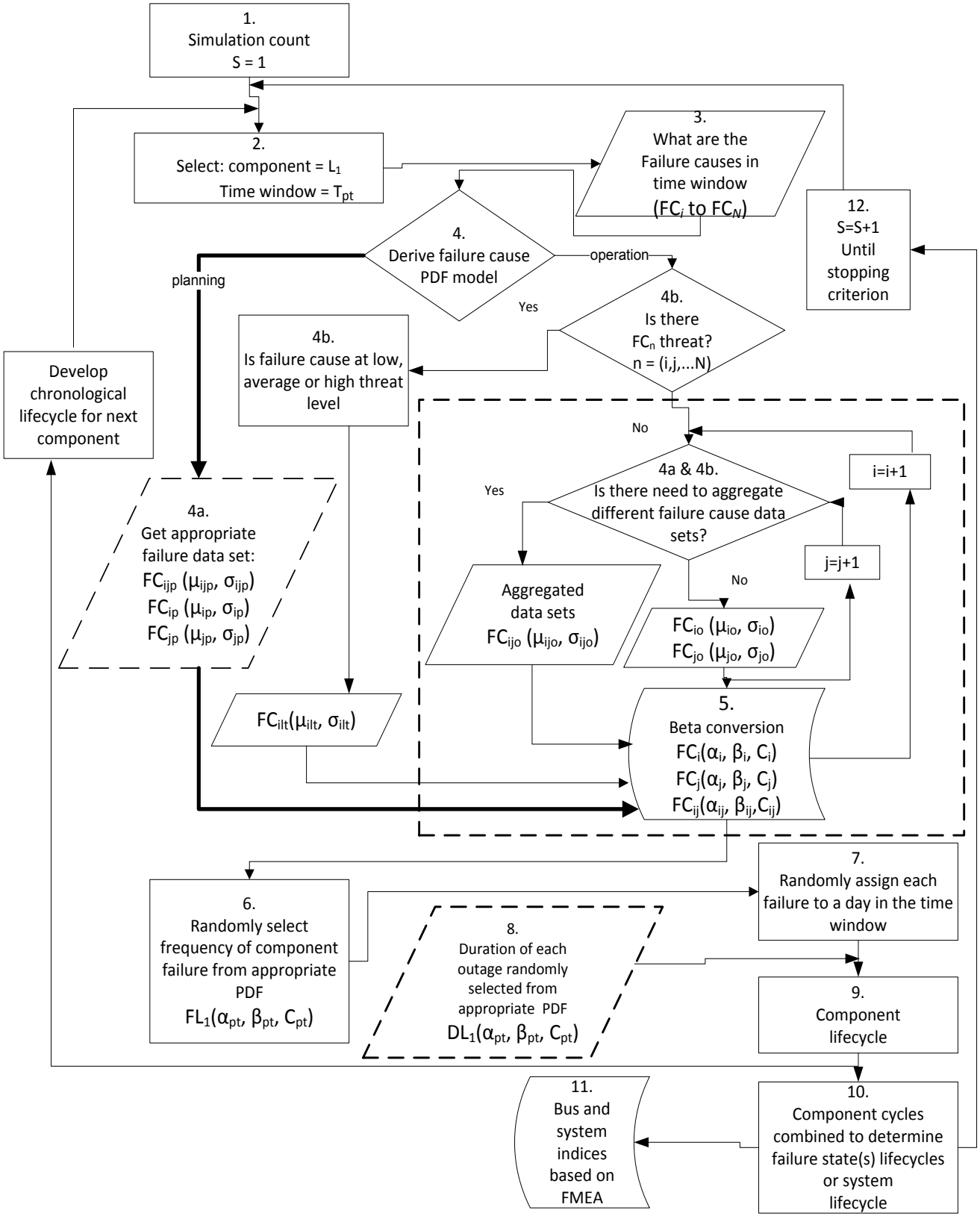

Figure 4.6: Flow chart representing TDPA simulation procedure

4b. For operational analysis an aggregated data set, FC_{ijo} (μ_{ijo}, σ_{ijo}) can also be derived for a component exposed to more than one failure cause. Additionally, the severity level of a given failure cause is considered in operational analysis. A component's exposure to a threat varies according to the prevailing conditions or the proximity of the component to the corridor of a moving threat such as fire or thunderstorms. Threat-severity-dependent failure data, FC_{ilt} (μ_{ilt}, σ_{ilt},), are derived from correlated historical weather data and failure data. As an example, dissimilar PDFs for high, low and average lightning threat level can be based on the failure data corresponding to high, low and average values of lightning ground flash density for a time window.

5) Derive the component's frequency of failure PDF, $FL_1(\alpha_{pt}, \beta_{pt}, C_{pt})$, from the appropriate failure data sets. The component's PDFs are derived from the failure statistics presented in the matrix cell identified using (2.9) and (2.10).

6) Generate the number of component failures in T_{pt}. The number of times a component fails in T_{pt} during each simulation run is randomly selected from $FL_1(\alpha_{pt}, \beta_{pt}, C_{pt})$. The Beta PDF represents the component's vulnerability to either a single cause (FC_n) or combination of multiple network risks (FC_{nm}) as given by (4.6).

$$FL_1(\alpha_{pt}, \beta_{pt}, C_{pt}) = \begin{cases} FC_{nq}(\alpha_{nq}, \beta_{nq}, C_{nq}) \\ \\ FC_{nmq}(\alpha_{nmq}, \beta_{nmq}, C_{nmq}) \end{cases} \quad (4.6)$$

n, m: failure cause index; n= (i, j, ……., N); m = (j, k,……., N)

N: total number of failure causes occurring in T_{pt}

q = either planning (p) or operation (o)

7) Randomly assign each failure event to a specific day within the analysis period using a uniform random generator.

8) Generate the duration of failure per event by randomly selecting from the component's duration of failure PDF, $DL_1(\alpha_{pt}, \beta_{pt}, C_{pt})$ aggregated and derived for each time window in the same way as for the component frequency-of-failure, depicted by the dashed lines in Figure 4.6.

9) Develop the component's chronological (up and down) state cycle for the analysis period. A failure event is represented by a string of bit zeroes. The length of a string depends on the duration sampled from $DL_1(\alpha_{pt}, \beta_{pt}, C_{pt})$. The number of strings depends on the failure frequency sampled from $FL_1(\alpha_{pt}, \beta_{pt}, C_{pt})$. The strings of bit "ones", in the component's original up-state lifecycle, corresponding to the failure days randomly selected are replaced by the string of zeroes to yield a new up-down lifecycle.
10) Repeat steps 2 to 9 for all components and combine the components' cycles to develop the system lifecycle and provide failure state cycles for different load points based on the FMEA analysis.
11) Analyze the system failure states to compute required load point and system reliability indices. Attach Beta PDFs to computed index data
12) The simulation is repeated until the coefficient of variation in a selected index is less than a specified threshold.

The same procedure is applied to both network planning and operation reliability analyses. The only variation in the procedures is the size of the matrix windows and the vulnerability models derived for a given component in each analysis. It should be noted that to improve the computation time of the simulation process, one could decide on a contingency level i.e. N-1, N-2 etc. As the contingency level increases, the number of components that influence failure within the network also increases. By predefining a contingency level at the FMEA stage, the number of failure states that would be yielded is reduced. This in turn reduces the number of component lifecycles that would be generated in the simulation process. This research investigates the most likely failure events in either a planning or operation analysis. Higher contingency levels that account for extreme failure events were thus not required.

The key differences between the conventional and TDPA based sequential MCS techniques are summarized below:

1) The conventional sequential MCS calculates the time-to-failure (TTF) during the simulation procedure. The exponential PDF is commonly used due to its simplistic inverse transform [Billinton & Sankarakrishnan, 1995]. While other PDFs have also been applied in subsequent sequential MCS applications [Goel, 2000], the Beta PDF has thus far been overlooked. This could be attributed to the complexity in deriving the Beta inverse transform. The TDPA does not calculate TTF and thus overcomes the need to derive the Beta inverse transform. The TDPA applies the Beta PDF to simulate the number and duration of failures in a period as well as randomness in the time of failure.
2) Conventional sequential MCS builds the chronological cycle of a component by simulating the TTF and TTR. It starts with the up state, and then adds each set of outage states for the total length of the analysis period e.g. 8760 hours. The TDPA builds the same chronology by simulating how many down states will appear (using the frequency of failure PDF), when each down states begins (using a uniform distribution for now) and how long each down state lasts (using the failure duration PDF). At all other times the system is in an up state, but these do not have to be calculated.
3) Chronology is easily identified when long-term periods are considered. Conventional sequential MCS is thus usually applied in planning studies to compute annual or annualized indices. The TDPA recognizes chronology based on either seasonal to time-of-day variations. It can thus be consistently applied to either planning or operation studies.

4.4 POTENTIAL LIMITATIONS OF THE TDPA

Allocation of failures in a time window: Failure data can be analyzed to determine the distribution or for this research the Beta PDF that represents the actual distribution of failure events within a time-window. This is a specification assigned during the collation of failure data and would contribute to a more comprehensive analysis of failure data. This set of data was not available for this thesis.

For illustration purposes a uniform distribution was applied so that this aspect has negligible influence on the variation induced in the results. The density of number of events is captured in the Beta PDF model derived for a given time window. It is expected that weekend and weekday variations mainly impact on the duration of a failure event and not its occurrence.

Accounting for failures that occur at the boundary of time windows: This aspect is dealt with during the collation of data. The time windows developed are flexible and vary depending on the network. The dimensions of the time-window are developed so as to capture those periods that have the highest density of failure events. A given time window thus reflects the periods in which the network is most vulnerable to the considered threats. The collator of failure data thus has to decide on the matrix dimensions and then the time window to which a given failure event is allocated. The TDPA is then applied based on the matrix and corresponding failure models developed.

Accounting for two down states overlapping for the same component: The TDPA derives the total number of failures occurring in a time window and then assigns them to different days in the time window. The thesis assumes more likely failure events so that each down state is not extreme. The length of each failure event is such that the next failure will find the component in an up-state. The repair times are thus sufficiently small that two down states do not overlap and the distribution of failures is dependent on the variability of the contributing network threat. The phenomenon may however be significant in operational studies that consider short-term windows lasting only a couple of hours. This is because the failure events would now be allocated on an hourly basis. The simulation procedure can however be adjusted so that the next failure event is assigned when the previous event has ended.

4.5 ANALYZING THE PERFORMANCE OF THE TDPA

This section will first test the performance of the TDPA on a published test system and compare it to that of the conventional sequential MCS approach. The effect of aggregating input failure data sets on a reliability study will also be analyzed.

Various reference networks exist for testing reliability techniques and models. According to Billinton et al [1989], "*a technique, however elegant it may be, should first be applied to a small system which can be easily solved and appreciated by the student using hand calculations before being extended to computer development."* For this reason, Billinton et al [1989] came up with the Roy Billinton Test System (RBTS) shown in Figure 4.7.

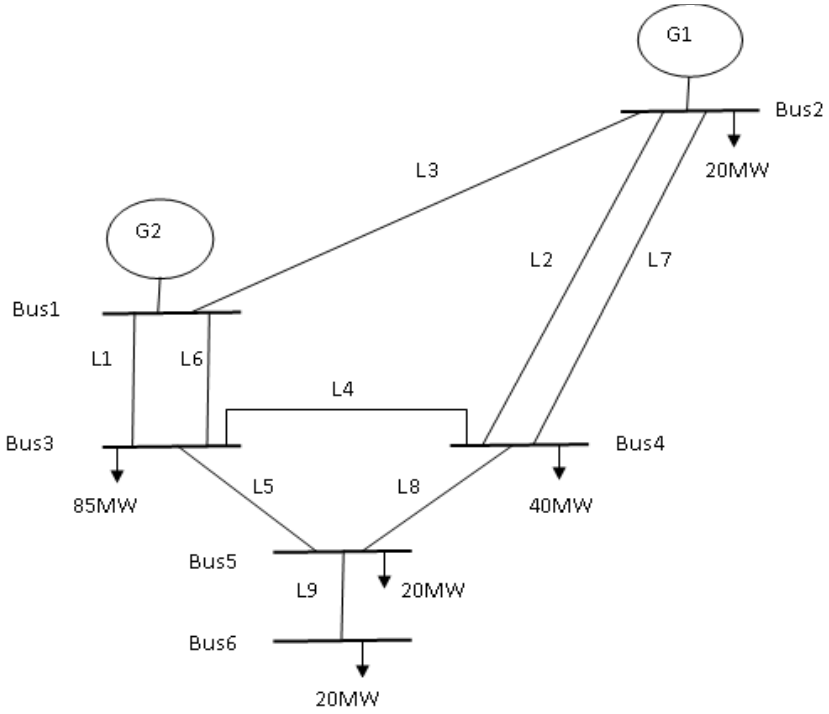

Figure 4.7: Roy Billinton Test system [Billinton et al, 1989]

It is simple enough to enable easy application and comparison of different techniques but still ensures that the studies have enough detail to reflect the actual complexities involved in practical reliability analysis. The results published in literature for the RBTS provide a benchmark against which the TPDA can be assessed.

Three case studies are investigated on the test system. The case studies analyzed were developed based on the models of failure parameters typically inputted in a reliability simulation. The case studies include:

- Base case: Constant input failure parameters
- Case two: Impact of dispersion in input failure parameter PDFs
- Case three: TDPA with practical (skewed) Beta PDF shapes

4.4.1 Base case: Constant input failure parameters

The conventional sequential MCS and the TDPA use different processes to develop the required chronological cycles for a sequential MCS. The SDM uses an inverse translation function to derive time to failure and repair parameters. The TDPA, as described in Section 4.3, however develops frequency and duration of failure PDFs. When the same failure data sets are considered, the two methods should be able to yield the similar results. This base case study was thus used to determine if the TDPA can replicate an analysis previously performed using the conventional sequential MCS. The base case thus validates the TDPA simulation by comparing its computed results against those from the conventional sequential MCS. To validate the TDPA based simulation, it should yield results similar to those computed by the conventional sequential MCS when applied to the same system. It was thus necessary to replicate the same conditions or reliability inputs considered by the conventional sequential MCS. With reference to the RBTS this included:

- The conventional sequential MCS when applied to the RBTS considered an annual analysis [Billinton & Sankarakrishnan, 1995; Li, 2003]. The time window considered by the TDPA has a period of one year and 24 hour time slot.
- The conventional sequential analysis considered deterministic (average) values for the RBTS component failure rate and repair duration [Billinton & Sankarakrishnan, 1995; Li, 2003]. The TDPA analysis developed symmetrical Beta PDF models from failure rate and repair duration data sets that have average values corresponding to those used in the conventional MCS analysis.

The outage frequency and duration parameters of RBTS components are presented as deterministic values (average) [Billinton & Tang, 2004]. The conventional sequential MCS would thus use the exponential PDF to describe the corresponding TTFs and TTRs. To represent the same deterministic averages value in the TDPA, a symmetrical ($\alpha = \beta$) Beta PDF with the same mean and a scaling factor equal to twice the mean is required.

Finally, a deterministic value can be represented by increasing the values of α and β so that the variance tends to zero, essentially making the PDF a spike, as illustrated in Figure 4.8. With the same mean and scaling value, the width of the PDF reduces.

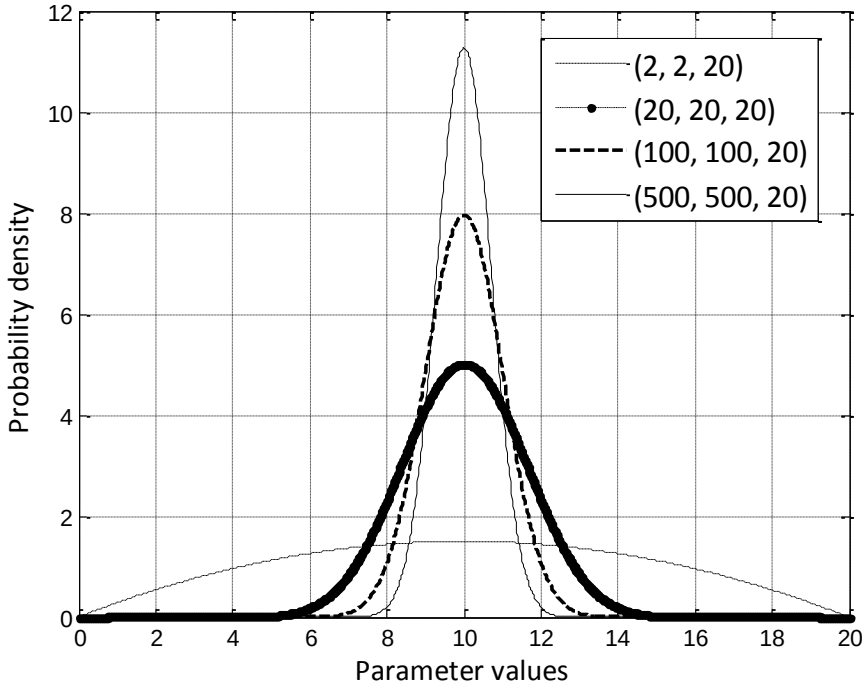

Figure 4.8: Gaussian-shaped Beta PDFs used in TDPA analysis

The Beta PDF with (α, β, C) = (500, 500, 20) is spike-like with a variance of 0.03. It is used in the TDPA base case to represent the average values of the failure and repair parameters of the RBTS. The average component failure rates and repair durations applied in each sequential MCS analysis are presented in Table 4.9, together with the corresponding scaling values required for the symmetrical Beta PDFs. While the standard deviation of a Beta PDF varies with the scaling factor, the coefficient of variation is maintained for a given set of shape parameters (α, β). Using the same set of (α, β) parameters ensured that the same level of 'spikiness' was applied to the components in Table 4.9.

The simulation reduction technique based on the covariance [Billinton & Li, 1994] was applied by both techniques. Three key aspects affect results computed from different analyses; the load point priority order, contingency level applied in the FMEA and the simulation stopping criterion.

Table 4.9: Inputs used in TDPA and conventional sequential MCS

Load point	Component	Conventional sequential and TDPA		TDPA	
		Average values		Scaling factor for Gaussian shaped PDFs	
		Failures (1/yr)	*Repair (hours)*	*Failures (1/yr)*	*Repair (hours)*
	L5,L8, L9	1	10	2	20
1 - 3	L1, L6	1.5	10	3	20
2	G20X4	2.4	55	4.8	110
2	G40	3	60	6	120
1	G20	5	45	10	90
2 - 4	L2, L7	5	10	10	20
1	(G40X2)	6	45	12	90

The load point indices computed by different analyses depends on the load point priority order assigned. The load shedding protocol has a significant impact on load point indices. A load point priority order is usually specified to guide the load shedding. The Interrupted Energy Assessment Rate (IEAR) index for each load point was used to determine the RBTS load point priority order presented in Table 4.10 [Billinton & Tang, 2004].

Table 4.10: IEAR index values for the RBTS load pointes [Billinton & Tang, 2004]

System load point number	IEAR($/kWh)	Priority order
2	7.41	1
3	2.69	5
4	6.78	2
5	4.82	3
6	3.63	4

System indices are not affected by the priority order but by the stopping criterion considered in the simulation process. The contingency level affects both load point and system indices.

The analysis considered an annualized load of 185 MW and a maximum of three simultaneous component outages in the FMEA. The RBTS indices computed, for an annualized system load, are available in literature [Billinton & Li, 1994; Li, 2003]. Billinton and Li [1994] considered a 6 % stopping criterion with no defined load priority order. The same priority order shown in Table 4.10 was applied by Li [2003] and a limit of 2,000,000 simulation runs specified.

The reliability indices computed for load point 6 and the overall system include the Probability of Load Curtailment (PLC) and Expected Frequency of Load Curtailment (EFLC) [Billinton & Kumar, 1990]. Table 4.11 shows a comparison of the system index values computed using the TDPA and those presented in literature. The TDPA results are computed for a 6 % stopping criterion.

Table 4.11: System reliability indices computed using the two sequential MCS techniques

Index	Conventional MCS [Billinton & Sankarakrishnan, 1995]	Conventional MCS [Li, 2003]	TDPA MCS
PLC	0.0099	0.0099	0.0098
EFLC (1/yr)	4.1	5.3	4.2
Simulation runs	150	2,000,000	78
CPU (seconds)	733	-	4.9

Load point 6 index values computed with the TDPA, for different stopping criteria, are compared with values presented by Li [2003] in Table 4.12.

Table 4.12: Comparison of load point 6 index values

Index	Conventional MCS [Li, 2003]	TDPA MCS (6%)	TDPA MCS (1%)
PLC	0.0014	0.0016	0.0015
EFLC (1/yr)	1.3	1.1	1.1
Simulation runs	2,000,000	78	2880

Tables 4.12 and 4.13 show that the TDPA index values are close to those presented in literature for the system and load point 6.

One can thus conclude that the TDPA was able to replicate the conventional sequential MCS analysis. It is important to state that the SUN and MECORE reliability software were used in Billinton and Sankarakrishnan [1995] and Li [2003] respectively. It is thus possible that higher contingency levels were considered which would mainly affect the EFLC index. It is also important to note that the Li [2003] states that 2,000,000 runs were deemed sufficient for simulation convergence. This could be a specification of the software used or due to application of a different simulation reduction technique.

Figure 4.9 shows the variation in the average PLC index value computed for load point 6 using the conventional and TDPA based sequential MCS techniques and a stopping criterion of 1 %. The rate of simulation convergence is influenced by the variability induced in the index computation. In the conventional sequential MCS, a component's up and down state lengths are derived from TTF and TTR PDFs with an infinite range. The conventional sequential MCS could thus yield extreme values which would disrupt the convergence process. The TDPA on the other hand, limits the down state durations to finite ranges which ensures that less variability is achieved in the computed index.

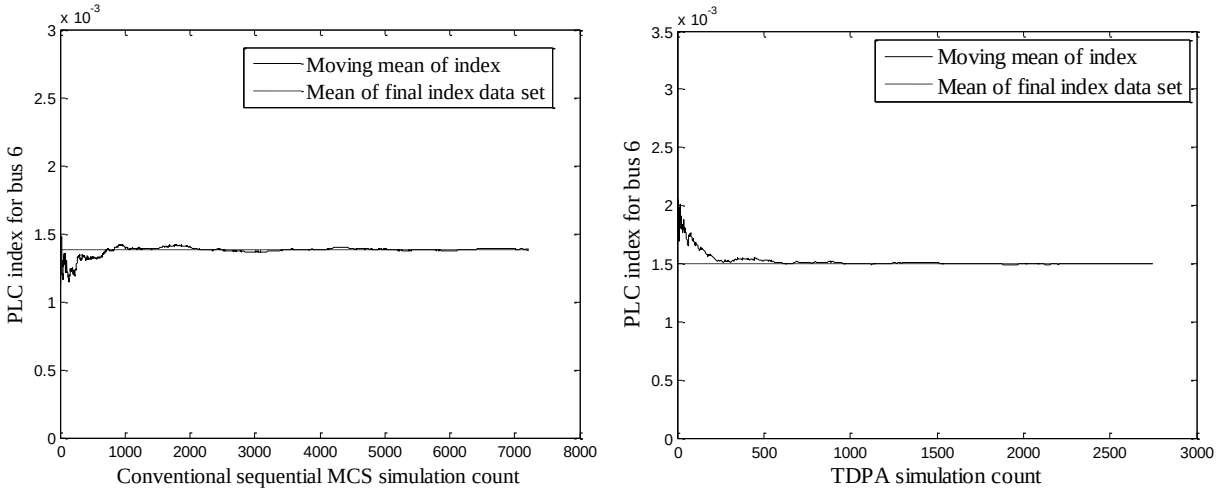

(a) **(b)**

Figure 4.9: Convergence of load point 6 PLC index for (a) Conventional sequential MCS (b) TDPA sequential MCS

Figure 4.9 shows that for the same simulation conditions the TDPA converged faster than the conventional sequential MCS. For a stopping criterion of 1 %, the conventional sequential MCS required more than double the number of simulation runs to reach convergence. The simulation computation time is a function of the number of simulation runs. While the two sequential MCS techniques yielded similar results, the TDPA appears to be significantly faster.

4.4.2 Case two: Impact of dispersion in input failure parameter PDFs

In reality, reliability parameters are not constant values. Variability in the parameters can be captured through the dispersion and skewness of the PDFs representing them. This section will test the impact of PDF dispersion on the performance of the TDPA. Figure 4.8 showed the symmetrical PDFs applied to modelling the reliability inputs i.e. component failure rates and repair durations. They have the same mean (10 hours) and scaling factor (20 hours). However, the variance about the mean is different, being 5.02, 0.61, 0.5 and 0.03 for the PDFs with shape parameters (2,2), (20,20), (100,100) and (500,500) respectively. The RBTS reliability analysis was performed using each of the Gaussian-shaped Beta PDFs as input models. The computed average load point and system indices are presented in Tables 4.13 and 4.14, using the same stopping criterion of 1 %.

Table 4.13: Reliability indices computed for load point 6

Index	**TDPA results for different Beta shape parameters**			
	(2,2,C)	*(20,20,C)*	*(100,100,C)*	*(500,500,C)*
PLC	0.0016	0.0015	0.0015	0.0015
EFLC (1/yr)	1.13	1.11	1.11	1.10

Table 4.14: System reliability indices

Index	**TDPA results for different Beta shape parameters**			
	(2,2,C)	*(20,20,C)*	*(100,100,C)*	*(500,500,C)*
PLC	0.0094	0.0099	0.0096	0.0093
EFLC (1/yr)	4.0	4.0	3.8	3.5

The indices computed change as the dispersion of the input PDFs is reduced. This is particularly evident from the system indices. To capture any underlying trend, more PDFs were considered. The level of 'spikiness' varied between that of the (2,2,C) and (500,500,C) Beta PDFs. Figure 4.10 shows the variation in the system PLC index as the dispersion of the Beta input PDF shapes is reduced. The indices were computed for different stopping criteria: 1 % and 0.1 %.

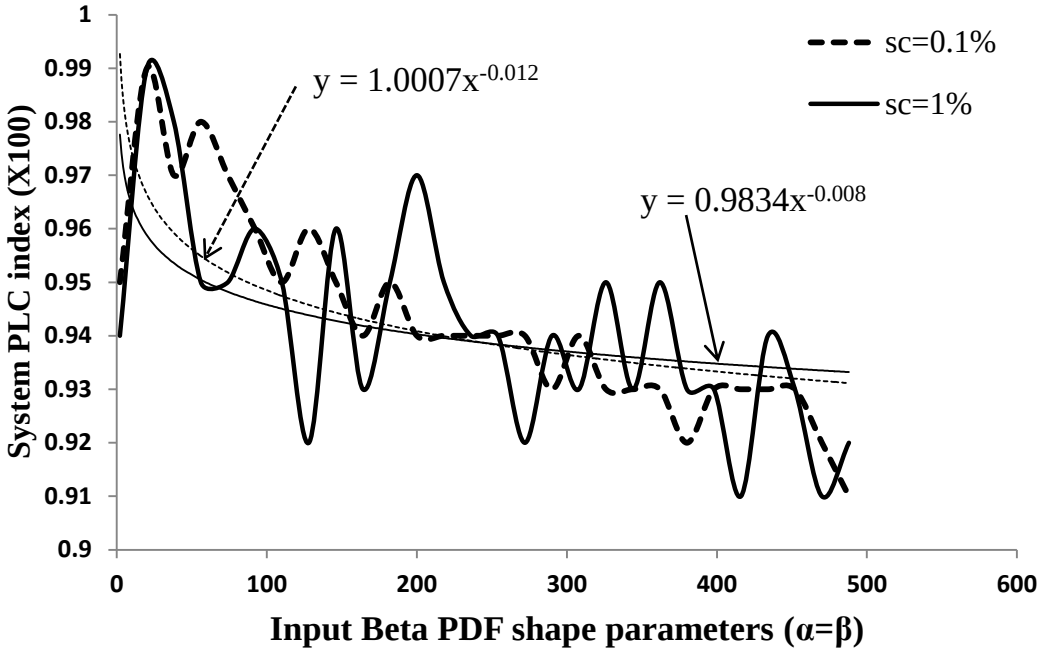

Figure 4.10: Variation in index values due to reduction in input PDF dispersion

Figure 4.10 clearly shows that the indices computed are influenced by the level of dispersion in the input PDFs. The variability in the index value is also affected by the stopping criterion. The indices computed are more variable when a higher stopping criterion is applied. The fitted trend lines indicate that as the dispersion is reduced, the index values computed tend towards that value computed with the least level of dispersion. This trend is noted for results computed for either a 1 % or 0.1 % stopping criterion. The results presented in Figure 4.10 show that it is not sufficient to represent reliability inputs using only average values. The input PDFs had the same mean but different index values were computed. The TDPA analysis showed that as the input representation was improved (spike-like PDF achieved), the indices computed tended towards a single value.

The fitted trend lines in Figure 4.10 tend towards similar index values at the point α = β = 500. Tables 4.15 and 4.16 show the system indices computed for different stopping criterion values. Table 4.15 was developed for the Beta PDF of (α, β) = (500, 500) and shows that index values computed using the TDPA, corresponding to different stopping criteria, are significantly close.

Table 4.15: Variation in system indices due to reduction in stopping criterion (α=β= 500)

Stopping criterion	**1** %	**0.1** %	**0.01** %
PLC	0.0093	0.0091	0.0092
EFLC (1/yr)	3.5	3.4	3.4

Table 4.16: Variation in system indices due to reduction in stopping criterion (α=β= 20)

Stopping criterion	**1** %	**0.1** %	**0.01** %
PLC	0.0097	0.0099	0.0098
EFLC (1/yr)	3.9	4.0	3.9

One could attribute this to the application of spike-like PDFs which as shown previously, yields indices closer to those computed from the conventional sequential MCS. Table 4.16, developed using PDF inputs with more dispersion around the mean i.e. (α, β) = (20, 20), however presents a similar internal observation. While the index values are higher than those presented in Table 4.15, the indices presented in each column of Table 4.16 are quite similar.

The significance of a stopping criterion to MCS based analysis cannot be discounted. For example, a stopping criterion of 6 % is quite high and as such, the indices computed would be quite variable due to a lack of convergence. The results in Tables 4.15 and 4.16 indicate that TDPA results depend significantly on the representation of the reliability inputs. For stopping criteria lower than 1 %, the simulation converged to more or less the same value. This is quite significant since a lower stopping criterion is associated with more simulation runs and thus, longer computation times.

4.4.3 Case three: TDPA with practical Beta PDF shapes

Section 2.4 discussed the need to account for variability in component parameters so as to achieve more practical and realistic reliability models. In this section the effect of using practical component failure data represented by skewed Beta PDF models (with high variance about the mean) is investigated.

The TDPA analysis presented in this section was performed with failure rate and repair duration Beta PDFs based on real failure data collected on the South African power network [Minnaar et al, 2012]. The statistics presented for bird related failures affecting 275 kV transmission lines were considered. The Beta PDF derived from the statistics was applied to the lines of the RBTS. The seasonal based data sets were aggregated to yield an annual data set. The normalized annual frequency of the line failure PDF is shown in Figure 4.11, together with the normalized duration of repair Beta PDF applied to all components. The right-skewed repair duration Beta PDF is similar to a lognormal distribution. Still using the RBTS network data, the generator failure rate PDF was maintained as a symmetrical Beta PDF with $(\alpha,\beta) = (500,500)$.

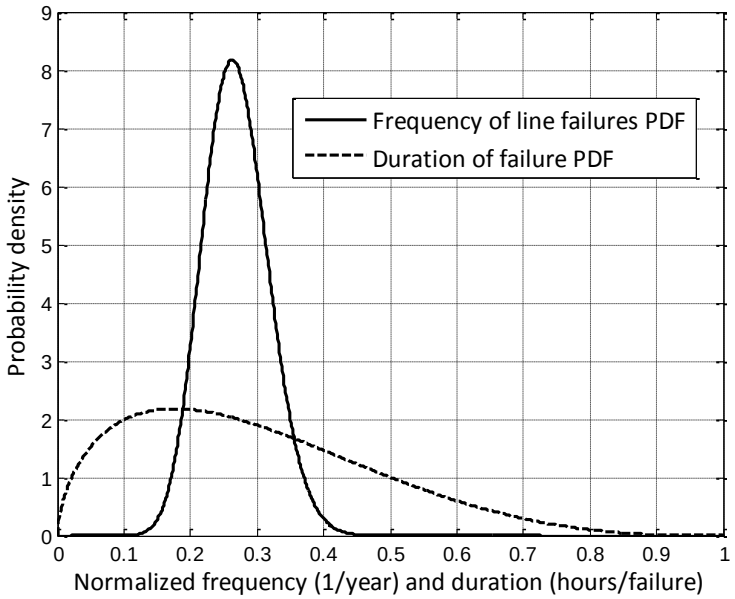

Figure 4.11: Bird related transmission failure PDFs based on South African data

The line failure rates were represented by the practical failure data, scaled so that the RBTS average line failure rates shown in Table 4.9 were maintained.

A comparison of the scaling factors applied to the Gaussian and practical Beta PDF shapes is presented in Table 4.17, for line failure rates, and Table 4.18 for repair duration.

Table 4.17: Corresponding scaling factors for different Beta PDF inputs (failure rates)

Model	Line failure rates (1/year)			
RBTS mean values	1	1.5	4	5
Spike-like PDFs (α,β) = (500,500)	2	3	8	10
Practical PDFs (α,β) = (20,66)	3.5	5	13.2	16.5

Table 4.18: Corresponding scaling factors for different Beta PDF inputs (repair duration)

Model	Component repair duration (hours)		
	Lines	*Generators*	
RBTS mean values	10	45	55
Spike-like PDFs (α,β) = (500,500)	20	90	110
Practical PDFs (α,β) = (1.6,3.8)	34	151.9	185.6

The system indices computed using the TDPA with practical PDF inputs are presented in Table 4.19. A stopping criterion of 1 % was considered. The indices are higher than those previously computed when the symmetrical shaped (α,β) = (500,500) PDF was applied.

Table 4.19: Comparison of TDPA results for different Beta PDF inputs

System index	Symmetrical	Practical, skewed
PLC	0.0093	0.0095
EFLC (1/yr)	3.5	4.1

The variation in the mean of the load point 6's PLC index is shown in Figure 4.12. An increase, not only in the mean of the index (0.00165), but also in the number of simulations required for convergence (3500) is indicated.

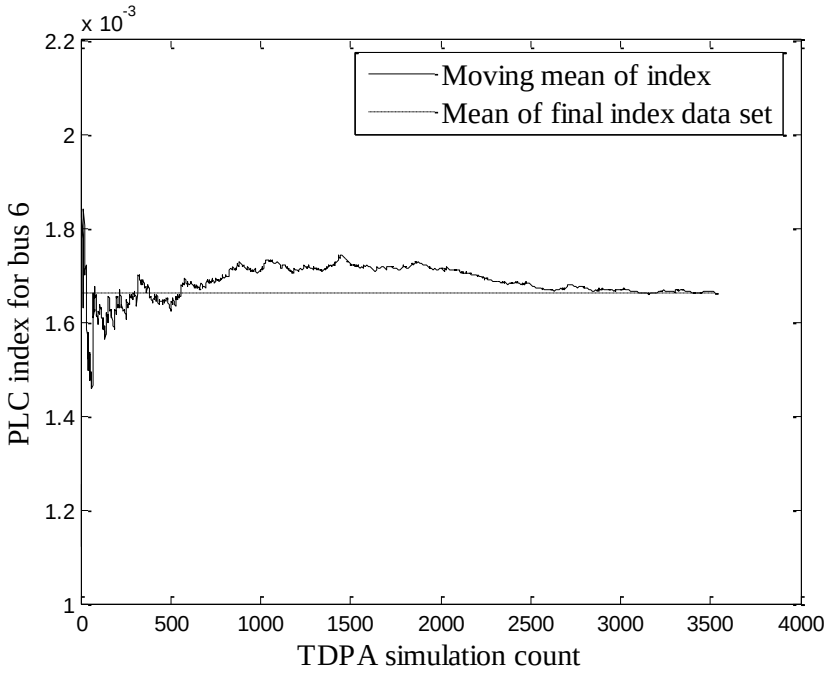

Figure 4.12: Variation in mean PLC index for bus 3 with practical Beta PDF inputs

Representing computed system indices as PDFs instead of simple average values (spikes) illustrates the effect of practical variability. Instead of determining the average values, PDFs were fitted to the index data sets computed from each simulation. The results are shown in Figure 4.13 for the system probability and frequency of load curtailment.

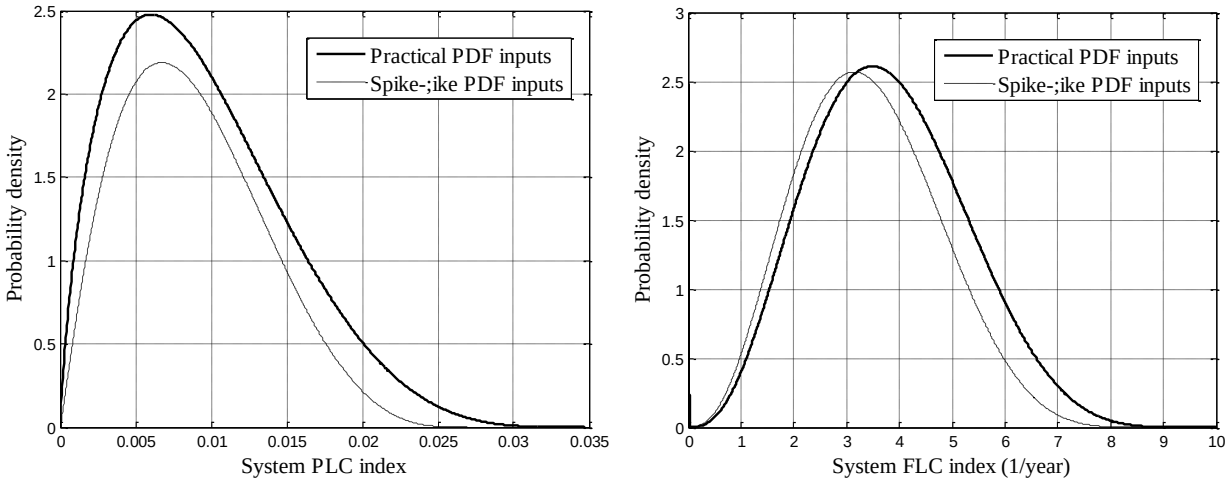

Figure 4.13: (a) Frequency and (b) duration of system load curtailment computed with deterministic (symmetrical, small variance) and practical PDFs as inputs

The skewness of the computed index distributions is clearly affected by the failure parameter models used (input PDFs). When the skewness of a probability distribution changes, for example the shapes in Figure 4.13 (a) became more left skewed, the values near the tails become more significant as practical outcomes. A PDF model provides the full range of values a given index can take. Values can thus be selected from an index PDF with particular levels of confidence attached according to the analysis or the decisions to be made. Decisions with potentially high financial impact may justify high levels of confidence or an indication of how the expected outcome varies with the risk. The concept of confidence level also applies to reliability inputs, particularly if deterministic values are used. The mean or 50^{th} percentile value with a 50 % level of confidence corresponds to the average index usually derived from a simulation study.

4.4.4 Computation times

A disadvantage of sequential MCS processes is the computation time required. A comparison of the number of simulations and computation time required by the SDM analyses in literature and the custom SDM code written for this thesis is presented in Table 4.20.

Table 4.20: Comparison of computational efficiency of two SDM simulation processes

Conventional Sequential MCS code	Simulation runs	Computation time (seconds)
Billinton and Sankarakrishnan [1995]	150	733
Custom SDM code written for this thesis	7000	4.9

It is important to note that Billinton and Sankarakrishnan [1995] required fewer simulations than the custom SDM code. Their computation time was however significantly higher than that required by the custom SDM code. This could be a case of capability of computing system used to run the code.

Table 4.21 compares the computation times required by the custom SDM code written for this thesis and that written for the TDPA, for different stopping criteria. The analyses were performed on the same computer and the same approach to programming applied[3].

Table 4.21: Computation times for TDPA and sequential MCS for same system and parameters

Stopping criterion	6 %	1 %	0.1 %
Conventional sequential	< 5mins	< 2.8hrs	>> 2.8 hrs
TDPA with spike-like PDFs	< 5s	< 2.5mins	< 12mins
TDPA with practical PDFs	< 6s	< 3.2mins	< 21mins

The times for corresponding stopping criteria are significantly different, with both TDPA methods considerably faster than the conventional sequential MCS. The TDPA's faster speed, even with realistic Beta PDFs, can be attributed mainly to its simulation of the down states (zeros), which are inserted into the initial lifecycle of up states (ones). The higher speed and capability to model short periods (e.g. 6 hours) suggest the TDPA method might be suitable for on-line operational reliability assessment.

A difference is noted in the computation times of the two TDPA analyses. The dispersion in the reliability inputs is higher when the practical PDF models are applied as opposed to spike-like PDFs. A comparison of the shapes in Figures 4.9(b) and 4.12 shows that variability in the reliability inputs influences the computed reliability indices. Practical PDFs are however more dispersed so that the convergence of the corresponding simulation is expected to be slower. The performance of the TPDA in each analysis is however still comparable for stopping criteria higher than 1 %.

[3] The simulations were run on an HP Intel (R) Core (TM)2 Duo CPU with a 2 GHZ processor. The programming was performed in carried out in the R2009b edition of MATLAB software).

4.6 SUMMARY

The chapter addressed the gaps identified in literature. A new reliability evaluation technique was presented and its performance tested on the Roy Billinton Test System. The research questions addressed in this chapter included:

Qn.2: How applicable are probability Density functions in network reliability analyses?

The suitability of the Beta PDF for use in a reliability analysis was tested. Different PDFs were fitted to reliability input and output data sets. The goodness-of-fit tests ranked the Beta PDF as one of the best fits for the data sets considered. The Beta PDF has had limited application in reliability studies thus far. For this research, the Beta PDF is scaled by the maximum value recorded in the data set being described. Maximum values based on extreme value theory can be applied in analyses aimed at investigating extreme events.

Qn.6: How can continuous probability distributions be incorporated in either planning or operational reliability analyses?

The Herman and Gaunt [2010] matrix failure model was extended so that Beta PDF-based models, required by the TDPA, could be developed for failure and repair rates in each cell. The new matrix model provides a better and more realistic representation of reliability input parameters; dispersion and skewness in parameter distribution is represented. The planning PDF models derived did not have Gaussian shapes. The use of average values for annual planning studies is thus questionable. The occurrence and dispersion of outages is influenced by more factors in the short-term which should be included when developing and applying operational models.

4.5.1 Onward

Chapter 5 applies the TDPA to a real bulk power network. The input failure models derived for both planning and operational based reliability analyses are presented. South African adverse local weather threats are considered.

5. APPLYING THE TDPA TO A REAL POWER NETWORK

5.1 INTRODUCTION

Chapter four discussed the time-dependent probabilistic approach applied in this research. It discussed how vulnerability models can be developed for either a network planning or operational reliability analysis while using the same failure data sets. The simulation procedure required was also developed and the TDPA tested on a published test network. This Chapter will now apply the TDPA to a real power network and input Beta PDF models based on real failure data.

5.2 INPUT FAILURE MODELS DERIVED FOR PLANNING CASE STUDIES CONSIDERED

The bulk power network shown in Figure 5.1 represents a portion of the real South African transmission network and is used here because real and relevant data is available, allowing realistic conditions to be modelled. The network is composed of 36 buses with a total load of 6.3 GW. The maximum generating capacity is 2.2 GW with make-up in-feed (slack-bus) from Terminal 01. Transmission lines at a voltage level of 400 kV were considered. The base voltage and power for the network is 400 kV and 100 MW respectively. Other network component ratings are presented in Appendix C.1.

Figure 5.1 shows two distinct geographic regions; the frontal and thunderstorm regions. The regions are based on the rainfall activity of South Africa which is significantly higher in one half of the country. As a result, the weather patterns and intensities also vary such that the likelihood of occurrence and severity of a given failure cause is different in each region. Depending on the location of a given component, its exposure to a given threat could be understated or overstated. The sub-regions in which each external threat is dominant are also shown in Figure 5.1.

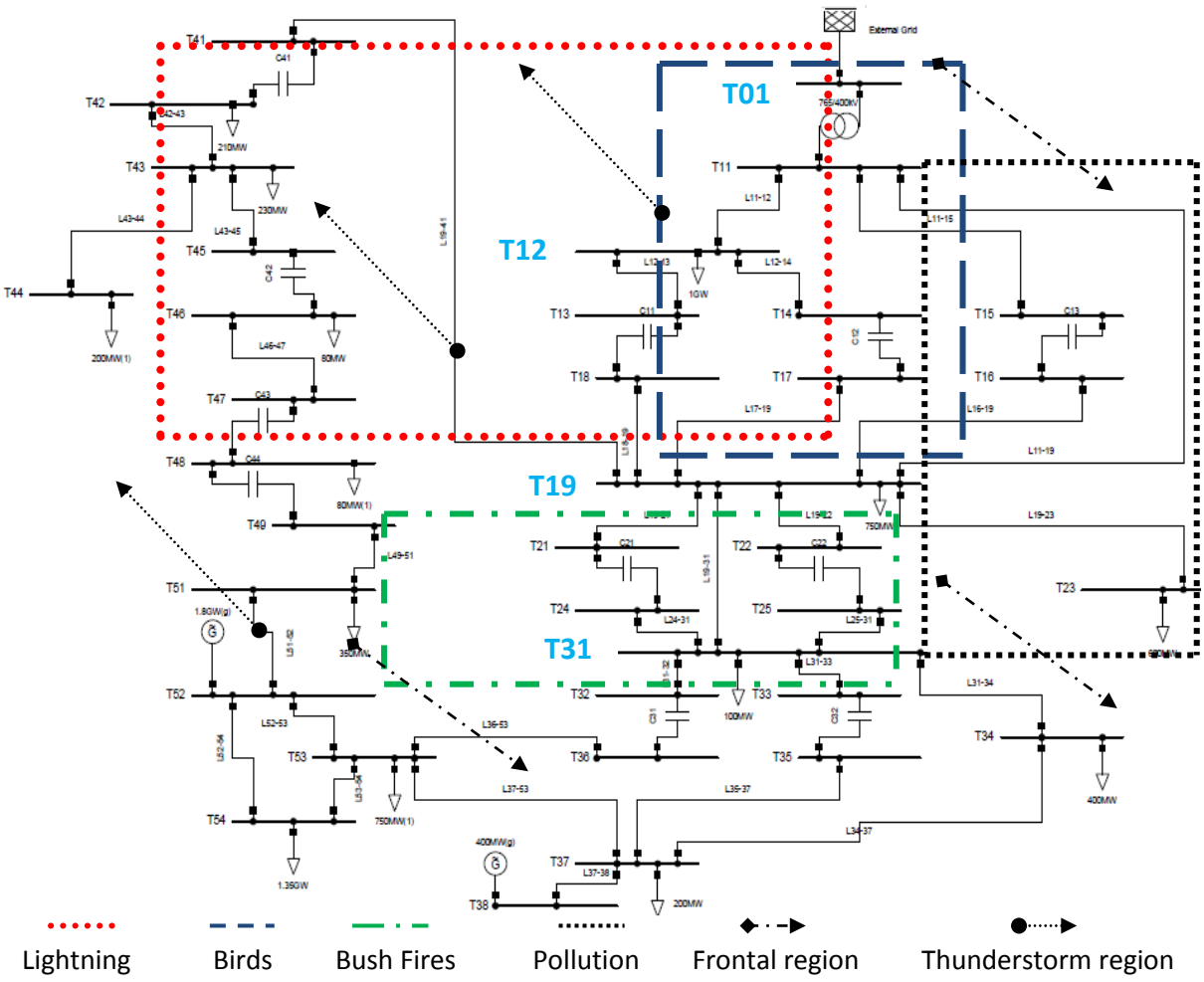

Figure 5.1: Portion of South African bulk network showing sub-regions of external network risk influence

The main external network threats influencing component failure of the bulk network in Figure 5.1 were determined as birds, lightning, bush fires and pollution. The sub-regions in which these external elements have significant influence are also shown in Figure 5.1.

5.2.1 Network component restoration time model

The Beta PDF in Figure 5.5 represents a restoration time model for the network components. The shape is also similar to models derived from South African repair data. The mean of the data set used is 10 hours. The model was applied in both planning and operational analyses.

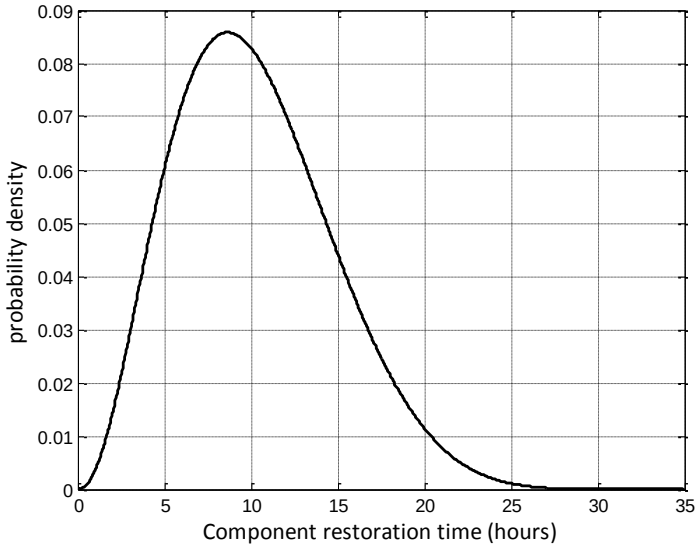

Figure 5.2: Beta PDF model for component restoration time (hours/failure)

The shape of the PDF in Figure 5.2 indicates that while repairs that take less than 10 hours occur more often, repairs lasting more than 10 hours are still likely. The factors that affect repair of components at either operation or planning are similar. The same model was thus applied in both planning and operational reliability analyses for all types of component outages.

5.2.2 Network failure frequency models used as planning reliability inputs

The failure data presented by Minnaar et al [2012] was collated to yield regional failure data. The contributing matrix models corresponding to each failure cause for both frontal and thunderstorm regions are presented in Appendix C.2.

Failure statistics, corresponding to a given threat, in the frontal and thunderstorm regions were aggregated to yield the overall network failure statistics. The failure data set of every component, in each region, was first distributed into four 4X4 network risk matrix models. For example, in the frontal region, all component matrices developed for say lightning, were aggregated to develop a single 4X4 lightning failure model. A lightning failure model was similarly derived for the thunderstorm region. Each region was thus described by four network threat matrix models.

Using (4.2) to (4.5), the failure statistics of each component matrix, corresponding to a given external threat, were then aggregated to yield a regional matrix model for each network threat. Corresponding regional matrices were then aggregated to develop models for the entire network. The aggregation process, from component matrix to overall network matrix model, is illustrated in (5.1) and (5.2) for lightning related failures.

$$Lightning\ [frontal] = \sum_{f=1}^{n} L_f[Lightning] \tag{5.1}$$

$$Lightning[network] = Lightning\ [frontal] + \ Lighting\ [Thunderstorm] \tag{5.2}$$

$L_f[Lightning]$: 4X4 matrix model for lightning related failures of a component in the frontal region

$Lightning\ [frontal]$: aggregated failure model for lightning related failures in the frontal region (4X4 matrix)

$Lighning[network]$: aggregated failure model for lightning related failures in the whole network (4X4 matrix)

n: number of components in the frontal region

At this stage, each network threat matrix model is characterized by a quarter year period and different time-of-day. Annual composite models, required for planning, were then derived for each network threat by aggregating along different seasons; essentially increasing the analysis season to a calendar year. The failure data sets of the new annual matrix were analyzed per time window and the corresponding Beta PDF models derived. For each planning cell, four network threat Beta PDF models were derived. Each Beta PDF model is applicable to components located in the sub-region in which the given threat is dominant. The shape parameters (α, β, C) of the derived Beta PDF models are shown in Table 5.1 for each time slot.

Table 5.1: Shape parameters for annual time windows given South African conditions

Network risk	Period				
	00:00–06:00 hrs	00:06–12:00 hrs	12:00–18:00 hrs	18:00–24:00 hrs	00:00-24:00 hrs
Birds	(17.7,35.5,222.3)	(12,31.2,93)	(6.2,23.9,34.8)	(10.1,26.4,120)	(42.2,99,470.1)
Fire	(1.5,9.2,12.5)	(3.5,12,35.6)	(4.7,13.7,149.8)	(2.1,11.7, 20.3)	(8.1,26.7,218.2)
Lightning	(5,19.5,64.4)	(2.3,13.4,27.2)	(5.9,22.4,114.6)	(5.3,18.2, 87.7)	(18,69,294)
Pollution	(0.1,1.4,132.6)	(0.8,6.1,43.2)	(0.1, 1,13.2)	(0.5, 4.6, 26.8)	(0.5,5.2,215.8)

The discussion in Section 3.3 described the different models applied when stochastic external factors are considered in a reliability analysis. It was also stated that single deterministic values, computed as average values over many years, are conventionally used to model component parameters in planning reliability analyses. The use of an average value assumes that the distribution that describes the given data set has a Gaussian shape so that the mean value is the most likely value[4].

The shape parameters in Table 5.1 do not indicate that the planning PDFs have symmetrical shapes. This is important particularly with regard to the Central Limit Theorem [Papoulis, 1991; Leon-Garcia, 1994]. According to the theorem the summation of a large number of independent and identical random variables approximates to a variable with a Gaussian distribution. Using average values may thus misrepresent annual planning failure parameters.
Table 5.1 shows that network components are most vulnerable to outages between midnight and 06:00 am. Table 5.1 also indicates that annually, during this period, the main cause of component outages is bird streamers. The other significant time slot is between noon and 06:00 pm. The failures during this period were mainly fire and lightning related.

Figure 5.3 shows the plots of the planning Beta PDFs based on the annual network threat failure data sets covering the midnight to 06:00 am and noon to 06:00 pm time slots.

[4] For Gaussian shape, mean=mode=median

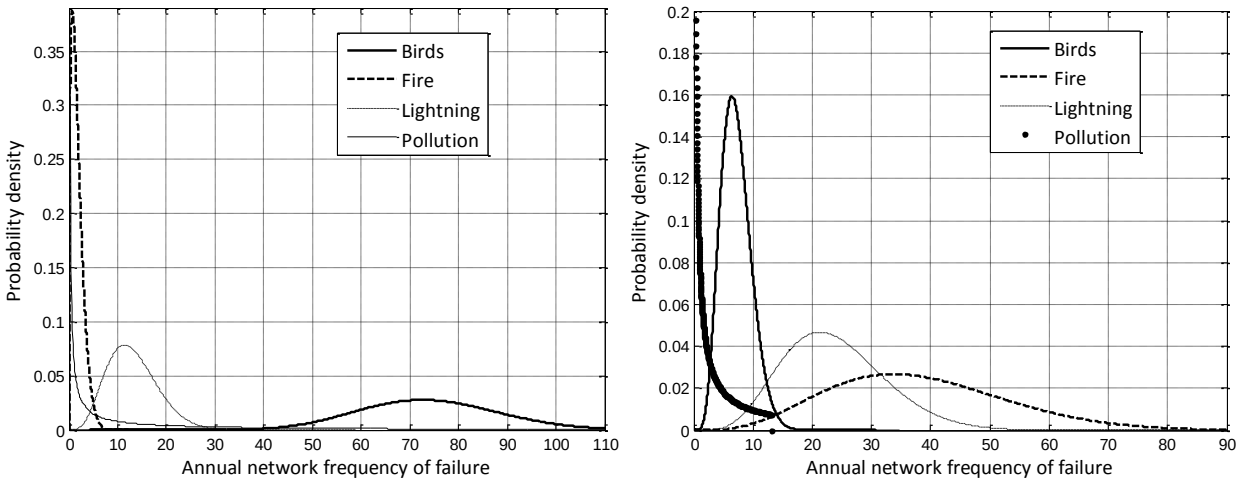

Figure 5.3: Annual network risk PDFs for different time slots (a) 00:00-05:59 am (b) 12:00-0559 pm

It is clear that the threat posed by the external threat is elevated between noon and 06:00 pm.

5.2.2.1 Analyzing failure data sets derived by the TDPA aggregation concept

Section 4.3.2 presented the planning failure PDF models for transmission lines developed using the TDPA. The models were based on aggregated failure data. It is important to check that the aggregation applied does not in fact compromise the failure data provided. The first step in determining this is comparing the composite planning failure data sets derived with data sets achieved without applying the aggregation. The failure statistics collated by Minnar et al [2012] were categorized into quarter-year seasons for each network threat. In Section 4.3.2, these were aggregated to develop the annual planning models. Table 5.2 presents all network failure statistics organized on an annual basis. The Beta shape parameters for each time window are presented in Table 5.3.

Table 5.2: Annual failure statistics for six hour intervals

S/P	0000-0559 hrs			0600-1159 hrs			1200-1759 hrs			1800-2359 hrs		
	mean	std	max	mean	std	max	mean	std	max	mean	std	max
Jan-Dec	**99.8**	**27.6**	**431.8**	**42.6**	**9.02**	**199**	**72.7**	**17.5**	**307.8**	**61.4**	**12.1**	**259.9**

Table 5.3: Shape parameters of the frequency of failure PDF models for all components

Season	Period				
	0000-0559 hrs	0600-1159 hrs	1200-1759 hrs	1800-2359 hrs	0000-2400 hrs
January-December	(9.8,32.7,431.8)	(17,63.5,199)	(12.9,42,307.8)	(19.4,62.8,260)	(45,150,1198.5)

The shapes of the Beta PDFs derived are shown in Figure 5.4. It is clear from the PDFs that the vulnerability of the network to failure varies during the day.

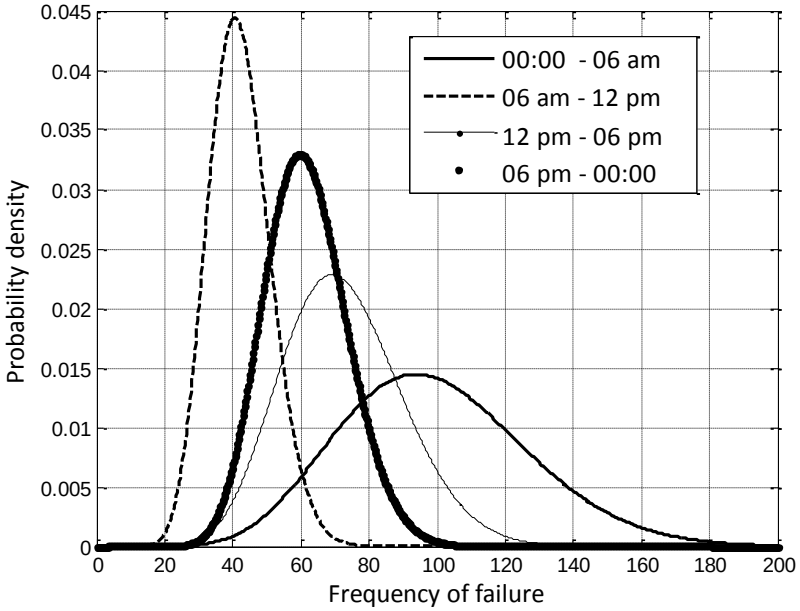

Figure 5.4: Time-of-day based frequency of failure Beta PDF models

The TDPA through aggregation should also be able to derive the models in Table 5.1 and Figure 5.4. The annual failure models based on network threats when aggregated yield a composite threat model. A comparison of the PDF models in Table 5.1 and the composite threat PDF models for each time slot derived is presented in Table 5.4.

Table 5.4: Shape parameters (α, β, C) for annualized time windows for the entire network

Selection/period	00:00–06:00 hrs	00:06–12:00 hrs	12:00–18:00 hrs	18:00–24:00 hrs	00:00-24:00 hrs
January-December	(9.8,32.7,431.8)	(17,63.5,199)	(12.9,42,307.8)	(19.4,62.8,260)	(45,150,1198.5)
Composite threat	(9.8,32.7,431.8)	(17.3,63.5,199)	(12.3,42.2, 312.4)	(18.1,12,254.8)	(43.9,149,1198)

The composite threat PDFs derived through aggregation are very similar to the PDFs computed from failure data categorized in terms of annual seasons (January to December) and six-hour intervals. It is clear that the shapes of the planning Beta PDF models presented and scaling factors for corresponding time slots are similar. This shows that the aggregation applied by the TDPA did not distort the contributing failure data sets.

5.2.3 Case studies analyzed in the TDPA planning reliability analysis

The planning case studies aim at showing the importance of using the right input failure models in a reliability analysis. The planning case studies presented in this section particularly investigate:

- The effect of using PDF-based models, over deterministic average values, for planning reliability inputs
- The effect of the aggregation concept applied by the TDPA on the reliability indices.
- The additional information derived when PDFs, as opposed to deterministic averages, are also used to represent the outputs of a reliability study.

The planning reliability analyses were carried out whilst considering an annual time line. Four different failure models were used to reflect the vulnerability of network components in the same time window. The case studies are thus used in this section to show how the perception on a network's reliability is influenced by the failure models applied. The four cases considered for each component frequency of failure model include:

- Base case analysis that considers average values
- Single composite PDFs for an annual planning study (region unspecific)
- Two half-year composite PDFs for an annual planning study (region unspecific)
- Annual beta PDFs based on geographic regions

Case 1: Base case analysis that considers average values

A base case analysis provides a set of values to be used for comparison with those values obtained from other tests carried out on a given system. This enables the evaluation of different action alternatives from a reliability viewpoint.

A base case analysis considers no proposed changes in the network topology, operating conditions or protection scheme [Alvehag, 2008]. Only unplanned failures are considered and the failure rates of the components are assumed to be constant. The component restoration times are also assumed to be unaffected by time-dependent activities. Component parameters, frequency and duration of failure, were thus represented using average failure parameter values. A base case average parameter value is usually an annualized value i.e. the parameter is represented on an annual basis. The frequency or duration of failure of a given component was derived from a failure data set that corresponded to component outages due to the network risk(s) to which it was exposed. If one considers the location of a network component, it can be determined that the dominant external element in the given location is the major contributor to the component's outages. One could thus match the outage pattern of a component or portion of the component to variation in severity of the dominant external element present in its vicinity.

This base case analysis considered the sub-regions in which each external element had significant influence. The component failure data sets corresponding to the dominant external element in each sub-region were used to derive the average component parameter values. All components in a given sub-region and thus exposed to the same dominant external element, were assigned the same frequency and duration of failure values. For components in overlapping sub-regions (crossing more than one sub-region), average values were determined from the failure data sets of the corresponding sub-regions and summated.

An average parameter value was applied to the full length of the transmission lines. Since it is an average value, a single level of risk is attached such that the component parameter assumes the same value annually. Table 5.5 presents the annual average frequency of failure for components exposed to the main external threats in the 12:00 to 18:00 hrs time slot. The values presented were computed from the composite failure data sets derived per external threat for the whole network (frontal and thunderstorm).

The PDFs corresponding to these composite failure data sets are shown in Figure 5.3. For the base case however, a spike-like PDF with $\alpha = \beta = 500$ was applied with the average values in Table 5.5.

Table 5.5: Average frequency of component failure due to different external elements

Network risk	All exposed components (failures/year)	Per component (failures/year)
Birds	7.2	0.8
Lightning	24.0	1.7
Bush Fires	38.2	4.2
Pollution	2.4	0.4
Birds and Lightning	(7.2+24.2) = 31.4	2.5

Case 2: Single composite PDFs for an annual planning study (region unspecific)

Unlike the base case analysis, frequency and duration of component outages were inputted as skewed PDFs. The full range of each network threat PDF was applied in the analysis as opposed to the base case which applied only the average values. For each external threat, annualized component failure data sets corresponding to the 12:00–18:00 hour time slot were again considered. The composite Beta PDFs derived for frequency of component outage due to some of the threats, lightning, birds and bush fires, were shown in Figure 5.3 (b). These, together with the component restoration model in Figure 5.2, were applied as reliability inputs in this case analysis instead of the average values used in the previous section. Similar to the base case analysis, a given external threat PDF derived was applied to affected components in either region i.e. same vulnerability model for both regions.

Case 3: Two half-year composite PDFs for an annual planning study (region unspecific)

A key concept with regards to the TDPA is the aggregation of failure data sets within a given time window or across different time windows to derive a composite PDF. The aggregation concept was checked at the input side of the TDPA in Section 5.2.2.1. It was shown that the input failure data sets were not compromised.

It is however important to ensure that one can yield similar reliability results if the PDF inputs applied describe either the contributing data sets or the corresponding composite data set derived.

The analysis in Case 2 applies single composite PDF models to all components exposed to the given threat. Instead of a single annual PDF, two half-year composite PDFs could also have been derived for each external threat. To further validate the concept of aggregating data sets, the indices computed using the half-year PDFs should be comparable to those attained using single annual-based PDFs. Each half-year PDF is derived from failures that occur either between January to June or, July to December. Figure 5.5 presents the frequency of failure Beta PDFs derived for fire and lightning related failures in each half-year between noon and 6 pm. The half-year PDFs describe the data sets that could be aggregated to yield the composite data set descried by the annual PDF.

The failure PDFs presented in Figure 5.5 show that the external threats affect components differently in each half of the year between noon and 6 pm. The frequency of lightning related component failures is lower in the second half of the year compared to the first. For fire, the highest and lowest number of failure will more likely be recorded in the first half of the year.

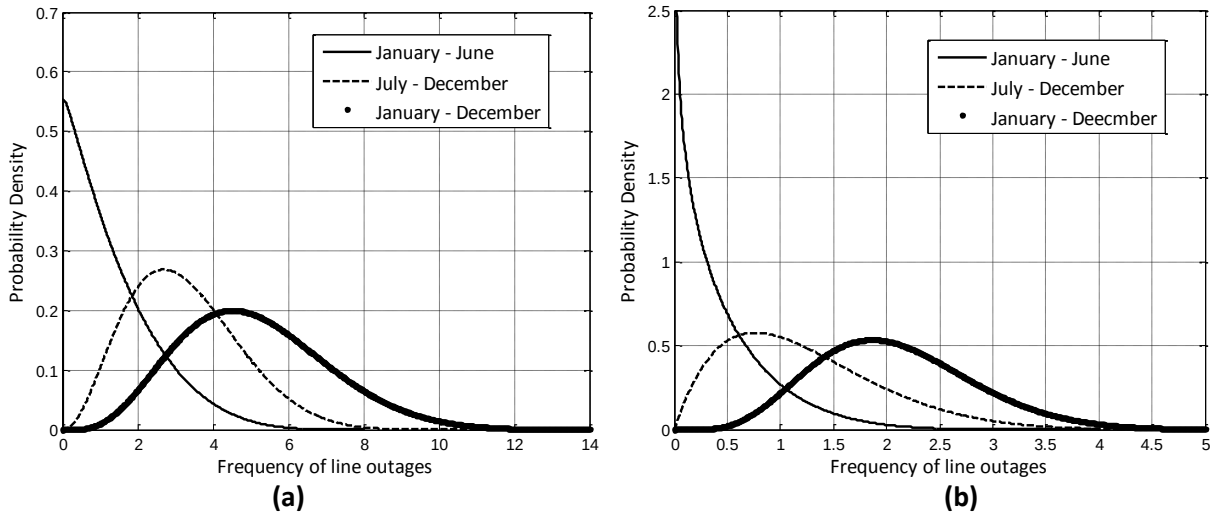

Figure 5.5: Half-year and annual PDFs for component failures due to (a) fire (b) lightning

The expression in (5.6) shows how the two half-year PDFs were applied for a given threat. The annual frequency of component failure is the summation of the failures that occurred in each half of the year. A component's annual failure frequency was thus determined in the simulation as a summation of the two values randomly selected from the relevant half-year external threat PDFs.

$$FL_i(\alpha_{yr}, \beta_{yr}, m_{yr}) = FL_i(\alpha_{fhyr}, \beta f_{fhyr}, m_{fhyr}) + FL_i(\alpha_{shyr}, \beta_{shyr}, m_{shyr}) \qquad (5.6)$$

$FL_i(\alpha_{yr}, \beta_{yr}, m_{yr})$: failure frequency generator from annual component PDF for threat i

$FL_i(\alpha_{fhyr}, \beta f_{fhyr}, m_{fhyr})$: failure frequency generator from first half-year component PDF

$FL_i(\alpha_{shyr}, \beta_{shyr}, m_{shyr})$: failure frequency generator from second half-year component PDF

Case 4: Annual Beta PDFs based on geographic regions

The base case analysis and case with single annual composite PDFs, applied the same model to components, irrespective of whether they lay in the frontal or thunderstorm regions. As such, the vulnerability of a component to a specific threat could either be understated or overstated. This section applies external threat models that relate to the geographic regions. The models are developed based on the actual conditions in the proximity of the affected component.

This is more realistic compared to the two previous cases. For each threat, two failure models were thus derived and applied to affected components while taking into account their geographical locations. These are shown in Figure 5.6 for bird and lightning related failures.

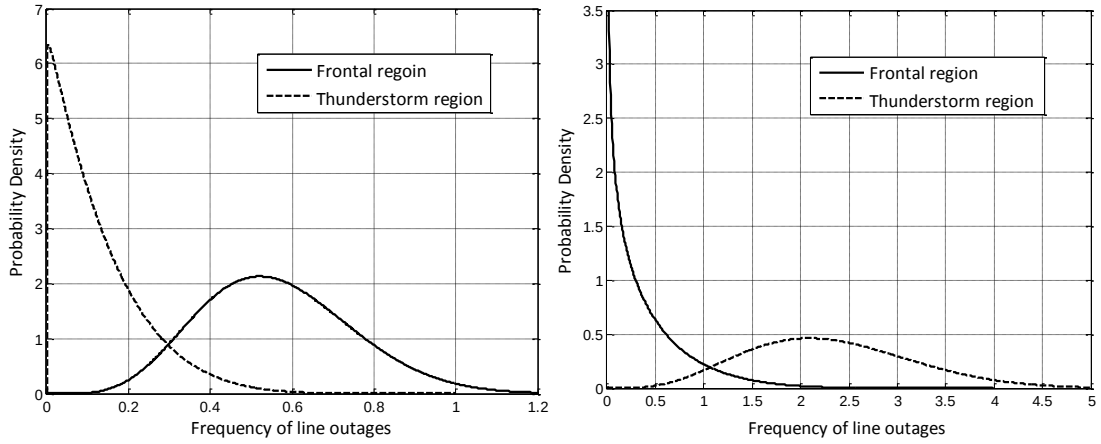

(a) **(b)**

Figure 5.6: Geographical based line failure PDFs for (a) birds (b) lightning

The shapes in Figure 5.6 clearly show that the influence of a network threat on network outages varies between the two regions.

5.3 INPUT FAILURE MODELS USED AS OPERATIONAL RELIABILITY INPUTS

This section highlights the need to use different failure modelling approaches in planning and operational reliability analyses. Even though each study considers the same network risks, different criteria are required when developing and applying the failure models. With the TDPA applied in a planning analysis, a single PDF is used to represent the parameter in each cell of the developed matrix model. These PDFs have been described as the average model of the component's parameter in a selected time window. External threats and the resulting component failure parameters are however quite intermittent in operational time windows. It could thus be necessary to base operational failure models on the different severity levels of the external threat.

While the planning analysis was carried out over the period of January to December, an operational analysis considers shorter periods. Three-month operational periods are considered here. PDF models will specifically be developed to represent vulnerability during the 1200-1800 hr over the first quarter of the year. Similar to Case 4 in the planning analysis, the operational failure models were developed with regard to the geographic regions.

The average component failure frequency PDFs corresponding to the different threats are shown in Figure 5.7. The PDFs represent a component's vulnerability, in each region, to external threats at an average level of severity.

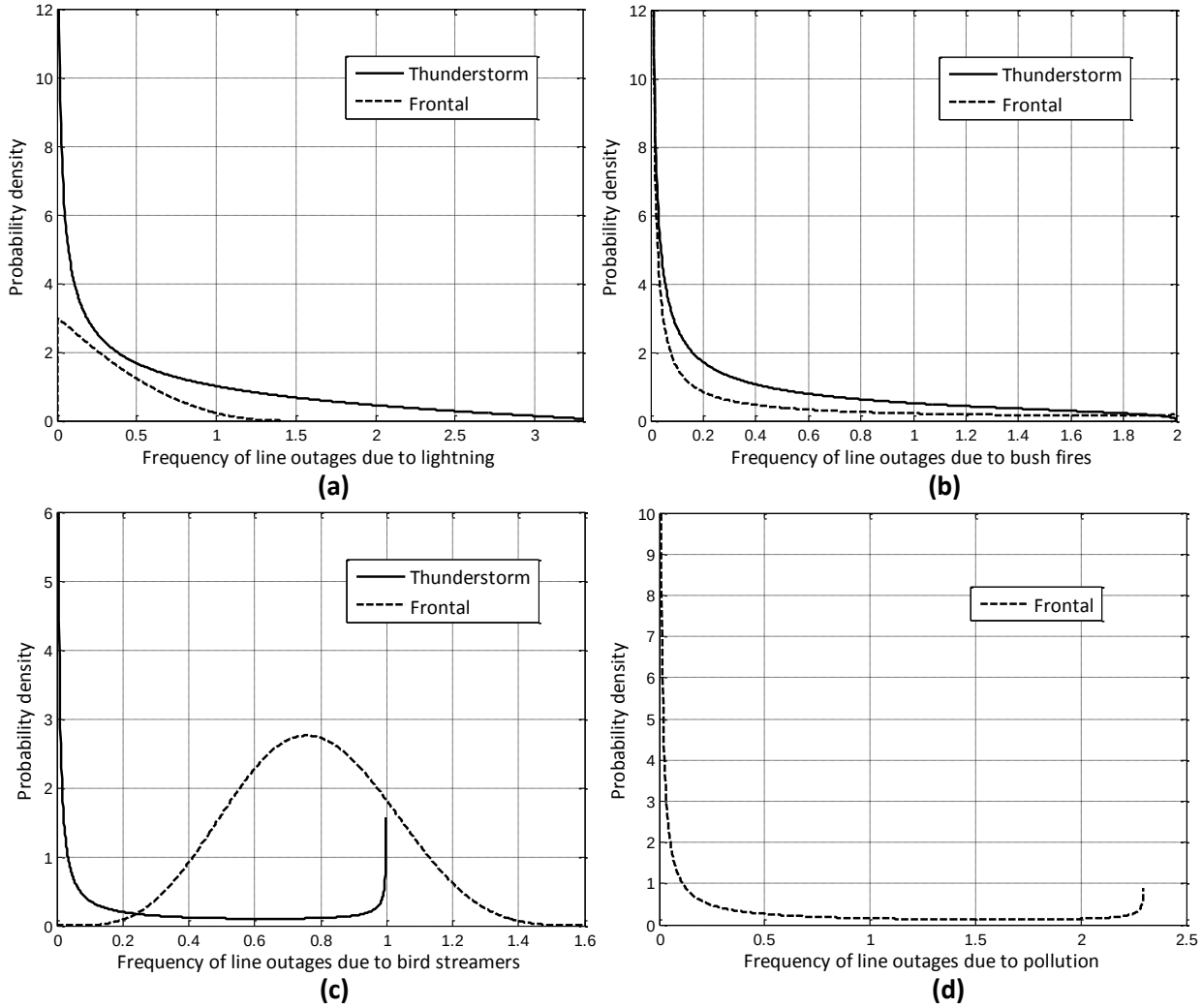

Figure 5.7: Operational component failure PDFs due to different external threats in each geographic region (a) lightning (b) fires (c) birds (d) pollution

It is clear from the PDFs that in the frontal region, during the first quarter of the year between noon and 6 pm, birds cause the most line outages. Lightning on the other hand contributes most to line outages in the thunderstorm region. No outages due to pollution were recorded in the frontal region. Overall, for the operational time window considered, lightning can be regarded as the dominant threat. Variability in lightning intensity, as opposed to other threats, would thus have a more significant influence on the network failures.

In reality, all the threats vary in severity. For illustration purposes the operational PDFs shown in Figures 5.7 (b)-(d) were applied to components exposed to fire, birds and pollution respectively. They correspond to the vulnerability of a component to the respective threats at an average level of severity. The composite PDFs shown in Figures 5.7 (a) were applied on days where the lightning flash density was close or equal to the average value[5] and were thus considered as the average severity lightning failure models in each region. The normalized low and high severity failure frequency PDFs for lightning related outages are shown in Figure 5.8. These were applied to lightning outages in either region.

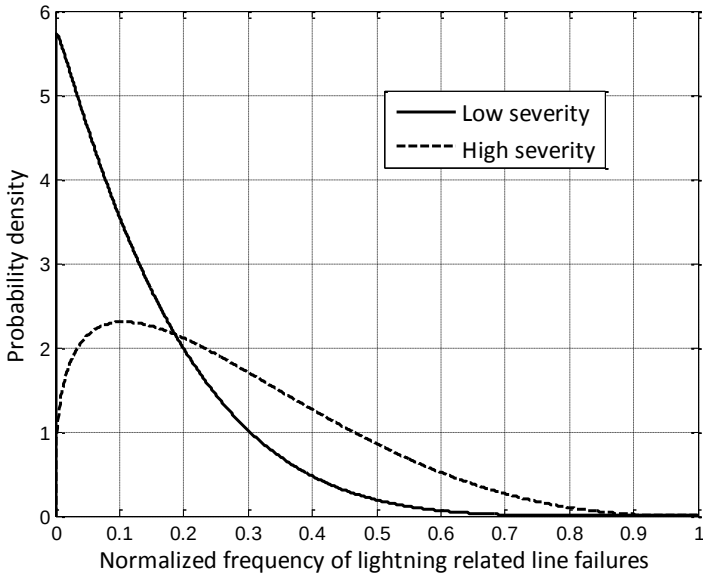

Figure 5.8: Threat-severity-dependent models for lightning related failures

5.4 ONWARD

The next chapter will present and discuss the simulation results of the planning and operational case studies presented.

[5] Days with average conditions simulated

6. RESULTS OF REAL NETWORK SIMULATIONS AND DISCUSSION

6.1 INTRODUCTION

The indices computed in each case, for every load point and the overall system, include the Probability of Load Curtailment (PLC), Frequency of Load Curtailment (FLC) and Duration of Load Curtailment (DLC). The values for FLC computed were rounded to the nearest whole number e.g. 3.2 = (3 events/year) and 3.5 = (4 events/year). The load point results are presented in this section for three buses: T12, T19 and T31. The performance of load points T12 and T31 is affected by components that lie only in the frontal and thunderstorm regions respectively. Load point T19 on the other hand is affected by components in both regions. Analyzing corresponding indices of the three load points provides an indication of how the network performs in each region.

Index values are dependent on the system topology and, operating philosophy and conditions [Wangdee & Billinton, 2005]. A given index would thus take on different values with every simulation run. More information could be derived from the outputs of a reliability analysis if probability distributions were used to describe them, compared to using the average values [Billinton & Huang, 2005]. The level of skewness of the distribution of a given index is very important when one has to interpret the given index [Billinton & Allan, 1996]. Since reliability indices are stochastic parameters, their underlying distributions can take on any shape. Similar to component parameters, index values fall within finite ranges. It could be useful to represent the indices using Beta PDFs.

The failure data collected and published by Minnaar et al [2012] was applied to the real network components using (6.1).

$$f_{cRt} = \frac{NF_{Rt}}{NC_{Rt}} \tag{6.1}$$

f_{cRt} : failure rate of a component due to a specific threat in a given region or sub-region

NF_{Rt} : number of failures, due to threat, in region or sub-region of influence

NC_{Rt} : number of components, in region or sub-region, exposed to given threat

6.2 NETWORK PLANNING SIMULATION RESULTS

The planning procedures of a power network rely on the perception of its reliability. Network components are however affected by a range of factors. The models used to capture vulnerability of network components to failure could be critical to the evaluation of its reliability and the decisions made thereafter. This section investigates the effect of using either deterministic or probabilistic component failure models in a planning reliability study. Unlike most published work, that only consider the magnitude of the reliability indices, the impact on the probability distributions of the computed indices is also analyzed.

6.2.1 Case 1: Base case analysis that considers average values

Spike-like Beta PDFs were used to represent the average values of the input failure parameters. The average values of the indices computed are presented in Table 6.1. It was stated in Section 4.3 that the 50 percentile (50 %) value of a distribution represents the median value of that given distribution. These are also presented in Table 6.1.

Table 6.1: Base case index values

Bus	PLC		FLC (events/year)		DLC (hours/year)	
	Mean	50 %	Mean	50 %	Mean	50 %
T12	0.0034	0.0035	5	5	29.6	30.5
T19	0.0057	0.0054	8	8	49.9	47.0
T31	0.0077	0.0066	11	9	67.1	57.5
System	0.021	0.022	31	32	185.5	193.5

From the average values, one deduces that load point T12 performs better than T19 and T31 in the selected time window. The power network's line diagram in Figure 5.1 shows that load point T12 is close to the external grid so that, unlike T19 and T31, supply to the load is not significantly affected by component outages. The performance of load point T12 could also be attributed to it location in the frontal region.

The external conditions are not as adverse as those in the thunderstorm region. Load point T19 borders the two regions while T31 is affected only by components located in the thunderstorm region. A comparison of the overall system indices, particularly FLC and DLC, shows that T31 is responsible for close to half of the outages that occurred in the test network. This indicates that T31 is one of worst performing load points.

Without plotting or analyzing the shape parameters of the index PDFs, one cannot determine the most likely index value. The mean values and 50 percentile values computed from the index data sets are similar, particularly the FLC values. This could indicate that the index PDFs have symmetrical shapes which would mean that the indices will most likely take on the mean values presented in Table 6.1. The shape parameters of the indices however tell another story. The Beta PDF shape parameters corresponding to each load point and system index are presented in Table 6.2. A Beta PDF exhibits a Gaussian shape when its shape parameters, α and β, are equal[6].

Table 6.2: Shape parameters of the base case indices

Index	**Shape parameters of the index Beta PDFs (α, β)**			
	T12	T19	T31	System
PLC	1.2, 1.8	1.8, 2.3	3.6, 5.6	2.5, 2.0
FLC (events/year)	1.05, 1.6	1.7, 1.6	3.0, 3.9	2.7, 2.0
DLC (hours/year)	1.2,1.8	1.9, 2.3	2.9, 4.5	2.8, 2.1

With the exception of the FLC index of load point T19, the shape parameters in each cell of Table 6.2 are not close enough to infer symmetrical shapes. In fact, for the load point indices, the PDFs are mainly right skewed (β > α). The system indices on the other hand are left skewed (β < α). Thus, from the base case analysis, a reliability index for the load points considered will in fact more likely take on a value greater than its mean. The system indices on the other hand will more likely have values less than the mean.

[6] See Figure 2.3

Figures 6.1, 6.2 and 6.3 show the probability, frequency and duration of load curtailment indices computed for the three load points and overall system. Despite using deterministic (average) values for every reliability input, the index PDFs take on shapes as exhibited by the differently skewed Beta PDFs.

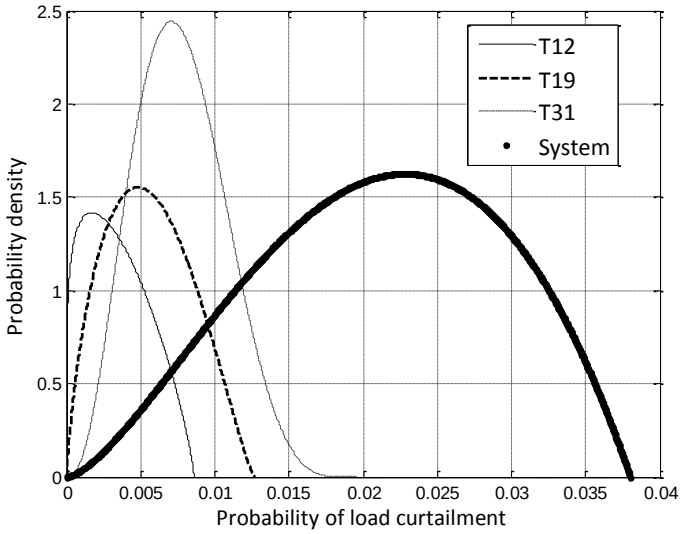

Figure 6.1: Base case PLC at different load buses and for the overall system

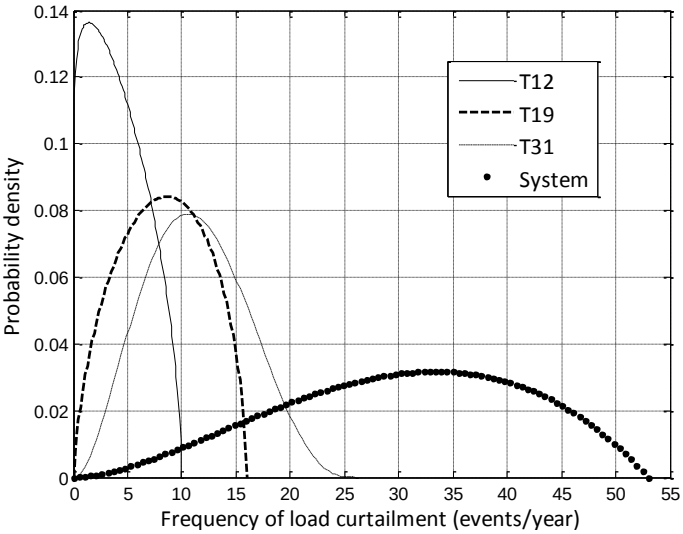

Figure 6.2: Base case FLC at different load buses and for the overall system

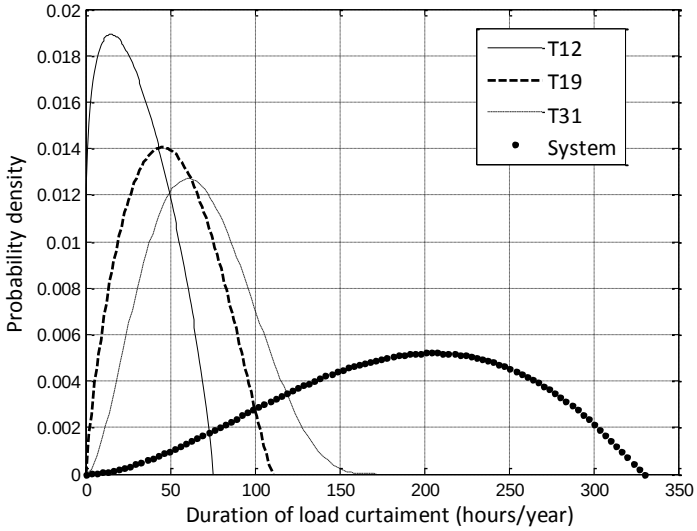

Figure 6.3: Base case DLC at different load buses and for the overall system

Reliability input parameters vary over a year so that, a maximum and minimum value can be determined each year; the failure data of different network components have variable ranges. One would thus expect the corresponding indices computed to also have specific ranges of values. Using single deterministic values, as inputs, however results in the simulation process selecting values from a significantly reduced range. For the base case, the parameter values selected are closer to the average values. The effect of this is shown in the base case index PDFs. All the indices have a minimum of zero and pattern observed in the shapes exhibited by the PDFs; right skewed for the load point indices and left skewed for the system indices.

The base case PDFs also show that, of the three load points, T31 is the worst performing bus in the selected time window. The peaks of the load point index PDFs show that T31 is the most likely to fail. The tail regions of the load point index PDFs, in Figures 6.2 and 6.3, show that T31 will experience the highest number and longest outages. The PDFs also show that T12 is the best performing load point with the least number of recorded failures and shortest duration of failures annually.

6.2.2 Case 2: Single composite PDFs for an annual planning study

Unlike the base case, more practical PDFs were considered. A comparison between index values computed from the two cases analyzed thus far is presented in Table 6.3.

Since the conventional approach used in the base case analysis usually presents the indices as average values, a comparison is made in Table 6.3 between the base case indices and the mean values of the indices computed in Case 2.

Table 6.3: Comparison of average index values

	PLC		FLC (events/year)		DLC (hours/year)	
	Base Case	1-year PDF	Base Case	1-year PDF	Base Case	1-year PDF
T12	0.0034	0.0073	5	6	29.6	64
T19	0.0057	0.015	8	12	49.9	130
T31	0.0077	0.018	11	14	67.1	155
System	0.021	0.062	31	48	185.5	545

Table 6.3 shows that T31 is still the worst performing load point and T12 the best performing. The analysis in Case 2 however yielded significantly different values; a significant increase is noted in all the indices. Using PDFs as reliability inputs thus shows that the components are more vulnerable to outages and as such, a higher number of load curtailments events occur throughout out the network. The use of PDFs also predicts longer load curtailment events. Using average values as inputs as shown in Table 6.3, yields reliability indices that could either understate or overstate the vulnerability of load buses and the overall system to the external threats that cause component outages. Similar to the case with deterministic values applied, the analysis with PDFs produces comparable results for T19 and T31 which infers that load point T19 is influenced more by thunderstorm conditions.

The shape parameters of the Beta PDF shapes displayed are presented in Table 6.4. While the system indices are still left skewed, no clear pattern can be identified from the load point indices.

Table 6.4: Beta shape parameters for case of single composite PDFs applied

Index	Shape parameters of the index Beta PDFs (α, β)			
	T12	T19	T31	System
PLC	5.2, 5.4	7.6, 10	8.2, 6.5	21.2, 8.2
FLC (events/year)	7.7, 5.8	10.9, 8.6	9.9, 4.0	23.0, 7.1
DLC (hours/year)	5.0, 5.3	7.5, 7.6	9.0, 7.3	19.6, 7.6

The shape parameters for the PLC index PDF for T12 and, DLC index PDFs for T12 and T19 indicate that the distributions are closer to symmetrical shapes. The index PDFs for T31 are all left skewed. Other index PDFs are either left or right skewed.

The PLC, FLC and DLC index PDFs computed in this case analysis for the selected load points and overall system are shown in Figures 6.4, 6.5 and 6.6 respectively. It is clear that some of the Beta PDFs are shifted horizontally. Using PDFs for reliability inputs allows selection of component parameter values from a range of possible values so that the reliability indices computed also fall within specific ranges. Using PDFs also ensures that the selection of input values was carried out while considering the likelihood of a parameter taking on a given value. The skewness of a given component parameter's PDF ensures that certain values are selected more in the analysis because the parameter is more likely to have such values.

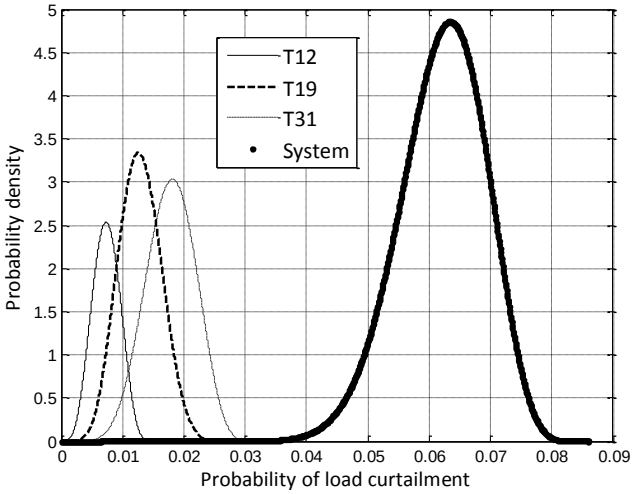

Figure 6.4: PLC at load buses and overall network for case of single composite PDFs

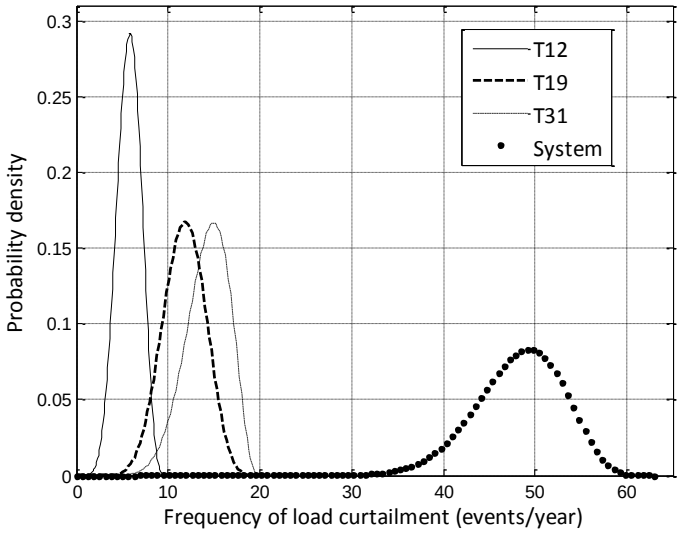

Figure 6.5: FLC at load buses and overall network for case of single composite PDFs

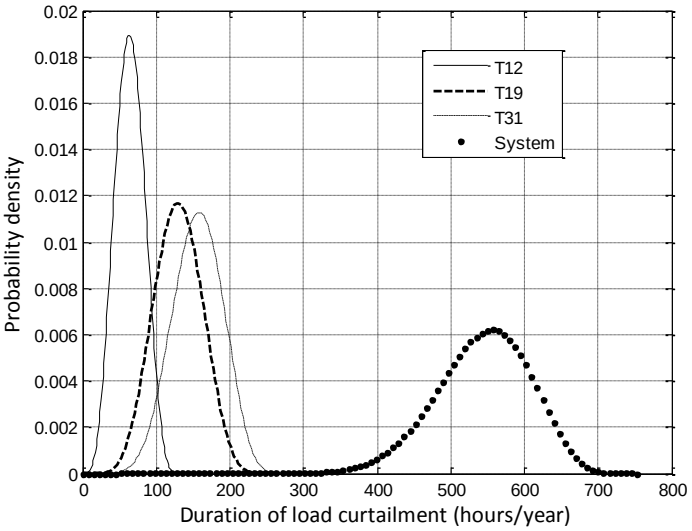

Figure 6.6: DLC at load buses and overall network for case of single composite PDFs

From the average values presented in Table 6.3, it was determined that T19 and T31 have comparable results. The PDFs also show that the corresponding indices have similar ranges. Analyzing T19 and T31 PDFs however shows that there is a difference in likelihood of an index taking on a given value. From Figure 6.6, the DLC indices for T19 and T31 have a range of about 50 to 250 hours/ year. However the DLC PDF for T19 has a Gaussian shape, $(\alpha, \beta) = (7.5, 7.6)$ while the T31's PDF is left skewed $(\alpha, \beta) = (9.0, 7.3)$. This implies that the DLC index for T19 will more likely take on values that lie around the mean while the same index for T31 will take on values greater than the mean.

From the PLC PDFs in Figure 6.4, the range is again similar, 0.002 to 0.03, but index for T19 will most likely take on values lower than the average while T31's will take on values higher than the average. Since the FLC index PDF of T31 is more left skewed than that of T19, the likelihood of FLC index taking on values closer to the minimum of the FLC range (5 to 20 events/year), is higher with T19. This is illustrated at the lower value tail regions of the FLC curves in Figure 6.5. The PDF of T19 is above that of T31. Such observations are missed when deterministic values are used to describe the indices.

6.2.1.3 Case 3: Analyzing effect of aggregation in the TDPA on computed indices

A comparison of the frequency of load curtailment index, for the overall system, computed from the TDPA analyses with single and two half-year composite PDFs applied as inputs is shown in Figure 6.7.

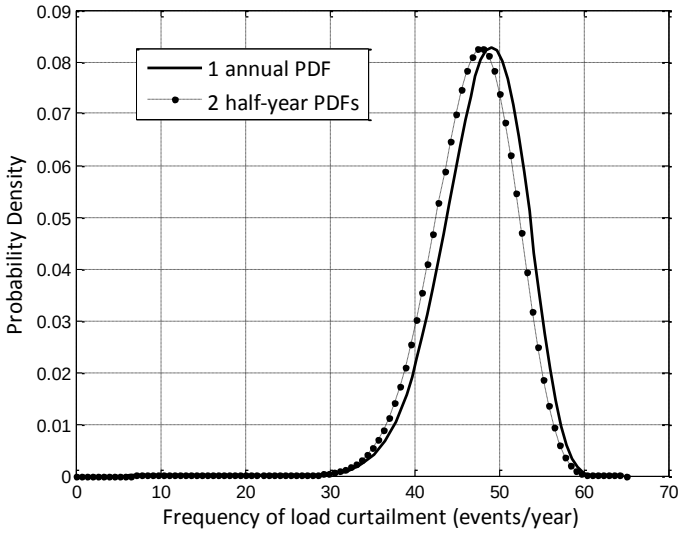

Figure 6.7: Comparative system FLC index PDFs derived from analyses using single composite and two half-year input PDFs

The index PDFs are quite similar. It can be observed from the PDFs that the two analyses, using either single annual or two half-year composite PDFs, yielded index values that fall within very similar ranges. A slight horizontal offset is observed. This could be attributed to the summation carried out in the simulation when deriving an annual component parameter value. Depending on the component, a simulation run could yield either higher or lower failure frequency values from the half-year failure PDFs than from a single annual failure PDF.

This difference is more evident in the maxima of the parameter values derived which in turn impacts on the maxima of the indices computed. The vertical offset could be a result of the dominance of one half-year PDF over the other. One half-year PDF could have a scaling effect on the values selected from the other PDF which affects the likelihood of occurrence of values that fall within the middle band; either increasing or decreasing the number of middle band values.

While the PDFs provide a good visual impression of the similarity between indices computed, it is important to also compare the values selected from each of set of PDFs. Table 6.5 shows index values selected at two levels of confidence; 50 % and 90 % level of confidence. The level of confidence, as discussed in Section 4.3.2, is an indication of the uncertainty allowed in a selected or computed value. Higher levels of confidence ensure lower uncertainty such that the most likely values can be selected or computed.

Table 6.5: Comparison of index values computed using annual and half-year PDFs inputs for 50 % and 90 % confidence levels

Index	T31				System			
	50 %		90 %		50 %		90 %	
	1PDF	2PDFs	1PDF	2PDFs	1PDF	2PDFs	1PDF	2PDFs
PLC	0.018	0.017	0.024	0.028	0.062	0.064	0.075	0.076
FLC (events/year)	14	14	18	23	48	49	58	58
DLC (hours/year)	155.5	152	214	246.5	541	561.5	659.0	665.5

The corresponding values in Table 6.5 are significantly close. This shows that the index data sets computed from the two analyses and their underlying distributions are also similar. One can thus deduce that aggregating, to derive composite data sets, does not compromise the original failure data and is valid.

6.2.1.4 Case 4: Annual beta PDFs based on geographic regions

The frequency and duration of load curtailment indices for the best and worst performing buses, T12 and T31 were computed.

These were compared with corresponding indices derived in Case 2. The corresponding FLC and DLC index PDFs, for each load point, are presented in Figures 6.8 and 6.9 respectively.

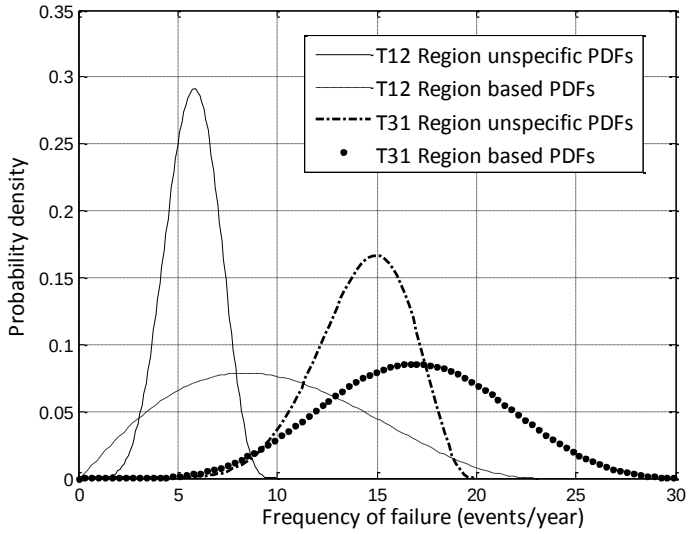

Figure 6.8: Comparative FLC indices based on single and regionally based composite input PDFs

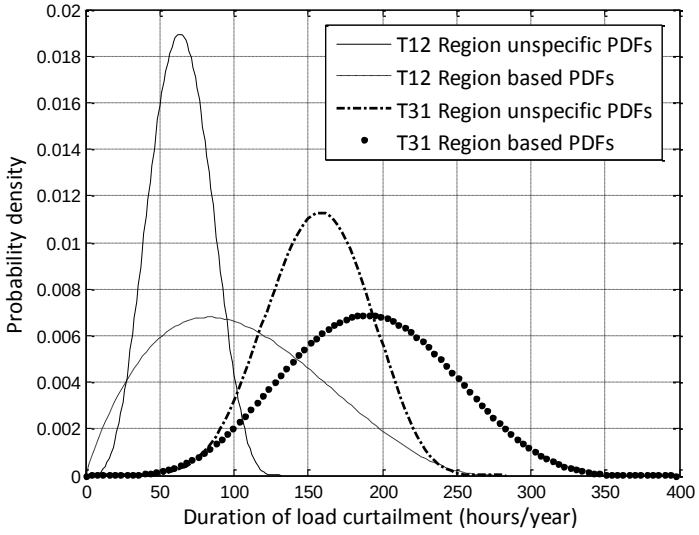

Figure 6.9: Comparative DLC indices based on single and regionally based composite input PDFs

A significant increase is noted on the indices computed for both load points. The shapes of the PDFs also change which affects the likelihood of a given index taking on different values. Consider indices computed for T31.

From Figure 6.8, the number of load curtailment events increases when regional based PDFs are applied. However, the likelihood of fewer load curtailment events also increases as seen from the lower tails of its FLC index PDFs. The lower tails of the DLC index PDFs almost overlap which shows that the likelihood of short load curtailments occurring is unaffected. The length of load curtailment events however increases when regional PDFs are applied.

A comparison of values selected from the different PDFs, with a 90 % level of confidence attached is presented in Table 6.6. Load point T12 is more affected when the external threats are modelled based on the geographic regions; the indices significantly increase.

Table 6.6: Comparison of index values selected for 90 % level of confidence

Index	T12		T31	
	Case 2	Case 3	Case 2	Case 2
PLC	0.011	0.026	0.024	0.032
FLC (events/year)	8	18	18	23
DLC (hours/year)	96	198	214	281.5

The performance of the two load points is affected by conditions in different geographic regions. While the conditions in the frontal region are less severe than in the thunderstorm region, the indices for T12 increase more significantly. The use of the single composite PDFs thus understated the likelihood of failure in the frontal region.

6.3 NETWORK OPERATIONAL SIMULATION RESULTS

This section will analyze the use severity-level-based PDFs in an operational analysis. The effect of considering threat-severity dependent levels in operational reliability of a power network, as opposed to the average level of severity applied in planning, will be investigated.

The section compares the reliability indices computed when the operational input failure models are based either on the multiple severity levels of a threat or the average severity.

The frequency and duration of load curtailment indices were computed for load points T12 and T31. The Beta PDFs representing the indices computed, with and without severity levels considered in the reliability analysis, are shown in Figures 6.10 and 6.11.

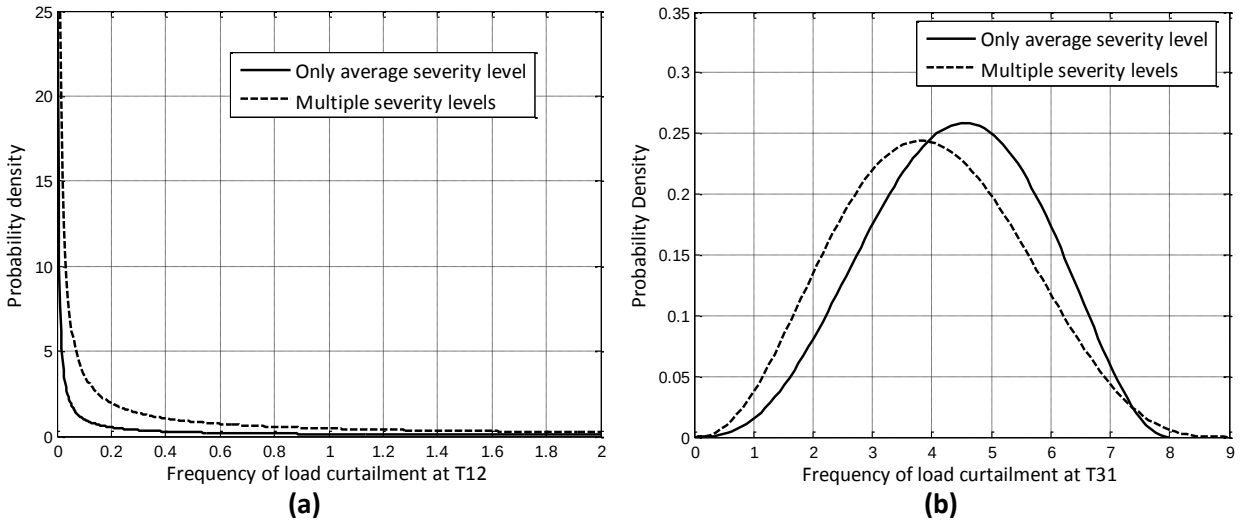

Figure 6.10: FLC index PDFs for (a) T12 and (b) T31 derived from the network operation analysis

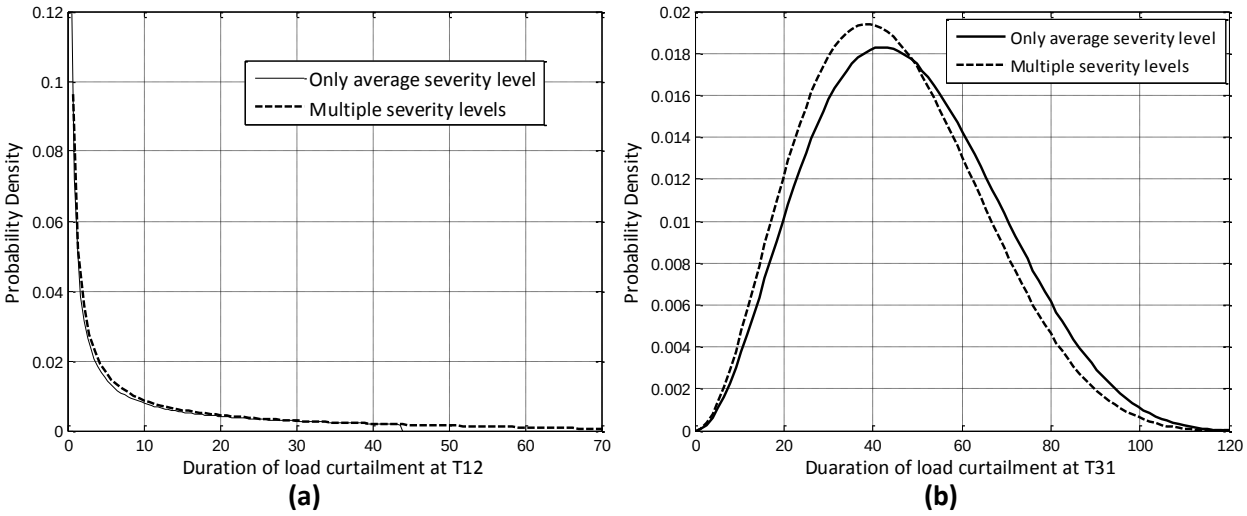

Figure 6.11: DLC index PDFs for (a) T12 and (b) T31 derived from the network operation analysis

The difference in the corresponding index PDFs shows that each load point is affected. While the index values increase, it is noted that T31 is influenced more than T12. This is attributed to the location of T31 in the thunderstorm region where lightning is more severe and would thus significantly impact the performance of T31.

The use of multiple severity levels of network threats provides a more realistic impression of component vulnerability. Even with T12 which is not as affected by lightning, the use of an average severity model erroneously understated the vulnerability of components to lightning. This is reflected in the increase in the FLC and DLC index PDFs for T12 when multiple severity level modelling is applied.

The index PDFs displayed for T31 are a good example of why using PDFs to describe reliability indices is more effective than the use of deterministic values. The skewness of T31's FLC and DLC index PDFs changes when multiple severity levels are considers. Variation in PDF skewness impacts on the likelihood of low and high extreme index values. A factor neglected when reliability indices are represented by deterministic values. Table 6.7 shows the values for T31's indices when represented either deterministically[7] or selected from the PDFs at 50 % level of confidence.

Table 6.7: T31 average index values and values selected at 50 % confidence level

Index	Average		50 % confidence level	
	Single average severity level	Multiple severity levels	Single average severity level	Multiple severity levels
FLC (events/T_w)	5.0	4.0	5.0	4.0
DLC (hours/T_w)	50.3	43.7	49.6	40.8

The results presented in Table 6.7 only predict better load point performance due to a change in failure model applied for lightning outages. The PDFs for T31 however indicate that adopting the multiple severity model increases the likelihood of the extreme values for load curtailment frequency and duration. From the upper bounds of T31 FLS PDFs, a higher likelihood of increased load curtailment events is inferred.

Table 6.7 presented values with 50 % risk (50 % confidence level). Table 6.8 shows the FLC and DLC index values selected with lower risk attached i.e. 90 % confidence level.

[7] Average of the index (EFLC)

The values presented in Table 6.8 confirm the observations made from the PDFs. The number of curtailment events is higher. However the duration of the events reduces when the failure model is changed to include the multiple severity levels.

Table 6.8: Index values selected with 90 % confidence level attached

Index	90 % confidence level	
	Single average severity level	Multiple severity levels
FLC (events/T_w)	6.0	7.0
DLC (hours/T_w)	74.0	79.3

A single dimension is achieved when analyzing reliability indices that have been represented deterministically. Conventionally average values are used which is equivalent to using values with 50 % risk level attached. With PDFs, the full range of possible index values was achieved. Analyzing Tables 6.7 and 6.8 shows that the impression of a network's performance is dependent on the risk or confidence level allowed in the index value selection. This directly impacts on the decisions based on the computed reliability indices.

6.4 DISCUSSION OF THE RESULTS FROM THE TDPA SIMULATIONS

Three areas of the decision making process can be targeted when attempting to reduce uncertainty; the inputs considered, the methodology applied and the results on which the decisions will be based. This section will show how the TDPA helped:

- Improve the representation of reliability inputs
- Allowed for the selection of the appropriate component vulnerability models
- Improved on the interpretation of the indices computed

6.4.1 Representation of reliability inputs

The results from planning analysis showed that the representation of reliability inputs as PDF is more superior to the use of average deterministic values. The PDFs enabled uncertainty in reliability inputs to be accounted for. The use of Beta PDFs ensured that the inputs could be described while capturing any dispersion and skewness. With PDFs, the full range of failure parameter values was also inputted in the analysis. This provided more realistic results.

Most of the software packages used by power utilities for reliability analyses require component parameters inputted as deterministic values. They also present the computed reliability indices in the same form. To improve the performance of such software, the TDPA could be adopted. After developing the PDF based component parameter models, a decision would then be made on the level of confidence to be attached to the deterministic values selected from the various input PDFs. In the planning analysis, the chosen level of confidence would be applied to all component models. For an operational analysis, the confidence level could vary from component to component. The time window selected and particularly the severity of the threats to which each component is exposed would determine the confidence level applied. For components exposed to the threats at either high or average level of severity, parameter values should be selected with high confidence levels attached. The margin between parameter values selected from low severity-level threat models, at either high or low confidence levels, is negligible. As such, for components exposed to threats predicted at a low level of severity, low confidence levels can be attached to the selection of parameter values.
It should be noted that while indices computed the software packages would still be deterministic values, they would be based on significantly improved reliability inputs.

The Case 2 planning analysis presented in Section 6.3.1 showed that the same results could be achieved with either single annual or two half-year failure data sets developed per component. This justified the concept of aggregation performed when developing the TDPA matrix models. This method of failure data manipulation could have its advantages.

Traditionally component failure parameters are derived on an annual basis i.e. failure or repair rate per year. Using the TDPA, component behaviour over any year can be described using PDFs that represent each significant period in a year. Each component's reliability performance would thus be represented by a number of composite PDFs describing its behaviour over different periods and times in a year. This would capture all the statistically relevant data while also showing the variability in component and network performance over a given planning period. It must be stated that the number of periods and corresponding PDFs developed depend on the available data. The data must be sufficient to ensure that statistically relevant PDFs are achieved. A case could also be made for deriving annual indices from short-term or medium-term analyses. Indices from short or medium term analyses could be aggregated to yield composite indices. Simulations carried out in planning analyses usually require more computation time than those in operational analyses because of the number of years that have to be simulated. The simulation time could be reduced by performing simulations for each significant period and then deriving composite indices for planning purposes.

6.4.2 Applying the appropriate component vulnerability models

The planning results showed that the choice of modelling approach and the application of the selected model have a bearing on the indices computed. The decisions based on the evaluated level of reliability would in turn be influenced. Each of the models described can still be used. One however has to consider the sensitivity of the analysis and the anticipated application of the indices computed. With average deterministic values, the performance of the load points could be ranked. Inputting single annual composite PDFs however provided a better indication of the actual performance of the load points. The use of single composite PDFs however disregarded the variation in external threats due to geographical regions. These two types of models are thus more suitable for general analyses which provide an overview of the network's performance in a time window.

More sensitive analyses require that the network conditions simulated closely match the actual. As such, the vulnerability models should reflect the effect of varied conditions in different geographic regions. Using regional based PDFs in the TDPA ensures that the performance of each load point can be predicted, for any investment scenario, while taking into account the conditions that actually affect the individual buses. For example:

- Network supply and loading conditions during peak hours can be more accurately represented. This ensures that practices, such as energy efficiency techniques, that aim to reduce the load in specific areas in the network can be implemented more effectively

- The timing of maintenance practices has to be carefully scheduled so that there is minimum impact on the network. The seasonal and time-dependent approach of the TDPA ensures that the most suitable period in the year and time slot can be selected after running a reliability analysis.

Most of the studies relating to adverse external network conditions have been limited to distribution networks so that the impact of the adverse elements are localized in a single geographical region and all network components are affected in the same way. In reality, adverse conditions such as weather storms are not localized and the impact has variable levels of severity depending on the path and span of a given storm. Using average values or planning models, for operational studies leads to poor diagnosis on the state of the network. Components closer to the eye of a storm are more susceptible to outages. Components in the peripherals would be less affected. Also, the severity of a weather storm diminishes with time. The component vulnerability models developed should thus account for their proximity to the storm's corridor and the time of exposure to the storm.

Applying PDFs in the operational TDPA ensured that different severity-dependent models could be developed for the dominant threat. The failure model applied in the reliability analysis may be more critical to network operation. In planning, more time is available to correct planned actions based on inaccurate reliability analyses.

For operation, network decisions and the subsequent actions have to be made in real time. The reliability indices computed impact on network operation practices such as line switching and load curtailment. If the vulnerability of the network is overstated, unnecessary switching and load curtailment could result. Operators may be unprepared due to understated network vulnerability which could result in extreme outage events.

6.4.3 Interpretation of the reliability indices

Representing computed indices using PDFs improved on their description. The computation of a finite range of possible values for each load point index is particularly useful to utilities that have to measure their performance against standards set by the national regulators. The range of index values provides a quick impression on the network's performance with regard to the possibility of a penalty or reward.

The different index shapes exhibited by the PDFs reflected the effect of variability in external threats on different load points and overall system. From the shape parameters, and thus the skewness of the PDFs, one could identify the likelihood of an index taking on low or high values. The selection of an index value, other than the mean is quite significant. Network planners base their decisions on reliability study results. A balance between financial investments in a network and providing optimal reliability levels is always required. Effective decision making requires minimal uncertainty in the process. Using PDFs, allows selection of index values at different levels of confidence (conversely risk). This provides a measure of quantifying the uncertainty in a decision based on the selected index value. The decision to use either high or low levels of confidence is dependent on the purpose and type of analysis. It is clear that values with high confidence levels attached should be used for low levels of uncertainty. Decisions with potentially high financial impact may justify the application of high levels of confidence. An indication of how the expected outcome varies with the risk may also suffice.

6.5 SUMMARY

Qn.7: Does the use of PDFs in either network planning or operation studies yield more useful results for each scenario?

The use of PDFs in the planning analyses improved the representation of reliability inputs so that a more realistic impression of the network's reliability was achieved.

While the concept of average vulnerability models is valid for planning, the models should be applied appropriately. The perception of system reliability that is provided by computed indices depends on the input failure models applied. Furthermore, the risk level attached to index values also affects a reliability analysis. Variation in the severity of the threats is more distinct in network operation so that the average vulnerability model is not sufficient. Multiple severity level models are thus required. More information was also available when the reliability indices were represented as PDFs; the actual range of each index and the skewness of the index PDF were represented. A planner or operator is thus able to quantify the uncertainty in the index values selected.

6.5.1 Onward

The simulations thus far show how the TDPA can be applied to either network planning or operational studies. The component vulnerability models required by each analysis were described and the results computed discussed. The next chapter show how PDFs can be applied to link planning and operational analyses. The chapter will show how long-term vulnerability models can be translated into operational ones. The chapter will particularly investigate the impact of global threats on a network already predisposed to local weather threats. It analyzes the effect of network exposure to adverse space weather threats, specifically Geomagnetically Induced Currents (GICs), on a reliability analysis. GICs can be categorized as long-term threats but cause severe damage in operational time windows.

7. ANALYZING IMPACT OF THREATS WITH IMMEDIATE AND DEFERRED EFFECTS ON POWER NETWORK: GEOMAGNETICALLY INDUCED CURRENTS (GICs)

7.1 INTRODUCTION

The TDPA simulations carried out thus far analyzed the reliability of a network exposed to local external threats. In Chapter 5, the network threats were considered as affecting either planning or operation. The results of these reliability simulations were presented and discussed in Chapter 6. Some network threats can not however be regarded to have a distinct impact on only planning or operation. This Chapter will consider such a network threat; geomagnetically induced currents (GICs).

The May 2013 ruling by the Federal Energy Regulatory Commission (FERC) for new reliability standards recognized the potentially severe, wide-spread impact of GICs on the reliable operation of the bulk power systems [FERC, 2013]. Exposure to GICs is global and can have either immediate or deferred effects on network reliability. The most significant impact of GICs on power systems is damage to large power transformers.

It has been reported that the sun goes through a solar cycle every 11 years and that the intensity of GICs depends on the intensity of the solar flares [Molinski et al, 2000; Hutchins & Overbye, 2011]. GICs could thus be categorized as long-term network threats affecting planning. GIC events however occur for short periods during which severe damage can also be caused. A single event, lasting just a few minutes, has the potential to cripple portions of a power grid for weeks, even years [Hutchins & Overbye, 2012]. GICs thus present a unique kind of external threat to networks whereby network operators have to include elevated risk of failure due to potential GIC events. The risk of network failure could also be elevated in operational time windows due to deferred or neglected maintenance of components.

This chapter will use the TDPA to show how operational failure models can be derived whilst accounting for the elevation in risk of failure due to a threat with short and long term effects. It should be stated that collection of transformer failure data, for the South African power network, with respect to GICs is ongoing. Hypothetical failure models were thus derived.
This however puts no limitation on the methodology presented i.e. the GIC failure models can be changed. The transformer failure models derived are however based on real experiments carried out within the research group at the University of Cape Town. Some of the experimental results are presented herein.

7.2 FAILURE MECHANISM OF POWER TRANSFORMERS

Bossi et al [1983] consider a transformer to have failed if the unit has to be removed from service to be repaired. This is quite a restrictive definition. Failure of a transformer as viewed from network operators regards the impact of taking it out of service on the reliability of the network [Lapworth, 2006]. The IEEE developed guidelines for the collection and reporting of transformer failures. The establishment of a databases and statistical analysis of data through the calculation of failure rates was recommended [IEEE, 1986]. The IEEE transformer committee developed the failure rate evaluation rating presented in Table 7.1 [Kachler, 2001]. According to the evaluation scheme, failure rates can vary from being excellent to unacceptable.

Table 7.1: Failure rate evaluation scheme proposed by the IEEE [Kachler, 2001]

Transformer failure rate (λ_{tr})	Evaluation
$\lambda_{tr} \leq 0.5\%$	Excellent
$0.5\% < \lambda_{tr} \leq 1\%$	Good
$1.0\% < \lambda_{tr} \leq 1.5\%$	Satisfactory
$1.5\% < \lambda_{tr} \leq 2\%$	Acceptable
$\lambda_{tr} > 2\%$	Not Accepted

A summary of transformer failure rates from different surveys is provided in Table 7.2. The table is based on failure rates of differently rated transformers from a number of national utilities spanning a period of 37 years (1968 to 2005). The table shows that transformer failure rates vary with age and application.

The causes of transformer failure can be grouped into three main categories [Allan & White, 1995; Sokolov, 2005]:

- Failures due to weak specification, design deficiencies, manufacturing weaknesses or material defects
- Failures due to system disturbances, operational factors, or interactions between the transformers and other equipment on the system,
- Failures which result from maintenance operations, repairs or refurbishment that have or have not been undertaken.

Table 7.2: Failure rates from surveys from 1968 to 2005 [Jagers, 2011]

Survey Source	Application/ Classification	Failure Period	Manufacturing Period	Failure Rate (%)
Cigré International Survey	All voltage levels (60kV-700kV)	1968 - 1978	Pre 1978 2	2
United Kingdom	All voltage levels	Pre 1987	Pre 1987	< 2
United Kingdom	Generator Step-Up, Major failures	1974 - 1995	Pre 1995*	1.2
ZTZ Service Database, Ukraine	Generator Step-Up & Transmission Rated power ≥ 100MVA	2000 - 2005	Pre 2005	1 - 2
US-NGRID, United States	Distribution 115kV, 69kV & <69kV	-	-	0.35 - 0.8
Hydro Quebec, Canada	All voltage categories, major failures	-	-	<0.5
American Electric Power	345kV & 765kV	Pre 1986	Pre 1986 *	1.3 - 2.9
American Electric Power	345kV & 765kV	Post 1986	Post 1986 *	0.35 - 1.35
Australia & New Zealand	Costly failures	Pre 1996	Pre 1996	0.4
* Indicates studies where the manufacturing period was given.				

William and Bartley [2003] however state that transformer failures, whether due to a combination of mechanical, electrical or thermal factors, ultimately involve and result from breakdown of the transformer insulation.

They performed an analysis of transformer failure statistics received from different insurance companies for a 5 year period (1997 to 2001). The highest total amount paid out, as shown in Table 7.3, was to insurance claims reporting insulation failure.

Table 7.3: Insurance claims paid out for different transformer failure causes [William & Bartley, 2003]

Cause of Failure	Number of failures	Total Paid out ($Millions)
Insulation Failure	24	149.97
Design /Material/Workmanship	22	64.70
Unknown	15	29.78
Oil Contamination	4	11.84
Oil Contamination	4	11.84
Overloading	5	8.57
Fire /Explosion	3	8.05
Line Surge	4	4.96
Improper Maintenance /Operation	5	3.52
Flood	2	2.24
Loose Connection	6	2.19
Lightning	3	0.66
Moisture	1	0.18

The deterioration of transformer insulation is a time function of temperature, moisture content and oxygen [IEEE, 1995]. The insulation temperature is however the main controlling parameter [Jian et al, 2007]. Section 3.2.3 described the saturation of transformers due to induced GICs. The relative permeability of the magnetic core tends to 1 as the level of saturation increases. GICs thus generate fringing magnetic flux i.e. flux flowing outside the core. Gaunt and Coetzee [2007] state that "w*ithout adequate control of the flux under saturation conditions, local heating in parts of the transformer may not be cooled effectively, leading to rapid temperature increase. The intensity of overheating depends on the saturation flux paths, cooling flow and the thermal condition or loading of the transformer".*

The windings hottest-spot temperature (HST) and dissolved gas (DG) in the insulation oil are used as indicators of the stress (insulation damage) imposed on a transformer.

A transformer failure occurs when the withstand strength of the transformer with respect to one of its key properties is exceeded by operating stresses. Fu et al [2001] state that the winding HST in the top or in the centre of the transformer windings is the highest temperature subjected to the insulation system. As the winding temperature increases, the mechanical strength of the winding insulation material decreases. The potential for transformer failure thus increases. Also, gas bubbles may also form which facilitates the breakdown of the dielectric characteristics of the transformer oil.

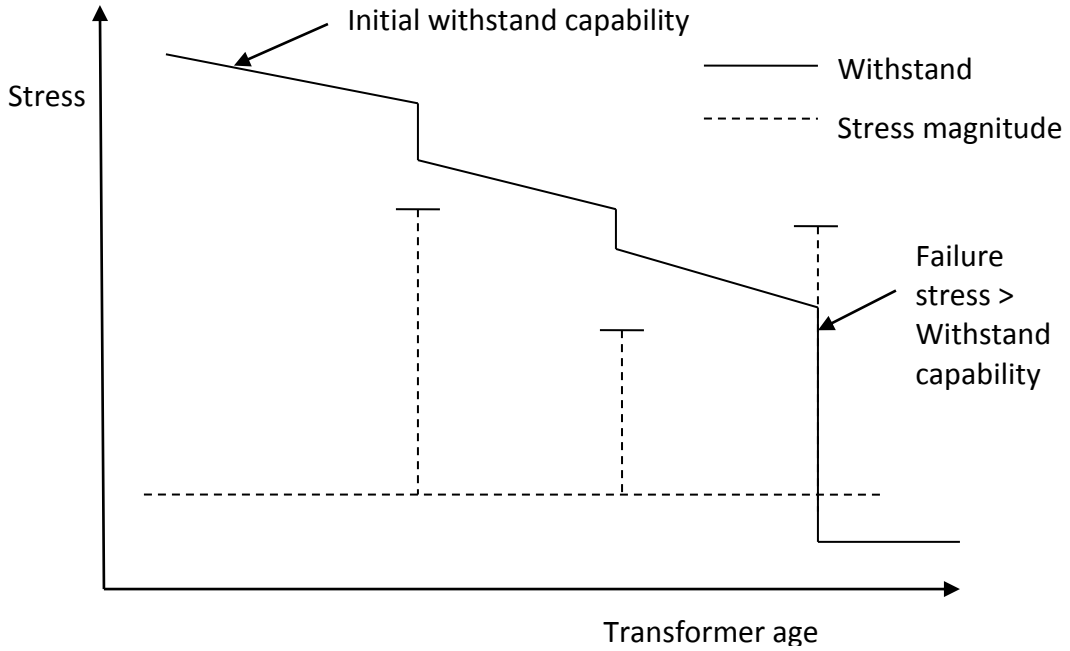

Figure 7.1: Risk of transformer failure due to insulation degradation [Herman et al, 2011]

Figure 7.1 shows the stress in a transformer putting it at risk of damage and the failure of a transformer weakened by prior stresses [Herman et al, 2011]. The figure shows that the susceptibility of transformers to further damage and failure increases as the withstand capabilities of the insulation progressively deteriorates because of stresses. A threshold can thus be specified based on either the HST or a DG analysis. Measurements of HST or DG beyond the threshold would indicate that the transformer has entered a critical region where failure is imminent.

7.3 FACTORS INFLUENCING TRANSFORMER FAILURE

The failure rate of transformers is not a constant parameter. Transformer insulation life and thus the failure threshold, is a function of factors such as the age and application of the transformer, and its operating conditions such as MVA loading and ambient temperature. A transformer load carrying ability study was performed by Wong [1994]. The author investigated the correlation between the time-varying transformer loading profiles and ambient temperature profiles and analyzed the impact on the transformer thermal behaviour. An on-line transformer diagnostic system has also been proposed [Meliopoulos et al, 1998]. It predicts transformer loss of life based on historical data. A risk-based probabilistic method was proposed by Fu et al [2001]. It considered insulation failure due to transformer overloading. The ambient temperature and transformer loading were regarded as stochastic quantities so that a range of possible HST could be derived.

Van Schijndel et al [2007] predicted the susceptibility of a transformer to failure based on age through the degree of polymerization (DP). The DP test assesses the age of the insulation paper of the transformer windings. The Doble laboratory tests [Doble Website] showed that "*generally, paper in new transformers has a DP of about 1000. Aged paper with a DP of 150-200 has little remaining mechanical strength, and therefore makes windings more susceptible to mechanical damage during movement, particularly during extreme events such as through-faults.*"

Figure 7.2 shows the DP- value predicted for a given transformer based on the probabilistic approach proposed by Van Schijndel et al [2007]. The accuracy bandwidths derived for the DP value, DP (t), and the DP-threshold are also shown. According to Figure 7.2, the mechanical strength of a new transformer is high but deteriorates as it gets older to a value below a critical threshold.

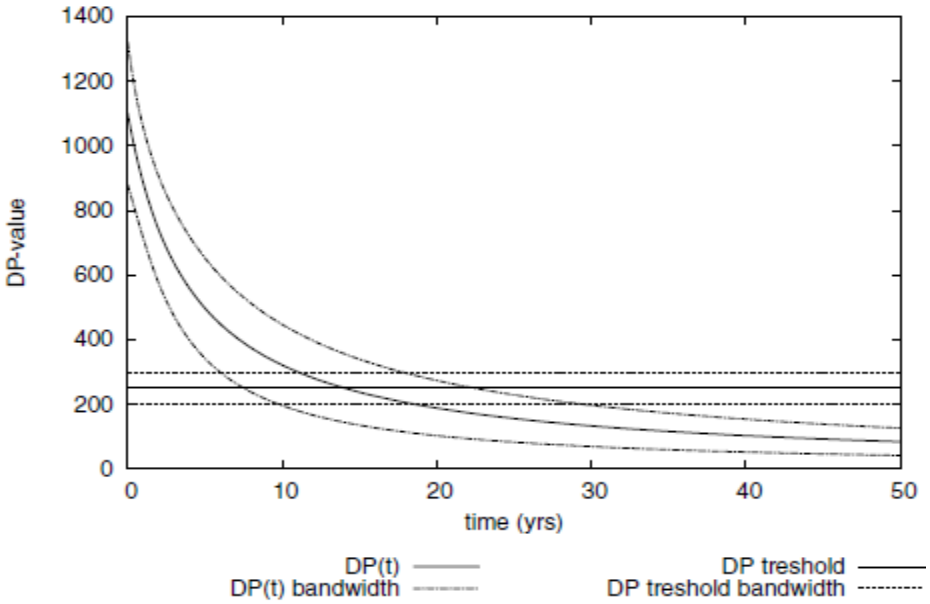

Figure 7.2: Variation in DP-value and DP-threshold with transformer age [Van Schijndel et al, 2007]

Jagers [2011] analyzed the failure rate patterns of transformers with new and older designs and reviewed related studies from different authors. The studies showed that transformer failure patterns vary with the transformer manufacturing period and design.

Generation Step-up transformers are usually operated close to their ratings compared to distribution units. As such, their insulation has to withstand more stress. Jagers [2011] also displayed the variation in transformer failure rates based on the transformer voltage groups.
Table 7.4 shows transformer failure data categorized according to the application, voltage group and manufacturing period. The table shows that failure rate increases with transformer size (application and voltage group).

Table 7.4: Average annual failure rate according to manufacturing period, transformer application and highest system voltage for transformers with tap changers [Jagers, 2011]

Application & Voltage Groups	PRE 1978		POST 1978	
	Failures (1/yr)	Failure Rate (%)	Failures (1/yr)	Failure Rate (%)
60 ≤ kV <100	**17**	**1.5**	**2**	**0.3**
Power Station TRFRs	15	1.8	-	-
Substation & Auto TRFRs	2	0.8	2	0.3
100 ≤ kV < 300	**82**	**2.2**	**69**	**2.6**
Power Station TRFRs	65	2.5	5	6.5
Substation & Auto TRFRs	17	1.5	64	2.5
300 ≤ kV < 700	**113**	**5.2**	**60**	**4.8**
Power Station TRFRs	18	2.4	13	**3.4**
Substation & Auto TRFRs	95	6.6	47	**5.5**
60 ≤ kV < 700	**212**	**3.0**	**131**	**2.8**
Power Station TRFRs	98	2.4	18	3.9
Substation & Auto TRFRs	114	6.0	113	2.7

7.4 MODELLING TRANSFORMER FAILURES DUE TO GICs

This section will show how failure models of long-term threats are translated into operational failure models. The model will account for component failure due to either excessive stress imposed by a random shock or due to accumulated damage from multiple shocks.

Other than age and application, the severity and rate of deterioration of the transformer insulation is also influenced by external random shocks. The transformer is deemed to be in a critical condition as soon as the damage, due to an extreme shock, or the cumulative damage, due to multiple shocks, exceeds a predetermined threshold [Wang & Pham, 2011]. The lifetime of a transformer is usually specified by the owner (utility). The manufacturer then designs for a failure model that enables the transformer withstand different shocks over its lifetime.

GICs have however been reported to cause extensive damage to affected transformers shortly after exposure. The failure of transformers in Tutuka, Matimba and Lethabo power stations, in South Africa, after the '*Halloween storm*' at the beginning of November 2003 testifies to this. The units are monitored regularly with on-line DG analysis applied to some.

Gaunt and Coetzee [2007] reported that "*a transformer at Lethabo power station tripped on protection on 17th November. There was a further severe storm on 20th November. On 23rd November the Matimba #3 transformer tripped on protection and on 19th January 2004 one of the transformers at Tutuka was taken out of service. Two more transformers at Matimba power station (#5 and #6) had to be removed from service with high levels of DGA in June 2004. A second transformer at Lethabo power station tripped on Buchholz protection in November 2004*." The manufacturer based models have to be adapted to reflect the threat GICs pose to network operation.

While the likelihood of transformer failure is dependent on the state of the transformer i.e. age, loading and design, it can also be regarded as a function of the characteristics of a GIC shock event. The signature of the induced GICs, either magnitude or duration, should be such that the hotspot(s) generated in the transformer is sufficient to cause damage. The time of occurrence of a GIC event is also significant because of the effects induced GICs have on transformer performance.

The NERC report [2012] compiled investigations from different authors ranging from the prediction of space weather, calculation of GICs, effect on power systems to operation mitigation strategies. It was reported that GICs impact on voltage and angle stability. Also saturated transformers produce unusual MVAr and MW swings [Hutchins & Overbye, 2012]. Berge et al [2011 (2)] presented a linear increase in the reactive power absorbed by a transformer as the induced GIC levels increased. The effect on the transformers output power was not reported on. The definition of a transformer failure state should thus be extended to include a drop in performance that impacts on the stability and reliability of a network.

While the NERC report [2012] showed how the transformer temperature increases with the simulated induced GICs, variation in transformer reactive power consumption and output (voltage and power) was not investigated.

The laboratory experiment described in Appendix D was used to confirm the reported effects of GICs on a transformer, particularly on its input MVars and output MW. The lab set up is shown in Figure 7.3. Current (dc) was injected through the transformer neutrals to simulate GICs.

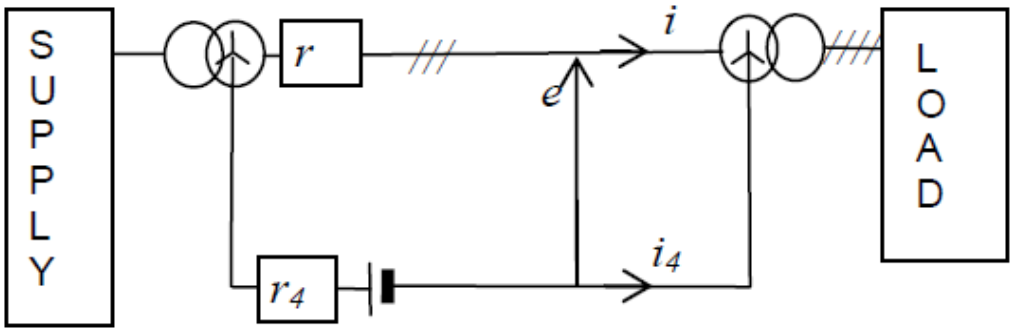

Figure 7.3: Laboratory test system to simulate injection of GIC into the neutral of the load transformer [Gaunt & Malengret, 2012]

The source transformer was significantly over-rated so that the dc component had negligible effect on its magnetisation characteristics. A small isolated three-phase generator was used as the power supply and care was taken to ensure that the applied voltage across the load transformer did not correspond to over-excitation. The dc current was increased gradually and the effect on the load transformer's reactive power (Q) consumption and apparent power output (S) noted. The experiment was replicated and some of the results are presented in Figure 7.4.

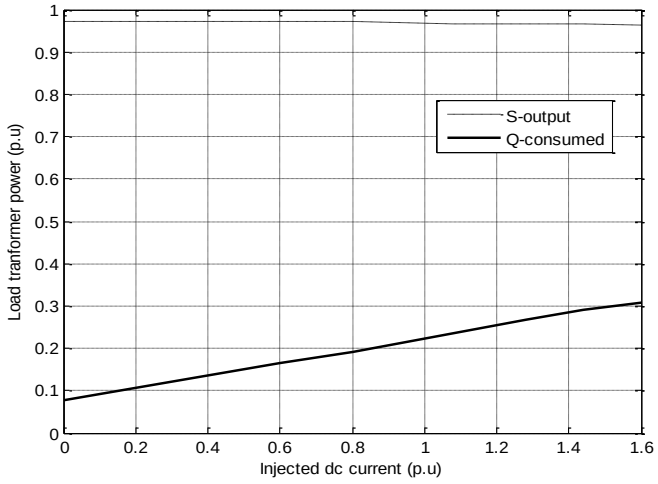

Figure 7.4: Variation in apparent power (S) and reactive power (Q) characteristics of load transformer with dc injection

Figure 7.4 shows that while the power output dropped, the amount of reactive power absorbed increased with increase in dc injection. The risk posed by a GIC event can thus be classified either in terms of:

- the accelerated failure of a transformer after the event (severity of expected damage)
- and/or reduced transformer capability during the event

Transformer failures due to GICs should thus be defined with respect to the GIC event i.e. whether GIC event is extreme or not.

7.3.1 Transformer failure model due to an extreme GIC event

The shocks experienced by transformers have variable magnitude and occur at random times. One of the commonly applied shock models is the extreme shock model [Wang & Pham, 2011]. The model considers exposure to an individual shock such that a system fails as soon as the magnitude of the shock effect goes into a critical region. Such shocks are deemed as extreme.

Figure 7.5 describes the failure pattern of a transformer with and without the influence of an extreme GIC shock. A critical region is identified by a threshold such that the transformer is highly likely to fail due to breakdown of its insulation when in this region.

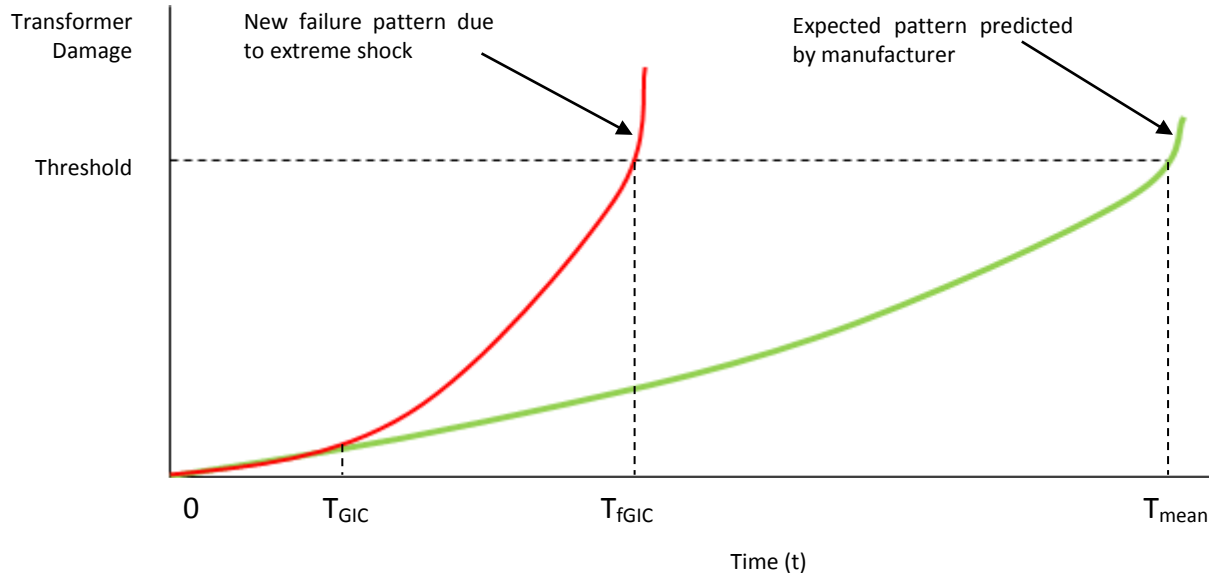

Figure 7.5: Description of transformer failure patterns; predicted and due to extreme shock

It should be stated that despite the representation in Figure 7.5, T_{GIC} and T_{fGIC} are considerably shorter than T_{mean}. Three key times are also shown in Figure 7.5:

- T_{GIC}: Time of exposure to a GIC shock. Can be categorized further than just the year of exposure by including the season and time-of-day
- T_{fGIC}: Time of failure due to GIC event. If a GIC event is extreme, the transformer fails shortly after exposure. The transformer thus fails (T_{fGIC} - T_{GIC}) hours or days after exposure
- T_{mean}: Expected time-to-failure. This is usually specified by the utility and considers the ability of the transformer to withstand all expected stresses in its lifetime. Power transformers usually have a life span of more than 30 years.

The likelihood of a transformer failing, $P(t < T_{mean})$, has three components as shown in (7.1). These relate to the probability of a given GIC event occurring, the state of the affected transformer, and its manufacturer based failure trend.

$$P(t < T_{mean}) = 1 - (HI * P_{trfr} * P_{GIC}) \quad (7.1)$$

- P_{GIC} is the probability that the GIC event that occurs is extreme i.e. can lead to over saturation of the transformer or cause extreme damage to the transformer windings. GIC events that cause such effects could have a specific signature. The probability of a specific GIC event occurring can thus be computed from historical events. The probability of GIC events corresponding to different exposure durations or induced GIC magnitudes are derived while considering the effect on the transformer.

- HI is the health index of a given transformer. It describes the state of the network at the time of exposure to a GIC event. Using on-line monitoring systems and tests, the state of the transformer can be graded. The HI is thus a scalar between 0 and 1. Newer or 'healthy' transformers will have HI values closer to 1.

- P_{trfr} is the probability of a transformer surviving up till the time of exposure to the GIC event. It is based on the survival trend designed for by the manufacturer or specified by the utility. This represents the transformer failure model applied in planning analyses. Such a trend is developed from all shocks that the transformer endured and can be categorized into seasonal and time-of-day windows. The probability varies from transformer to transformer, in each window, based on age and application.

6.3.2 Transformer failure model due to multiple GIC events

In the absence of an extreme shock, a transformer could also fail due to the compound effect of multiple shocks. The probability of a transformer surviving up till the N^{th} shock is a function of the probabilities of surviving the previous shocks [Esary & Marshal, 1973].

The cumulative shock model according to Wang & Pham [2011], describes a system's break down when the cumulative shock magnitude exceeds the specified threshold. Figure 7.6 shows that the before the ultimate shock, the likelihood of transformer failure is elevated by each shock.

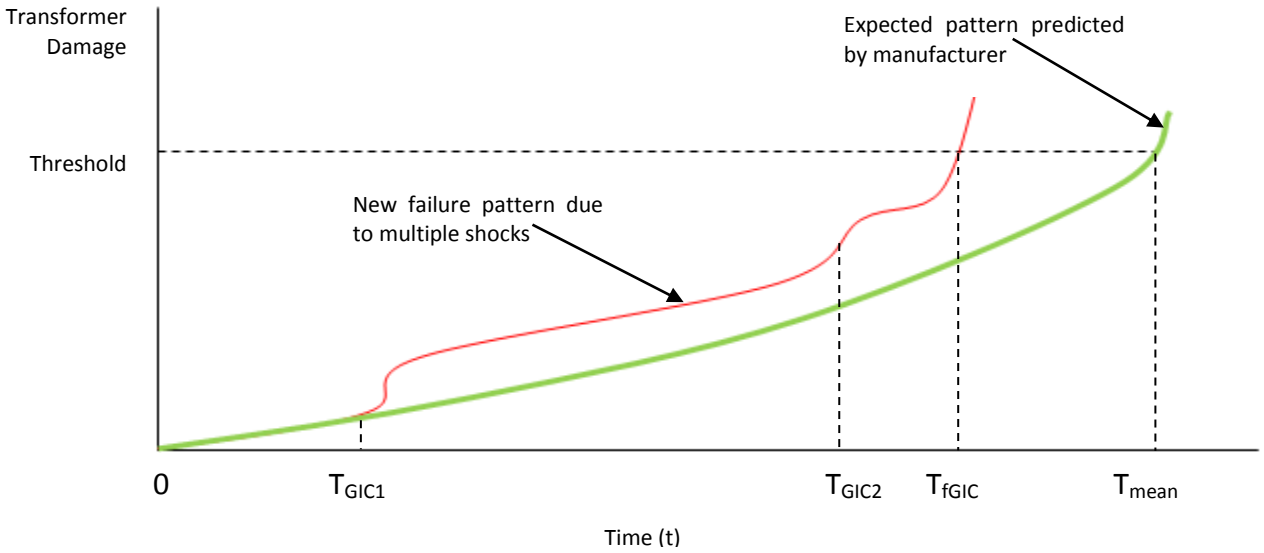

Figure 7.6: Description of transformer failure patterns; predicted and due to multiple shocks

The multiple GIC shock model considers transformer failure resulting only from insulation damage and not due to over saturation. The likelihood of failure is thus derived from (7.2). T_{fGIC} is the time-of-failure since exposure to the first GIC event.

$$P(t < T_{mean}) = 1 - (HI * P_{trfr} * \sum_{k=1}^{N} P_k) \quad (7.2)$$

The definitions for HI and P_{trfr} are as described in Section 6.3.1. P_k is the probability of a non-extreme GIC shock k occurring. The cumulative component in (7.2) is limited by the number of shocks required to push the transformer into the critical region.

7.5 INCLUDING EXPOSURE TO GICs IN A RELIABILITY ANALYSIS

In the absence of the extreme and multiple GIC shock models, the likelihood of failure is determined only from the failure PDF based on the manufacturer's design (P_{trfr}). This section will analyze the effect of using operational PDF models that describe the elevated risk of failure as opposed PDF models developed by the manufacturer.

The span of GIC exposure is widespread so that all transformers of a utility can be influenced simultaneously. As stated in Section 7.2, the impact of GICs on individual transformers would however depend on location, type of transformer, age, loading and application. The occurrence of global and local weather threats is independent of each other. The effect of GICs can thus be superimposed onto a network already influenced by local weather threats. It is important to note that the parameters described in the GIC shock models are stochastic so that the TDPA matrix model can be applied.

Hutchins and Overbye [2012] determine the magnitude and direction of GICs in a network by modelling and simulating the induced geoelectric field in a power flow software package. Utilities are however more interested in the effect of a given GIC event on the network. It is thus important to know the transformer response characteristic for different GIC storms. Berge et al [2011] investigated the impact different GIC magnitudes in a power flow study. A technique that correlated the magnitude of GICs and the reactive power absorbed by transformers was applied. As discussed in previous sections, the drop in power performance of transformers is only one of the categories of transformer failure due to GICs.

The two power flow studies thus provide an incomplete impression of the effect of GICs on a network. The impact of transformer damage can be investigated through a reliability analysis. The probability of transformer damage or failure due to GICs must be considered in the context of the local conditions that affect the network. A reliability analysis thus ensures that the occurrence of local threats is not overlooked. The flow chart in Figure 7.7 shows how effect of GICs can be included in the TDPA based simulation process discussed in Section 4.3.4.

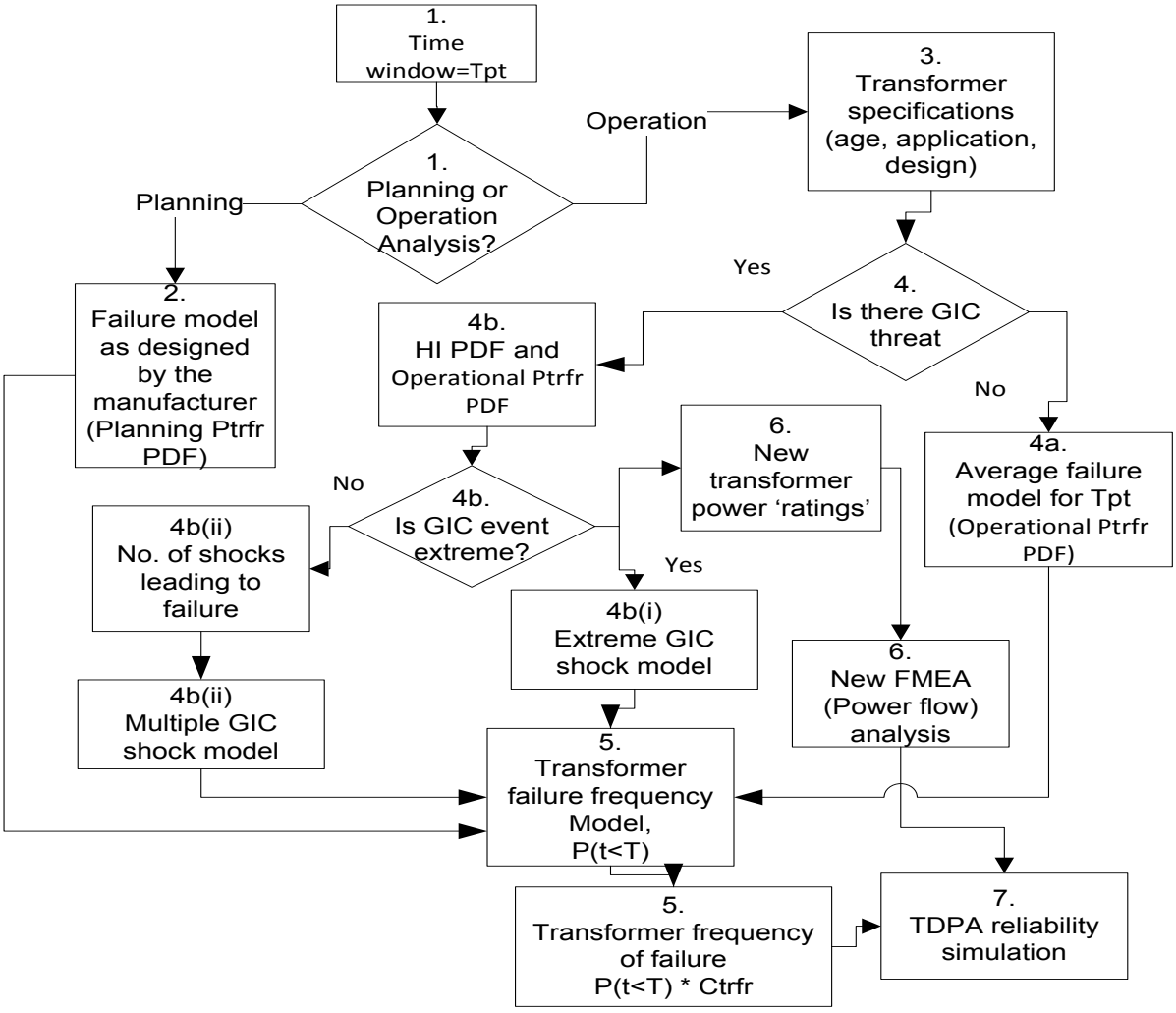

Figure 7.7: Simulation required for inclusion of transformer failures due to GICs

The key steps in the flowchart are described below:

1) Determine the time window depending on the type of analysis i.e. either planning or operation

2) For a planning analysis, the manufacturer based failure model is adopted for transformers. Same model could be applied to a group of transformers e.g. GSU failure model. Long-term PDF models can be developed from historical failure data

3) In a network operation analysis, the factors that influence transformer performance such as loading have to be considered while regarding the time window (specific season and time slot). The age and application of individual transformers becomes significant

4) Is there an impending GIC event?

4a) In the absence of GIC threat the manufacturer based failure model is only influenced by the operating conditions identified in Step 3. Short-term failure models are developed for each time window

4b) With a GIC threat predicted, the seasonal and time-dependent failure model is adapted. The new failure model depends on the type of GIC event.

4b (i) Model applicable to extreme GIC events

4b (ii) Model applicable to non-extreme GIC events

5) The frequency of transformer failure in a selected time window is derived from the appropriate model ($P(t<T)$ and scaling factor (C_{trfr})

6) The effect of a given GIC level on the MVars consumed and MW outputted by a transformer can be predetermined. Variation in the performance of a transformer also impacts on the power stability of a network. A power flow based FMEA could thus yield a different set of failure states for the load points

7) The transformer failure models and new FMEA are inputs to the reliability analysis

7.4.1 Application to a real bulk network

The effect of GICs on a network's reliability was analyzed for the time window characterized by the first quarter of the year and the noon and 6 pm time slot.

The bulk network presented in 5.2 was considered. The operational case study presented in Section 5.2 is modified to include the risk of transformer failure due to occurrence of GIC events.

For illustration purposes, the GIC events were categorized as either extreme or non- extreme. It must be stated that sub-categories of GIC events can be identified between the extreme and non-extreme categories. As such different PDFs could be achieved for different categories of GIC events. The PDFs in Figure 7.8 were assumed for probability of a transformer surviving till the time of exposure to a GIC event and the probability of either an extreme or non-extreme GIC event occurring. The shape parameters are presented in Table 7.5.

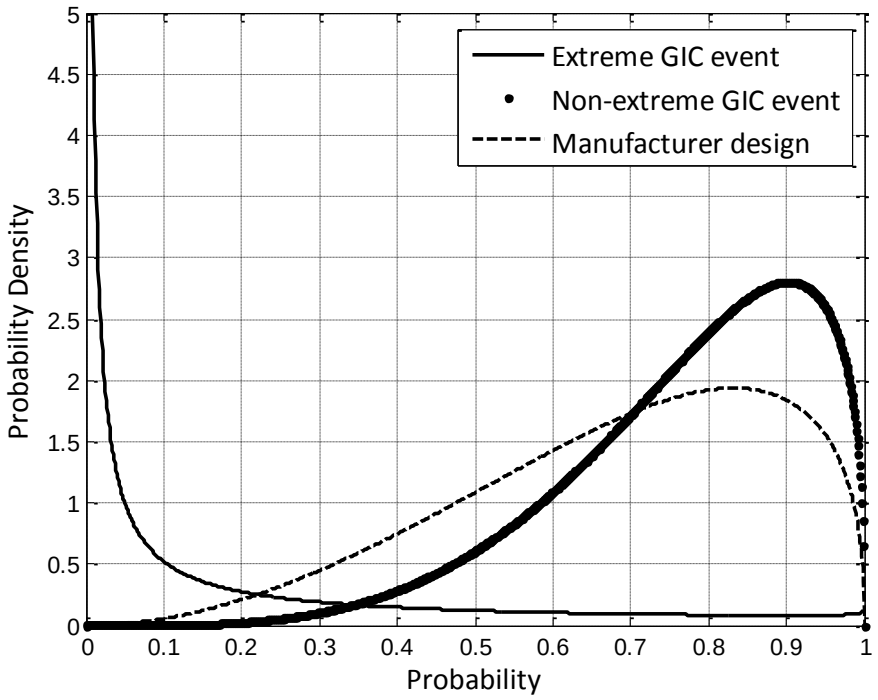

Figure 7.8: Hypothetical PDFs representing probability of types of GIC events occurring and of transformer survival up till the occurrence of a GIC event as designed by the manufacturer

Table 7.5: Shape parameters of transformer survival and GIC event PDFs

Type of PDF	Shape Parameters
Transformer survival (P_{trfr})	3, 1.4
Extreme GIC event	4.7, 1.5
Non-extreme GIC event	0.06, 0.9

The results of two operational reliability analyses are presented in this section. The first analysis did not consider the occurrence of GICs.

The transformer failure model was thus based on the survival PDF shown in Figure 7.8 which represents the survival of the unit based on the manufacturer's design. The second analysis considered the occurrence of GIC events. The models presented in Section 7.4 were applied to the transformers. The manufacturer-design based PDF was thus scaled in each GIC model using either the extreme or non-extreme GIC PDFs shown in Figure 7.8. In each simulation run, a uniform random number generator was used to determine whether a given GIC event was extreme or non-extreme. A uniform distribution was used to represent the transformer health index in the selected time window.

A comparison of the frequency and duration of load curtailment indices computed for each case is presented in Figures 7.9 and 7.10 respectively. The indices are presented for load point T31.

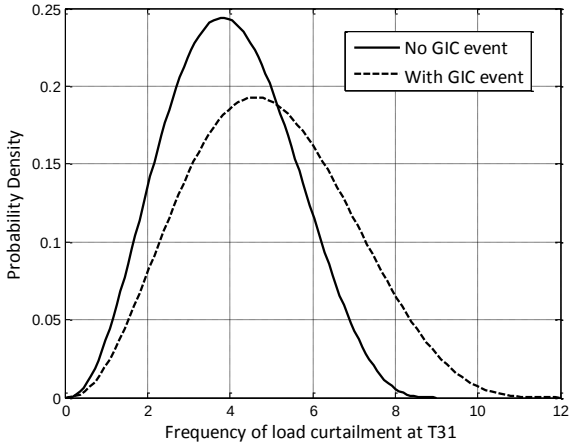

Figure 7.9: Effect of GIC exposure on the FLC index of load point T31

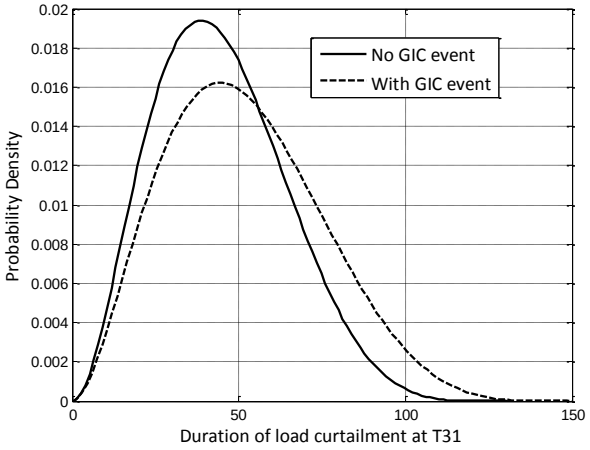

Figure 7.10: Effect of GIC exposure on the DLC index of load point T31

The inclusion of GIC events in the operational analysis leads to an increase in the frequency and duration of load curtailment events at load point T31. This is indicated in the reduced likelihood of few load curtailment events and increased likelihood of upper end extreme curtailment events. This was expected since the GIC shock models account for an elevation in likelihood of transformer outages. A similar impact is noted in the DLC index PDFs in Figure 7.10.

The effect of using the GIC shock models is further analyzed in Table 7.6. The table quantifies the increase in index values due to the use of the GIC shock models. A comparison of index values selected at 50 % and 90 % confidence level is presented. Table 7.6 shows an increase in the indices at two levels of confidence considered.

Table 7.6: Comparison of effect of GIC exposure on index values at 50 % and 90 % confidence level

Index	50 % confidence level			90 % confidence level		
	No GIC	With GIC	% increase	No GIC	With GIC	% increase
FLC (events/T_w)	3.9	4.5	15.3	6.0	7.8	30
DLC (hours/ T_w)	40.8	54.6	33.8	76.2	87.3	14.6

The increase in the indices presented shows that the GIC shock models were able to account for the elevation in risk during the operational time window considered.

7.6 IMPLICATIONS OF RELIABILITY BASED GIC STUDY

The life-time of a transformer is one of the specifications provided by utilities to guide the manufacturer's design. For planning a failure rate can be assigned to a category of transformers, either generation step-up or transmission units, in the network. The failure rate is modelled deterministically and usually varies due to aging. The use of manufacturer based failure models, particularly in operational time windows is not sufficient. When operational time windows are considered, the transformer's operating conditions have to be considered when determining its likelihood of failure.

Factors such as loading, moisture content and external threats usually influence the transformers so that the risk of failure is elevated. The performance of the considered load point deteriorated when failure models that capture the elevation in risk of failure were applied in the reliability analysis. The TDPA models incorporated a health index. The index provides a means of changing the probability of component failure and system risk in general. It indicates the state of the network and its components in different time windows. As such, the influence of different seasonal and time-dependent factors on the failure of a component can be graded.

The analysis showed that the impact of GICs can be included in a reliability analysis. Utilities strive to minimize costs while trying to mitigate the effects of predicted threats. One of the mitigation strategies proposed and adopted by networks where GIC have caused extensive damage in the past include the use of series-capacitors in the network. Network transformers could also be replaced with units that have a high GIC withstand level. These strategies are planning issues and require high time and capital investments especially considering that GIC events do not last long. Temporary approaches based on power flow analyses have also been recommended [Berge et al, 2011(1); Hutchins & Overbye, 2011 &2012]. The network is reconfigured, either through line or transformer tripping, to reduce the magnitude of GICs in the transformers. These approaches however do not take into account the real-time availability of all network components when a GIC warning is received. Previous chapters showed that network components are already influenced by local weather threats which could aggravate the impact of a GIC event.

The GIC reliability analysis developed models that allow the impact of GIC threats on an already stressed network to be investigated and quantified. Line switching changes the topology of the network and the potential load point and network failure states. The TDPA reliability analysis would thus be performed for each topology achieved until the optimum (with least impact) reliability levels are achieved. This provides operators with a means of monitoring and analyzing the vulnerability of their networks for a forecasted GIC event.

Operators would thus be able to modify the network depending on the scale of impact of the predicted GIC event without neglecting the local threats that affect it. Reconfiguration of the network is not a solution to the GIC problem but a means of managing or reducing the impact on a network. Permanent solutions can also be incorporated but the decision to use either or both depends on the utility (size and structure) and the severity of GIC storms experienced.

8. CONCLUSIONS AND FUTURE WORK

This chapter presents a review of the research questions and the main conclusions drawn. Ideas for future work that the research has opened are also identified.

8.1 ASSESSING THE VALIDITY OF THE HYPOTHESIS

This thesis was based on a hypothesis. The answers to the research questions aimed at validating the hypothesis are summarized below:

Q1) Measurement of reliability and presentation of results

Sequential MCS is the most suitable reliability evaluation technique for bulk networks. The variability in performance of network components due to, among other reasons, a stochastic environment can be captured in an analysis. It is also able describe failure parameters as PDFs and also derive the underlying distributions of the indices computed. Reliability indices are conventionally represented as deterministic values. However, using PDFs provides a better description of the indices. More information is derived from the inspection of the dispersion and skewness of the index distributions.

Q2) Effect of external network threats and vulnerability approaches proposed

Network performance is significantly influenced by the environment. The threats faced by networks can be categorized as either local or global. Local weather threats like lightning have specific regions of influence while global threats like GICs can influence the whole network.

A number of approaches have been proposed to capture the vulnerability of network components to external threats. The models however have different limitations such that they can not be applied effectively in both planning and operational reliability analyses.

Q3) Impact of seasonal and time-dependent variations on component reliability parameters

A seasonal and time-dependent pattern can be fitted to the occurrence and severity of impact of each type of threat.

The use of average deterministic value cannot capture such variability. Time windows that describe a specific season in the year and time-of-day can be developed. PDF models developed for each window exhibit a variety of shapes so that the variation in the likelihood of component failure can be captured and quantified.

Q4) Suitable PDF for capturing season and time-dependent variations in failure parameters

Due to the variability induced in component failure parameters, PDFs that can be left and right skewed are more useful in reliability analyses. The research showed that the Beta PDF can be used in place of other commonly applied PDFs.

Failure parameters are based on historical record and thus have a finite range. Only the Beta PDF can be scaled to a finite range. It was thus the most suitable PDF for the research presented.

Q5) Bulk network required for research

South Africa has a diverse climate and as such the power grid is exposed to a range of external local threats. Literature shows that the network is also exposed to GICs. Real failure data was also available for use in the analyses considered. The South African power grid thus makes an interesting and suitable case study. The test network was thus developed based on the South African network and external conditions.

Q6) Incorporation of PDFs in reliability analyses

A matrix vulnerability model that describes different seasons and time-of day was considered. The model was developed so that Beta PDF models could be developed for failure parameters in each window. Since the conventional sequential MCS unrealistically applies a constant model for failure rates, a new simulation technique was developed. PDF models could thus be applied for both failure and repair rates in the analysis. The research first showed that the new technique could replicate analyses performed using the conventional approach before applying it to the test network.

Q7) Significance of using PDFs in reliability analyses

PDFs are very significant to practical reliability analyses. The research showed that realistic reliability inputs could be derived with PDFs. A different perception on the network's reliability was also achieved when the reliability indices were also represented using PDFs. It was possible to make inferences about the parameters and indices being described based on the skewness of their respective distributions. The PDFs also aided decision making at both planning and operation levels. They provided a range of values with different level of risk or confidence attached. Planners and operators would thus be able to quantify the risk induced in their decision making when a given level of reliability is selected. The form of risk based decision making proposed in the thesis has not been used before. The PDF results thus showed that the conventional approach, as used in the base case planning analysis, could be applied only as one of the steps in a reliability analysis.

Q8) Modifying planning failure models for use in operational reliability analysis?

A key miscalculation made by operators is the use of planning failure models in their analyses. Misleading results are usually obtained. Decisions based on such results could have drastic ramifications. The research showed that long-term failure models can be translated into operational models. PDFs were used to model the long-term failure models, the likelihood of occurrence of a given operational threat and the health index that indicates the state of the network in an operational time window. The models derived modified the long-term failure models so that the elevation in risk of failure during operation could be accounted for.

The research questions were addressed. The research was thus able to show that simulation-based probability density functions that describe network interruptions, caused by adverse global and space weather conditions, can be used for effective network planning and operation decisions.

8.2 MAIN CONTRIBUTIONS OF THE THESIS

The research applied the Beta PDF in the analyses performed. The Beta PDF has had limited application in reliability studies. It may even have never been applied in conjunction with sequential MCS reliability assessment. The research showed that it can perform just as well as the other commonly used PDFs and may actually be more suited for operational and annual planning reliability studies where extreme events are not considered. The characteristics of the Beta PDF are such that it facilitates the modelling of variables with finite range. This makes it appropriate for modelling not only historical failure data but also reliability indices. It must be stated that further research may be required for the development of even better Beta PDF based models for reliability variables. The research could analyze the methodology applied in deriving shape and scaling parameters of the best fitting Beta PDF model.

The research improved and thoroughly arranged the sampling area of a sequential MCS. The matrix vulnerability model applied ensures a more realistic arrangement of failure data for either planning or operational reliability analyses. This allowed for the correlation between failure events and seasonal and time-of-day variations to be carried out simultaneously. The use of probabilistic models in each matrix cell ensures that the distinct variations or uncertainty in reliability inputs can be accounted for during the sampling process of the sequential MCS. The use of PDFs at the sampling stage and even for the representation of reliability indices enables planners and operators to quantify the level of uncertainty allowed in their decision making process.

The thesis proposed a new reliability evaluation technique that is computationally more efficient than its root conventional sequential MCS. The technique is not only computationally faster than the conventional sequential MCS but also ensures that the results computed are more dependent on the input failure models. The accuracy of the TDPA is comparable to that attained with a sequential MCS. The new technique can be consistently applied to planning and operational studies while taking into account the

distinct effect on the reliability inputs. The technique has significant potential for real time reliability applications.

The thesis provided a base modelling procedure applicable to scenarios in which a component's risk of failure is elevated due to occurrence of a threat. The threats considered have immediate and deferred effects on exposed network components. The thesis attempted to model the impact of a single threat on a component's short and long-term failure models. The ability to transform long-term failure models into operational models ensures that reliability analyses can be used to analyze the impact of impending storms. The TDPA was used to evaluate the effect of such threats on a network's reliability. The TDPA based reliability analysis could thus be considered as a tool in operational threat mitigation strategies; applicable to any threat and not only GICs

8.3 CONCLUDING REMARKS

The research focused on the modelling of component failure parameters. It can however be extended to other aspects of power networks such as integration of renewable energy systems and the effects of demand side management techniques on a network stability and reliability.

The experience acquired by planners and operators whilst working with their utilities is an invaluable asset. One can not however ignore the rapid changes in the power industry, particularly with regard to the network risks and the way the risks are managed. The time-dependent probabilistic approach developed in this research provides a means of quantifying the uncertainty allowed in network planning and operating practices. This should help ensure that better and more effective decisions are made within the power industry.

REFERENCES

Allan D J, White A, *Transformer Design for High Reliability*, Proceedings of 2nd IEEE International Conference on the Reliability of Transmission and Distribution Equipment, No. 406, 66-72, March 1995

Alvehag K, *Impact of Dependencies in Risk Assessments of Power Distribution System,* Licentiate Thesis, Royal Institute of Technology, School of Electrical Engineering, Stockholm, Sweden, 2008

Alvehag K, Soder L, *A Stochastic Weather Dependent Reliability Model for Distribution Systems*, 10th International Conference on Probabilistic Methods Applied to Power Systems, Puerto Rico, 1-8, 2008

Alvehag K, SÖder, *A Reliability Model for Distribution Systems Incorporating Seasonal Variations in Severe Weather*, IEEE Transactions on Power Delivery, Vol. 26, No.2, 910-919, 2011

Almeida S A B, Engelbrecht C S, Pestana R, Barbosa F P M, *Prediction of Faults caused by Lightning for Transmission System Operations*, 4 ELECTRA, No. 4, February 2011.

Almeida S A B, Pestana R, Barbosa F P M, *The main causes of Incidents in the Portuguese Transmission System-Their Characterization and how they can be used for Risk Assessment*, 6th International Conference on the European Energy Market, Leuven, 2009

Awodele K, Edimu M, Gaunt C T, Herman R, *Choice of Beta Probability Distribution Function for a Power System Reliability Assessment*, submitted to Electric Power Systems Research Journal, February 2012

Awodele K, Ip Cho N F S, *Impact of Different Load Models on Reliability Evaluation in Power Systems*, 46th International Universities Power Engineering Conference, Soest, Germany, 2011

Aydogmus Z, Cebeci M, *A New Dynamic Model of Polluted HV Insulators,* IEEE Transactions on Dielectrics and Electrical Insulation, Vol. 11, No. 4, 577-584, 2004

Amer R Y, *Temperature and Resistivity Distribution on the Insulator Surface,* 5th International Symposium on High Voltage Engineering, Braunschweig, Germany, 1987

Balijepalli N, Venkata S S, Richter C W, Christie R D, Longo V J, *Distribution System Reliability Assessment due to Lightning Storm*, IEEE Transactions on Power Delivery, Vol. 20, No. 3, 2153-2159, 2005

Banks D, Schäffer J, *The Potential Contribution of Renewable Energy in South Africa*, Executive Summary of Project Report, Available at: http://www.eepublishers.co.za/images/upload/Gener%201.pdf

BBC News, *Europe recovers from deadly storm,* http://news.bbc.co.uk/2/hi/7849887.stm#map (viewed: 13/10/2009)

Bebic J, *Power System Planning: Emerging Practices Suitable for Evaluating the Impact of High-Penetration Photovoltaics*, GE Global Research Report, February 2008

Bekker H J T, Britten A C, Stevens D J, Bolgna F T, Watridge G M, *Light Pollution on Glass Disc Insulators as an Underlying Cause of Flashovers in Eskom's 275 and 400 kV Networks*, 11th International High Voltage Engineering Symposium, 103-106, London, 1999

Beshir M J, Cheng T C, Farag A S A, *Comparison of two Bulk Power Adequacy Assessment Programs: TRELSS and COMREL,* IEEE Transmission and Distribution Conference Proceedings, Los Angeles, 431-437, 1996

Berge J, Marti L, Varma R K (1), *Modelling and Mitigation of Geomagnetically Induced Currents on a realistic Power System Network*, IEEE Electrical Power and Energy Conference, Winnipeg, 2011

Berge J, Varma R K, Marti L, (2), *Laboratory Validation of the Relationship between Geomagnetically Induced Current (GIC) and Transformer Absorbed Reactive Power*, IEEE Electrical Power and Energy Conference, Winnipeg, 2011

Bevers E, Saint B, *NRECA Reliability Reporting Survey and the new RUS Interruption Reporting Requirement,* IEEE Rural Electric Power Conference, A4 1-6, Albuquerque, New Mexico, 2006

Bhuiyan M R, *Inclusion of Weather Effects in Composite System Reliability Evaluation Using Sequential Simulation*, IEEE Generation, Transmission and Distribution Conference, Vol. 141, No. 6, 575-584, 1994

Billinton R, Acharya J, Consideration of Multi-State Weather Models in Reliability Evaluation of Transmission and Distribution Systems, IEEE Canadian Conference on Electrical and Computer Engineering, 619-622, 2005

Billinton R, Allan R N*, Reliability Assessment of Large Electric Power Systems*, Kluwer Academic Publishers, Boston/Dordrecht/Lancaster, 1988

Billinton R, Allan R N, *Reliability Evaluation of Engineering Systems*, *Concepts and Techniques*, New York, Plenum Press, ISBN: 0306440636, 1992

Billinton R, Allan R N, *Reliability Evaluation of Power Systems*, New York, Plenum Press, ISBN: 0306452596, 1996

Billinton R, Huang D, *Basic Considerations in Generating Capacity Adequacy Evaluation*, IEEE Canadian Conference on Electrical and Computer Engineering, 611-613, 2005

Billinton R, Kumar S, *Indices for use in Composite Generation and Transmission System Adequacy Evaluation*, International Journal of Electrical Power and Energy Systems, Vol.12, No. 3, 147-155, 1990

Billinton R, Kumar S, Chowddury N, Chu K, Debnath K, Goel L, Khan E, Kos P, Nourbakhsh G, Oteng-Adjei J, *A Reliability Test System for Educational Purposes-Basic Data,* IEEE Transactions on Power Systems, Vol. 4, No. 3, 1238-1244, 1989

Billinton R, Li W, *A Novel Method for Incorporating Weather Effects in Composite System Adequacy Evaluation*, IEEE Transactions on Power Systems, Vol. 6, 1154-1160, 1991

Billinton R, Li W, *Reliability Assessment of Electric Power Systems Using Monte Carlo Methods*, Plenum Press, New York, ISBN: 0306447819, 1994

Billinton R, Sankarakrishnan A, *A Comparison of Monte Carlo Simulation Techniques for Composite Power System Reliability Assessment*, Communication, Power and Computing Conference, Manitoba, 1995

Billinton R, Singh D G, *Reliability Assessment of Transmission and Distribution Systems Considering Repair in Adverse Weather Conditions,* IEEE Canadian Conference on Electrical and Computer Engineering, Vol. 1, 88-93, 2002

Billinton R, Singh G, *Application of Adverse and Extreme Adverse Weather: Modelling in Transmission and Distribution System Reliability Evaluation*, IEEE Proceedings Generation, Transmission and Distribution, Vol. 153, No. 1, 115-119, 2006

Billinton R, Tang X, Selected Considerations in Utilizing Monte Carlo Simulation in Quantitative Reliability Evaluation of Composite Power Systems, Electric Power Systems Research, Vol. 69, No.2-3, 205-211, 2004

Billinton R, Wangdee W, *Estimating Customer Outage Costs due to a Specific Failure Event*, IEEE Proceedings Generation, Transmission and Distribution, Vol. 150, 668–672, 2003.

Billinton R, Wangdee W, *Predicting Bulk Electricity System Reliability Performance Indices using Sequential Monte Carlo Simulation*, IEEE Transactions on Power Delivery, Vol. 21, No. 2, 909-917, 2006

Billinton R, Wu C, *Predictive Reliability Assessment of Distribution Systems Including Extreme Adverse Weather*, Canadian Conference on Electrical and Computer Engineering, Vol. 2, 719-724, Toronto, 2001

Billinton R, Wu C, Singh G, *Extreme Adverse Weather Modelling in Transmission and Distribution System Reliability Evaluation*, 14th Power Systems and Computation Conference, Sevilla, 2002

Blake S, Taylor P, Creighton A, *Methodologies for the Analysis of both Short-term and Long-term Network Risks,* 20th International Conference on Electricity Distribution, Prague, No. 24, June 2009

Bollen M H J, *Effects of Adverse Weather and Aging on Power System Reliability,* IEEE Transactions on Industrial Applications, Vol.37, No.2, 452-457, 2001

Bollen M H J, Wallin L, Ohnstad T, Bertling L, *On Operational Risk Assessment in Transmission Systems – Weather Impact and Illustrative Example*, 10th International Conference on Probabilistic Methods Applied to Power Systems, Rincon, 2008

Borgenstam C, Sandstroem A, *Why VASA Capsized*, AB Grafisk Press, Stockholm, ISBN: 9185268607, 1995

Borges C L T, Falcao D M, Mello J C O, Melo A C G, *Composite Reliability Evaluation by Sequential Monte Carlo Simulation on Parallel and Distributed Processing Environments*, IEEE Transactions on Power Systems, Vol.16, No. 2, 203-209, May 2001

Bossi A, Dind J E, Frisson J M, Khoudiakov U, Light HF et al, *An International Survey on Failures in Large Power Transformers in Service*, Cigré Electra, No.88, 21-48, 1983

Boteler D H, *Space Weather Effects on Power Systems,* American Geophysical Union, 347-352, 2001

Boteler D H, Shier R M, Watanabe T, Horita R E, *Effects of Geomagnetically Induced Currents in the B. C. Hydro 500 kV System*, IEEE Transactions on Power Delivery, Vol. 4, No. 1, January 1989

Breslow P B, Sailor D J, *Vulnerability of Wind Power Resources to Climate Change in the Continental united States,* Renewable Energy, Vol.27, 585-598, 2002

Brostrom E, Ahlberg J, Soder L, *Modelling of Ice Storms and their Impact Applied to a Part of the Swedish Transmission Network,* Power Tech, Laussanne, 1593-1598, 2007

Brown R E, Gupta S, Christie R D, Venkata S S, Fletcher R, *Distribution System Reliability Assessment: Momentary Interruptions and Storms*, IEEE Transactions on Power Delivery, Vol. 12, No. 12, 1569-1575, 1997

Burnham J T, Bird Streamer Flashovers on FPL Transmission Lines, IEEE Transactions on Power Delivery, Vol. 10, No. 2, 970-977, 1995

Carer P, Briend C, *Weather Impact on Components Reliability: a Model for MV electrical Networks,* 10th International Conference on Probabilistic Methods Applied to Power Systems, Puerto Rico, 2008

Carpaneto E, Chicco G, *Evaluation of Probability Density Functions of Distribution System Reliability Indices with a Characteristic-Functions Approach*, IEEE Transactions on Power Systems, Vol. 2, No. 9, 724-734, 2004

Cha S-T, Jeon D-H, Bae I-S, Lee I-R, Kim J-O, *Reliability Evaluation of Distribution System Connected Photovoltaic Generation Considering Weather Effects,* 8th International Conference on Probabilistic Methods Applied to Power Systems, Iowa, September 2004

Chen Q, *The probability, Identification and Prevention of Rare Events in Power Systems,* PhD Thesis, Iowa State University, USA, 2004

Cheng D, Zhu D, Broadwater R P, Lee S, *A graph trace based reliability analysis of electric power systems with time-varying loads and dependent failures*, Electric Power Systems Research Vol.79, 1321–1328, 2009

Chisepo H, *Electrical and Magnetic response of Transformers to Geomagnetically Induced Currents,* MSc. Candidate, University of Cape Town, 2012

Chowdhury A A, Koval D O, *High Voltage Transmission Equipment Forced Outage Statistics including Different Fault Types,* 10th International Conference on Probabilistic Methods Applied to Power Systems, Rincon, 2008

Council of European Energy Regulators (CEER), T*hird Benchmarking Report on Quality of Electricity Supply,* Quality of Supply Task Force Report, December 2005

Cross N, Herman R, Gaunt C T, *Investigating the usefulness of the Beta PDF to describe Parameter in Reliability Analyses,* International Conference on Probabilistic Methods Applied to Power Systems, Stockholm, 2006

Deaves D M, Lines I G, *On the Fitting of Low Mean Wind Speed Data to the Weibull Distribution,* Journal of Wind Engineering and Industrial Aerodynamics, Vol. 66, No. 3, 169-178, 1997

Deshmukh M K, Deshmukh S S, *Modelling of Hybrid Renewable Energy Systems*, Renewable and Sustainable Energy Reviews Journal, Vol. 12, 235–249, 2008

Doble Website, *Doble Laboratory Testing-Degree of Polymeriazation,* http://www.doble.com/services/lab_services_testing.html [viewed on 21/06.2012]

Dzobo O, Gaunt C T, Herman R, *Investigating use of Probability Distribution Functions in Reliability-Worth Analysis of Electric Power Systems*, International Journal of Electrical Power and Energy, Vol.12, 110-116, 2012

Edimu M, *Evaluation of Reliability Indices of a Composite Power System using Probability Distributions,* MSc Thesis, University of Cape Town, 2009

Edimu M, Gaunt C T, Herman R (1), *Applying Probability Distribution Functions to Model System Failures Due to Adverse Weather*, 17th Power Systems Computation Conference, Stockholm, 2011

Edimu M, Gaunt C T, Herman R (2), *Using Probability Distribution Functions in Reliability Analyses,* Electric Power Systems Research Journal, Vol. 81, 915-921, 2011

Endrenyi J, Reliability Modelling in Electric Power Systems, New York, John Wiley and Sons, 1978

Esary J D, Marshal A W, *Shock Models and Wear Process*, The Annals of Probability, Vol. 1, No. 4, 627-649, 1973

Eskom Annual Report 2006, *Western Cape Electricity Supply*, http://www.eskom.co.za/annreport06/pdf/Western%20Cape%20electricity%20supply.pdf (viewed: 16/08/2009)

European Renewable Energy Council (EREC), *Global Energy Scenario-January 2007,* http://www.energyblueprint.info/677.0.html (viewed: 27/06/2011)

Falcao A, Bollen M, *Exceptional Events and Force Majeure Events and their use in the Electricity Sector,* 20th International Conference on Electricity Distribution, Prague, No. 233, June 2009

Federal Energy Regulatory Authority, *Final Rule: Reliability Standards for Geomagnetic Disturbances,* Order No.: 779, May 2013

Fells Associates Report, *A Pragmatic Energy Policy for the UK,* August 2008

Filho V X, Couri J J G, Steinberger J M, Salgado E, Pilotto L A S, Martins N, Carvalho A R C, Roitman M, Bianco A, Chipp H J, Gomes P, *The March 11th 1999 Blackout: Short-Term*

Measures to Improve System Security and Overview of the Reports Prepared by the International Experts, CIGRE Large Disturbance Workshop, Paris, 2000

Fong C C, Grigg C H, *Bulk Power System Reliability Performance Assessment,* Reliability Engineering and System Safety, Vol. 46, 25-31, 1994

Fox News, *Brazil Blackout Sparks Concerns about Infrastructure,* http://www.foxnews.com/world/2009/11/12/brazil-blackout-sparks-concerns-infrastructure/ (viewed: 18/03/2011)

Fu W H, James D M, Vittal V, *Risk Assessment for Transformer Loading*, IEEE Transactions on Power Systems, Vol. 16, No. 3, 346-353, 2001

Gaunt C T, Coetzee G, *Transformer Failures in Regions incorrectly considered to have Low GIC-risk*, IEEE PowerTEch, Lausanne, July 2007

Gaunt C T, Malengret, *Why we use the term non-active power, and how it can be measured under non-ideal power supply conditions*, presented at IEEE PES PowerAfrica Conference and Exposition, Johannesburg, July 2012

Gençoğlu M T, Cebeci M, *The Pollution Flashover on High Voltage Insulators,* Electric Power Systems Research, Vol. 78, 1914-1921, 2008

Goel L, *Monte Carlo Simulation-based Reliability Studies of a Distribution Test System*, Electric Power Systems Research, Vol. 54, 55-65, 2000

González-Fernández R A, Leite da Silva A M, *Reliability Assessment of Time-Dependent Systems via Sequential Cross-Entropy Monte Carlo Simulation,* IEEE Transactions Power Systems, Vol. 26, No. 4, 2381-2387, 2011

Gray H L, Schucany W R, *Lower Confidence Limits for Availability Assuming Lognormally Distributed Repair Times*, IEEE Transactions on Reliability, Vol. R-18, No. 4, 157-162, 1969

Gu S, Chen J, Tong X, Li X, Zhang R, *Evaluation of Lightning Flashover Risk of HV Overhead Transmission Lines*, Asia-Pacific Power and Energy Engineering Conference, Chengdu, 1-5, 2010

Gupta A, Nadarajah S, *Handbook of Beta Distribution and its Properties*, Florida, CRC Press, ISBN: 0824753968, 2004

Habib S E D, Khalifa M, *A New Monitor for Pollution on Power Line Insulators, Part 1: Design Construction and Preliminary Tests,* IEEE Proceedings, Vol. 133, No. 2, 105-108, 1986

Haghifam M R, Omidvar M, *Wind Farm Modelling in Reliability Assessment of Power System,* 9th International Conference on Probabilistic Methods Applied to Power Systems, Stockholm, 11-15, 2006

Haldar A, Mahedavan S, *Probability, Reliability and Statistical Methods in Engineering Design*, New York, John Wiley and Sons, ISBN: 0471331198, 2000

Haroonabadi H, Haghifam M R, *Generation Reliability Evaluation in Power Markets Using Monte Carlo Simulation and Neural Networks,* 15th International Conference on Intelligent System Applications to Power Systems, Curitiba, November, 2009

He J, Sun Y, Cheng L, *Fast and Accurate Online Short-Term Reliability Assessment,* Probabilistic Methods Applied to Power Systems, Singapore, 352-357, 2010

Heier S, *Grid Integration of Wind Energy Conversion Systems*, 2nd Edition, John Wiley and Sons, Chichester, ISBN: 139780470868997, 2006

Henderson M, *Power System Planning Process and Issues,* IEEE Power and Energy Society General Meeting, Calgary, 2009

Herman R, Gaunt C T, *A Practical Probabilistic Design Procedure for LV Residential Distribution Systems,* IEEE Transactions on Power Delivery, Vol. 23, No. 4, 2247-2254, 2008

Herman R, Gaunt C T, *Probabilistic Interpretation of Customer Interruption Costs (CIC) Applied to South African Systems*, 11th Probabilistic Methods Applied to Power Systems Conference, Singapore, 2010

Herman R, Gaunt C T, Edimu M, *Procedure for Investigating the Planned and Operational Reliability of Transmission Networks with GICs*, IASTED, Greece, 2011

Herman R, Heunis S W, *A General Probabilistic Voltage Drop Calculation Method for L.V Distribution Networks based on a Beta PDF Load Model,* Electric Power Systems Research, Vol. 46, No. 1, 45-49, 1998

Historic Model Ships (HMS), *The Swedish Vasa of 1628*, Available at: http://www.modelships.de/Wasa/VASA_eng.htm

Hutchins T R, Overbye T J, *Power flow studies in the presence of geomagnetically induced currents*, IEEE Power and Energy Conference, 1-4, Illinois, 2012

Hutchins T R, Overbye T J, *The Effect of Geomagnetic Disturbances on the Electric Grid and Appropriate Mitigation Strategies*, North American Power Symposium, 1-5, Boston, 2011

IEEE data analysis task force, Working Group on Statistics of Line Outages**,** *An IEEE Survey of U.S. and Canadian Overhead Transmission Outages at 230 kV and above*, IEEE Transactions *on* Power Delivery, Vol. 9, No. 1, 21-39, 1994

IEEE/ANSI C57.91-1995, *Guide for Loading Mineral-Oil-Immersed Transformers*, 1995

IEEE C57.117-1986, *Guide on Reporting Failure Data for Power Transformers and Shunt Reactors on Electric Utility Power Systems*, 1986

IEEE 1243-1997, *Guide for Improving the Lightning Performance of Transmission Lines*, 1997

IEEE 859-1987, *IEEE Standard Terms for Reporting and Analyzing Outage Occurrences and Outage States of Electrical Transmission Facilities*, 1988

IEEE Report, Working Group on Geomagnetic Disturbances and Power System Effects, *Geomagnetic Disturbance Effects on Power Systems*, IEEE Transactions *on* Power Delivery, Vol. 8, No. 3, 1206-1213, 1993

Integrated Resource Plan (IRP) report*,* October 2010 draft, Available at: http://www.doe-irp.co.za/archive.html

International Organization of Standardization (ISO), *International Standard: Quality Management and Quality Assurance Vocabulary,* ISO 8402, 1994

Jadrijev Z, Majstrovic M, Majstrovic G, *The Relationship between Reliability Indices and Daily Load Curve*, 20th International Conference on Electricity Distribution, Prague, No. 909, June 2009

Jagers J N, Khosa J, De Klerk P J, Gaunt C T, *Transformer Reliability and Condition Assessment in a South African Utility,* XVth International Symposium on High Voltage Engineering, Ljubljana, 2007

Jagers J N, *Comparing the Reliability of older and newer Transformer Designs*, MSc. Thesis, University of Cape Town, 2011

Jakarta Post, *Massive Blackout hits Java, Bali,* (Available at http://www.thejakartapost.com/news/2005/08/19/massive-blackout-hits-java-bali.html viewed: 22/03/2011)

Jandrell I, Blumenthal R, Anderson R, Trengrove E, *Recent Lightning Research in South Africa with a Special Focus on Kerunopathology*, 16th International Symposium on High Voltage Engineering, August 2009

Jian H, Lin C, Yuan-Zhang S, *Transformer Real-time, Reliability Model based on Operating Conditions*, Journal of Zhejiang University, Vol. 8, No. 3, 378-383, 2007

Kachler A J, *Unique Transformer Failure Statistics - An Important Contribution to Economics of Transformer Management, SC12 (Transformers)*, Cigré Colloquium, Dublin, 2001

Kappenman J G, Albertson V D, *Bracing for the Geomagnetic Storms*, IEEE Spectrum Magazine, 27-33, March 1990

Kappenman J G, Radasky W A, Gilbert J L, Erinmez I A, *Advanced Geomagnetic Storm Forecasting: A Risk Management Tool for Electric Power System Operations*, IEEE Transactions on Plasma Science, Vol. 28, No. 6, 2114-2122, December 2000

Kim –O, Singh, Including in Uncertainty in LOLE Calculation using Fuzzy Set Theory, IEEE Transactions on Power Systems, Vol. 17, No. 1, 19-25, February, 2002

Kinver M, *Britain 'faces power cuts threat',* http://news.bbc.co.uk/2/hi/science/nature/7618840.stm (viewed: 17/09/2009)

Kjolle G H, Holen A T, *Reliability and Interruption Cost Prediction using Time-dependent Failure Rates and Interruption Costs,* Quality and Reliability Engineering International, Vol. 14, 159-165, 1998

Koen J, Gaunt C T, *Disturbances in the Southern African Power Network due to Geomagnetically Induced Currents*, CIGRE, August, 2001

Kolowrocki K, Kwiatuszewska-Sarnecka B, *Reliability and risk analysis of large systems with ageing components*, Reliability Engineering and System Safety, Vol. 93, 1821– 1829, 2008

Koonce A M, Apostolakis G E, Cook B K, *Bulk Power Risk Analysis: Ranking Infrastructure Elements According to their Risk Significance,* Electrical Power and Energy Systems Journal, Vol. 30, 169-183, 2008

KOSTT Press Release-24/07/2007, *Kosovo Power System Power Blackout,* http://www.kostt.com/kosttcms/images/doc/Press_release-Kosova_Power_System_Blackout.pdf, (viewed: 20/03/2011)

Koval D O, Bin S, Shen S, Chowdury A, *Modelling Severe Weather Related High Voltage Transmission Line Forced Outages,* Transmission and Distribution Conference and Exhibition, 788-793, May 2006

Krahl S, Ohrem S, Haubrich H-J, *probability Distributions of Reliability Indices of Electricity Distribution Networks,* 20th International Conference on Electricity Distribution, Prague, No. 373, June 2009

LaCommare K H, Eto J H, *Cost of Power Interruptions to Electricity Consumers in the United States (U.S),* Environmental Energy Technologies Division, September, 2004, Available at: http://eetd.lbl.gov/ea/ems/reports/58164.pdf

Lanoie R, Mercure H, *Influence of Forest Fires on Power Line Insulation,* 6th International Symposium on High Voltage Engineering, New Orleans, USA, 1989

Lapworth J A, *Transformer Reliability Surveys*, Cigré Biennial Conference, A2-114, Paris, 2006

Lecomte E L, Pang A W, Russel J W, *Ice Storm '98*, Institute for Catastrophic Loss Reduction, December 1998

Lee M Q, Lu C N, Huang H S, *Reliability and Cost Analyses of Electricity Collection Systems of a Marine Current Farm-A Taiwanese Case Study,* Renewable and Sustainable Energy Reviews, Vol. 13. No. 8, 2012-2021, 2009

Lee S T, *Estimating the Probability of Cascading Outages in a Power Grid*, 16th Power Systems Computation Conference, Glasgow, 2008

Lee S T, *Probabilistic Reliability Assessment for Transmission Planning and Operation Including Cascading Outages,* IEEE Power Systems Conference and Exposition, Seattle, 2009

Leite da Silva A M, Endreny J, Wang L, *Integrated Treatment of Adequacy and Security in Bulk Power System Reliability Evaluations,* IEEE Transactions on Power Systems, Vol. 8, No. 1, 1993

Leite da Silva A M, Manso L A F, Mello J C O, Billinton R, *Pseudo-Chronological Simulation for Composite Reliability Analysis with Time Varying Loads,* IEEE Transactions on Power Systems, Vol. 15, No. 1, 73–80, 2000

Leon-Garcia A, *Probability and random Processes for Electrical Engineering,* New York, Addison-Wesley Publishing Company, ISBN: 020150037X, 1994

Li W, *Incorporating Aging Failures in Power System Reliability Evaluation,* IEEE Transactions on Power Systems, Vol. 17, No. 3, 918-923, 2002

Li W, *Operation Reliability of Power Systems*, Article in Wiley Encyclopaedia of Electrical and Electronics Engineering, Wiley Online Library, Available at http://onlinelibrary.wiley.com/doi/10.1002/047134608X.W8187/abstract, 2013

Li W, *Risk Assessment of Power System. Models, Methods and Applications*, New York, IEEE Press, ISBN: 0471631682, 2005

Li W, Xiong X, Zhou J, *Incorporating Fuzzy Weather-related Outages in Transmission System Reliability Assessment*, IET Generation, Transmission and Distribution Journal, Vol. 3, No. 1, 26-37, January 2009

Li Y, *Bulk System Reliability Evaluation in a Deregulated Power Industry,* MSc. Thesis, College of Graduate Studies and Research, University of Saskatchewan, Canada, 2003

Liu Y, Singh C, *A Methodology for Evaluation of Hurricane Impact on Composite Power System Reliability,* IEEE Transactions on Power Systems, Vol. 26, No. 1, 145-152, February 2011

Looms J S T, *Insulators for High Voltages*, London, Peregrinus limited, ISBN: 0863411169 1988

Loredo-Souza A M, Davenport A G, *The Effects of High Winds on Transmission Lines,* Journal of Wind Engineering and Industrial Aerodynamics, Vol. 74-76, 987-994, 1998

Lun Y F, Lam J C, *A Study of Weibull Parameters Using Long-term Wind Observations,* Renewable Energy, Vol. 20, No.2, 145-153, 2000

Lundstedt H, *The Sun, Space Weather and GIC Effects in Sweden,* Advances in Space Research, Vol. 37, 1182-1191, 2006

Makkonen L, *Modelling Power Line Icing in Freezing Precipitation*, Atmospheric Research Journal, Vol. 46, 131-142, 1998

Marakov Y V, Hardiman R C, *Risk, Reliability, Cascading and Restructuring,* IEEE PES General Meeting, Vol. 3, 1417-1429, 2003

Marantes S, Pais Da Silva A, *Variability Evaluation of Distribution Networks Quality of Supply Performance Indices,* 20th ICED, pp. 910, June 2009

Mason J P, Black, Veatch Ltd, *Lake Victoria: A Predictably Fluctuating Resource,* Hydropower and Dams, Issue 3, 1-4, 2006

Mason J P, *Using Short to Medium Term Climate Data to Improve Hydrological Understanding and Supplement Stochastic Predictions*, 20th African Hydropower Symposium, Lusaka, Zambia, September 2008

Meliopoulos A P, Cokkinides G J, James J R, *An online Transformer Diagnostic System,* TechCon, 23-35, 1998

Mettas A, Sawa M, *System Reliability Analysis: the advantages of using Analytical Methods to Analyze Non-repairable Systems*, Proceedings of Annual Reliabilioty and Maintainability Symposium, Philadelphia, January 2001

Michener H, *Where Engineer and Ornithologist Meet: Transmission Line Troubles caused by Birds,* The Condor, May-June, 1928

Minnaar U J, Gant C T, Nicolls F, *Characterization of Power System Events on South African Power Lines,* Electric Power System Research, Vol. 88, 25-32, 2012

Miranda V, Carvalho L M, Mauro A R, Leite A M S, Singh C, *Improving Power System Reliability Calculation Efficiency with EPSO Variants*, IEEE Transactions on Power Systems, Vol. 24, No. 4, 1772-1779, 2009

Mili M, Qiu Q, *Risk Assessment of Catastrophic Failures in Electric Power Systems*, International Journal of Critical Infrastructure, Vol. 1, No. 1, 38-63, 2004

Molinski T S, Feero W E, Damsky B L, *Shielding Grids from Solar* Storms, IEEE Spectrum, Vol. 37, No. 11, 55-60, November 2000

Molinski T S, *Why Utilities Respect Geomagnetically Induced Currents,* Journal of Atmospheric and Solar-Terrestrial Physics, Vol. 64, 1765– 1778, 2002

Nadarajah S, Kotz S, *The Beta Exponential Distribution*, Reliability Engineering System Safety Vol. 91, 689-697, 2006

Naidoo K, Ijumba N M, Britten, A C, *Bird Streamer Initiated Breakdown Characteristics under HVDC conditions*, International Conference on Power System Technology, Vol. 19, 1-7, Chongqing, 2006

National American Electric Reliability Corporation (NERC), *Effects of Geomagnetic Disturbances on the Bulk Power System*, 2012 Special Reliability Assessment Interim Report, Available at: http://www.nerc.com/files/2012GMD.pdf

Nelson, W, *Applied Life Data Analysis*, New York, John Wiley & Sons, ISBN: 0471094587 1982

Ngwira C M, *Geomagnetically Induced Current Characteristics in Southern Africa,* MSc. thesis, Rhodes University, June, 2008

Ngwira C M, *NASSP Space Weather Course 2011: Geomagnetically Induced Currents,* University of Cape Town, May 2011

North American Electric Reliability Corporation (NERC), *Special Reliability Assessment Interim Report: Effects of Geomagnetic Disturbances on the Bulk Power Systems*, February 2012

O'Connor P D T, *Practical Reliability Engineering*, Sussex, Wiley and Sons, 2002, ISBN: 978047084463

Ozgener O, Ozgener L, *Exergy and Reliability Analysis of Wind Turbine Systems: A Case Study,* Renewable and Sustainable Energy Reviews, Vol. 11, 1811-1826, 2007

Patel M R, *Wind and Solar Power Systems,* CRC Press, New York, ISBN: 0849316057, 1999

Pahwa A, Hopkins M, Gaunt C T, *Evaluation of Outages in Overhead Distribution Systems of South Africa and of Manhattan, Kansas, USA*, 7th International Conference on Power System Operation and Planning, Cape Town, South Arica, 2007

Papoulis A, *Probability, Random Variables, and Stochastic Processes*, 3rd Edition, Singapore, McGraw-Hill Inc., ISBN: 0071008705, 1991

Park J, Liang W, Choi J, El-Keib A A, Shahidehpour M, Billinton R, *A Probabilistic Evaluation of a Power System including Solar/Photovoltaic Cell Generator,* IEEE PES General Meeting, 1-6, 1999

Pham T G, Turkkan N, *Reliability of a Standby System with Beta-Distributed Component Lives*, IEEE Transactions on Reliability, Vol. 43, No. 1, 71-75, 1994

Power System Dynamic Performance Committee (PSDPC), *Causes of the 2003 Major Grid Blackouts in North America and Europe, and Recommended Means to Improve System Dynamic Performance*, Proceedings of IEEE Power Engineering Society General Meeting, Denver, 2004

Power System Outage Task Force (POSTS) for US and Canada, *Final Report on the 14th August 2003 Blackout in the United States and Canada: Causes and Recommendations,* April, 2004 [Available at: https://reports.energy.gov/BlackoutFinal-Web.pdf]

Pulkkinen A, *Geomagnetic Induction during Highly Disturbed Space Weather Conditions: Study of Ground Effects,* Ph.D. thesis, University of Helsinki, 2003

Rei A M, Schilling M T*, Reliability Assessment of the Brazilian Power Grid using Enumeration and Monte Carlo,* IEEE Transactions on Power Systems, Vol. 23, No. 3, 1480-1487, August 2008

Rei A M, Schilling M T, Melo A C G, *Monte Carlo Simulation and Contingency Enumeration in Bulk Power Systems Reliability Assessment*, 9th International Conference on Probabilistic Methods Applied to Power Systems, Stockholm, Sweden, 2006

Réseau de transport d'léctricité (RTE), *The French Electricity Report 2009,* January 2010, Available at: http://www.rte-france.com/uploads/media/pdf_zip/publications-annuelles/rte-be09-en-02.pdf

Reuters-US, *Factbox: Texas Power Plant, Customer Outages due to Cold,* 3rd /02/2011, Available at: http://www.reuters.com/article/2011/02/03/us-ercot-rollingblackouts-idUSTRE7124NA20110203

Reuters –Africa, *Update 5: Risk of Texas Electric Blackout ends,* 10th/02/2011, Available at: http://af.reuters.com/article/energyOilNews/idAFN1026917320110210

Sahinoğlu M, Longnecker M T, Ringer L J, Singh C, Ayoub A K, *Probability Distribution Functions for Generation Reliability Indices-Analytical Approach*, IEEE Transactions on Power Apparatus and Systems, Vol. PAS-102, No. 6, 1486-1493, 1983

Sannino A, Bollen M H J, *Effect of Adverse Weather on the Voltage Dip Mitigation Capability of a Static Transfer Switch*, European Transactions on Electrical Power, Vol. 13, No. 6, 2003

SANS 507-1:2007, Electricity distribution-Guidelines for the provision of electricity distribution networks in residential areas. Part 1: Planning and design of distribution networks, Standards, Pretoria South Africa

Schlabasch J, Rofalski K-H, *Power System Engineering Planning, Design, and Operation of Power Systems and Equipment*, Weinheim, Wiley-VCH, ISBN-13: 9783527407590, 2008

Singh C, Lago-Gonzales A, *Reliability Modelling of Generation Systems including Unconventional Energy Sources*, IEEE Power Engineering Review, Vol. PER-5, No.5, 33, 1985

Singh C, Mitra J, *Composile System Reliability Evaluation based on Monte-Carlo Simulation Combined with Outages Screening,* IEEE Transactions on Power Systems, Vol. 14, No. 2, 785-791, 1999

Sheskins D, *Handbook of Parametric and Nonparametric Statistical Procedures*, 5th Edition, Florida, CRC Press, ISBN: 1439858012, 2011

Smith R L, *Extreme Value Theorem and Reliability Applications*, Reliability Journal, Vol. 15, No. 3, 161-170, 2003

Sokolov V, Vanin B, *Evaluation and Identification of Typical Defects and Failure Modes in 110 kV-750 kV Bushings*, 64th Annual International Conference of Doble Clients, Boston, 1997

Solver T, Amelin M, *State Duration Based Monte Carlo simulation Model with Independent Failures for Distribution System Reliability Analysis*, 9th International Conference on Probabilistic Methods Applied to Power Systems, Stockholm, 2006

Song Y, He H, Zhang D, Guo J, *Probabilistic Security Evaluation of Bulk Power System Considering Cascading Outages,* IEEE International Conference on Power System Technology, Chongqing, October, 2006

South African Weather Service (SAWS), *Western Cape Weather Data*, Period: 2000-2010

Staco Energy Products website: http://www.stacoenergy.com/emergency-lighting-ups.htm (viewed: 17/05/2011)

Stager J C, Ruzmaikin A, Conway D, Verburg P, Mason P J, *Sunspots, El Nino and the levels of Lake Victoria, East Africa,* Journal of Geophysical Research, Vol. 112, d15106, doi:10.1029/2006jd008362, 2007

Streubel H, *The Influence of Non-uniform Contamination on the Flashover Voltage of Insulators,* 4th International Symposium on High Voltage Engineering, Athens, Greece, 1983

Sukhnandan A, A Theoritical and Experimental Investigation into Fire Induced Flashover of High Voltage Transmission Lines, MSc. Thesis, University of KwaZulu Natal, South Africa, 2004

Sukhnandan A, Hoch D A, *Fire Induced Flashovers of Transmission Lines: Theoretical Models*, 6th AFRICON Conference, George, South Africa, October 2002

Sundararajan R, Burnham J, Carlton R, Cherney E A, Couret G, Eldridge K T, Farzaneh M, Frazier S D, Gorur R S, Harness R, Schaffner D, Siegel S, Varner J, *Preventive Measures to Reduce Bird-Related Power Outages-Part II: Streamers and Contamination,* IEEE Transactions on Power Delivery, Vol. 19, No. 4, 1843-1847, 2004

Sutanto D, Lachs W R, *Control Measure for Improving Power System Reliability,* International Conference on Advances in Power System Control, Operation and Management, Hong Kong, 1991

Suntanto D, Outhred H R, Lee Y B, *Probabilistic Power Production Cost and Reliability Calculation by the Z-transform Method*, IEEE Transactions on Energy Conversion, Vol. 4 No. 4, 559-566, 2002

Taylor P V, Naidoo P, Hoch D A, Britten A C, *An Investigation into Anomalous Flashovers of Transmission Lines,* 3rd CIGRE South Africa Regional Conference, 1998

Tyco Electronics website, Porcelain Rigid Red Guano shield (RRGS), Available at: http://energy.tycoelectronics.com/index.asp?act=page&pag_id=2&prl_id=5&pls_id=29&prf_id=59&prr_parent=483

United Nations Framework Convention on Climate Change (UNFCCC), *Kyoto Protocol: Reference Manual on Accounting of Emissions and Assigned Amount,* http://unfccc.int/essential_background/background_publications_htmlpdf/items/2625.php (viewed: 18/09/2009)

Union for the Co-ordination of Transmission of Electricity (UCTE), *Final Report of the Investigation Committee on the 28th September 2003 Blackout in Italy,* April 2004 (Available at: www.rae.gr/cases/C13/italy/UCTE_rept.pdf)

United States Government Accountability Office (USGAO), *Meeting Energy demand in the 21st Century,* Committee on Government Reform, House of Representatives, March 2005

Van Casteren J F L, Bollen H J M, *Reliability Assessment in Electrical Power Systems: The Wiebull-Markov Stochastic Model,* IEEE Transactions on Industry Applications, Vol. 36, No. 3, 911-915, 2000

Van Rooyen C, Vooslo H, Harness R, *Watch the Birdie [Overhead Line Faults]*, IEEE Industry Applications, Vol. 9, No. 5, 55-60, 2003

Van Schijndel A, Wetzer J M, Wouters P A A, *Forecasting Reliability of Transformer Populations*, 19th International Conference on Electricity Distribution, Vienna, 2007

Vancouver Island Powerline website: http://www.vancouverislandpowerline.com/quebec_ice_storm.html (viewed: 17/05/2011)

Vosloo H F, *The Need for and Contents of a Life Cycle Management Plan for Eskom Transmission Line Servitudes,* MSc. Dissertation, Department of Geography, Environmental and Energy Studies, University of Johannesburg, Johannesburg, 2005

Vosloo H F, Britten A C, Burger A A, Muftic D, *The Susceptibility of 400 kV Transmission Lines to Bird Streamers and Bush Fires: A Definitive Case Study*. 6th CIGRE Southern African Regional Conference, Somerset West, Western Cape, August 2009

Walpole R E, *Probability and Statistics for Engineers and Scientists*, 8th Edition, Oxford, Pearson Education, ISBN: 978-8131715529, 2007

Wang C, Zheng G, Cheng T C, *Reliability Evaluation and Failure Analysis of Power Capacitors,* Journal of Tsinghua University, Vol. 31, No.4, 107-112, 1991

Wang P, Billinton R, *Time Sequential Distribution System Reliability Worth Analysis Considering Time Varying Load and Cost Models*, IEEE Transactions on Power Delivery, vol. 14, No. 3, 1046-1051, 1999.

Wang P, Billinton R, *Reliability Cost/Worth Assessment of Distribution Systems Incorporating Time-Varying Weather Conditions and Restoration Resources*, IEEE Transactions on Power Delivery, Vol. 17, No. 1, 260-265, 2002

Wang Y, Pham H, *Dependent Competing-Risk Degradation*, Safety and Risk Modelling and Its Applications, Springer Series in Reliability Engineering, 197-218, 2011

Wangdee W, Billinton R, *Utilization of Time Varying Event-Based Customer Interruption Cost Load Shedding Schemes,* 8th International Conference on Probabilistic Methods Applied to Power Systems, Iowa, 769-775, September 2004

Wen J, Zheng Y, Donghan F, *A Review on Reliability Assessment for Wind Power*, Renewable and Sustainable Energy Reviews Journal, Vol. 13, 2485–2494, 2009

William H, Bartley P E, *Failure Analysis of Transformers*, 36th Annual Conference of the International Association of Engineering Insurers, Stockholm, 2003

Wilkins J D, *The Bath-tub Curve and Product Failure Behaviour*, Reliability Hotwire, Issue 21, November 2002

Xianhe J, Wang C, Amancio A, Chen C, Cheng T C, *Reliability Analyses and Calculation for Distribution Transformers,* IEEE Transmission and Distribution Conference, Vol. 2, 901-906, 1999

Xiao, Y Q, Li Q S, Li Z N, Chow Y W, Li G Q, *Probability Distributions of Extreme Wind Speed and its Occurrence Interval,* Engineering Structures, Vol. 28, 1173-1181, 2006

Yongji G, Yongjian X, Kai X, Huiyi Y, *Composite System Reliability Evaluation based on Monte-Carlo Simulation with Outages Screening*, IEEE Transactions on Power Systems, Vol.14, No. 2, 785-790, 1999

Yun S-Y, Kim J-C, Moon J-F, Park C-H, Park S-M, Lee M-S, *Reliability Evaluation of Radial Distribution System Considering Momentary Interruptions,* IEEE Power and Energy Society General Meeting, Vol. 1, 480-485, 2003

Zapata C J, Silva S C, Burbano O L, *Repair Models of Power Distribution Components,* IEEE PES Transmission and Distribution Conference and Exposition, Latin America, 1-6, 2008

Zhang W, Billinton R, *Application of an Adequacy Equivalent Method in Bulk Power System Reliability Evaluation,* IEEE Transactions on Power Systems, Vol. 13, No. 2, 661-666, 1998

Zhou J, *Reliability Assessment Method for Pressure piping Containing Circumferential Defects based on Fuzzy Probability,* International Journal of Pressure Vessels and Piping, Vol. 82, 669-678, 2005

Zhou Y, Pahwa A, Yang S-S, *Modelling Weather Related Failures of Overhead Distribution Lines,* IEEE Transactions on Power Systems, Vol. 21, No. 4, 1683-1690, 2006

Zhou Y X, Xu X, Nie Q, Liang X D, Guan Z C, Cui J F, Li Z Y, Yuan Y C, Chen Y, Yu D M, *Bird Streamer Caused Flashover in EHV Transmission Line*, IEEE Transactions on Dielectrics and Electrical Insualtion, Vol. 16, No. 1, 69-76, 2009

Zhu D, *Electric Distribution Reliability Analysis Considering Time-varying Load, Weather Conditions and Reconfiguration with Distributed Generation*, PhD Thesis, Virginia Polytechnic Institute and State University, 2007

APPENDIX

A. SELECTED RELIABILITY INDICES

Below are some selected indices identified for use in reliability studies [Billinton & Kumar, 1990; Pereira & Balu, 1992; Billinton & Allan, 1996; Li, 2003].

A.1 Basic Indices

- Probability of Load Curtailment

$$PLC = \sum P_i$$

P_i = Probability of a state i causing load curtailment

- Expected Loss of Load (LOLE)

$$LOLE = \sum (P_i * D_i) \text{ days/period of study}$$

P_i = Probability of a given Capacity outage

D_i = Duration of Capacity outage

- Expected Loss of Energy (LOEE)/Expected Energy not Supplied (EENS)

$$LOEE = \sum (P_i * E_i) \text{ MWh}$$

E_i = Energy curtailed for a given capacity outage

- Expected Demand not Supplied (EDNS)

$$EDNS = \sum (C_i * P_i) \text{ MW}$$

C_i = Capacity outage due to state i

- Expected Frequency of Load Curtailment (EFLC)

$$EFLC = \sum (F_i - f_i) \text{ Occ/yr}$$

F_i = Frequency of departing state i

f_i = Portion of Fi that corresponds to not going through the boundary wall between the loss-of-load state set and the no-loss-of load state set

- Expected Duration of Load Curtailment (EDLC)

$$EDLC = PLC * 8760 \text{ hrs/yr}$$

- Average Duration of Load Curtailment

$$ADLC = EDLC/EFLC \text{ hrs/disturbance}$$

- Expected Number of Voltage violations (ENVV)

$$ENVV = \sum F_j$$

A.2 IEEE proposed Indices

- Bulk Power Interruption Index (BPII)

$$BPII = \sum \frac{C_i * F_i}{L} \text{ MW/MW-yr}$$

L = annual system peak load

- Bulk Power-Energy Curtailment Index (BPECI)

$$BPECI = \frac{EENS}{L} \text{ MWh/MW-yr}$$

- Severity Index (SI)

$$SI = (BPECI * 60) \text{ system Min/yr}$$

- Bulk Power-Supply Average MW Curtailment Index (BPACI)

$$BPACI = \frac{\mathbf{ELC}}{\mathbf{EFLC}} \text{ MW/disturbance}$$

- Modified Bulk Energy Curtailment Index (MBECI)

$$MBECI = \frac{EDNS}{L} \text{ MW/MW}$$

B. SOUTH AFRICAN LIGHTNING FLASH DENSITY MAPS

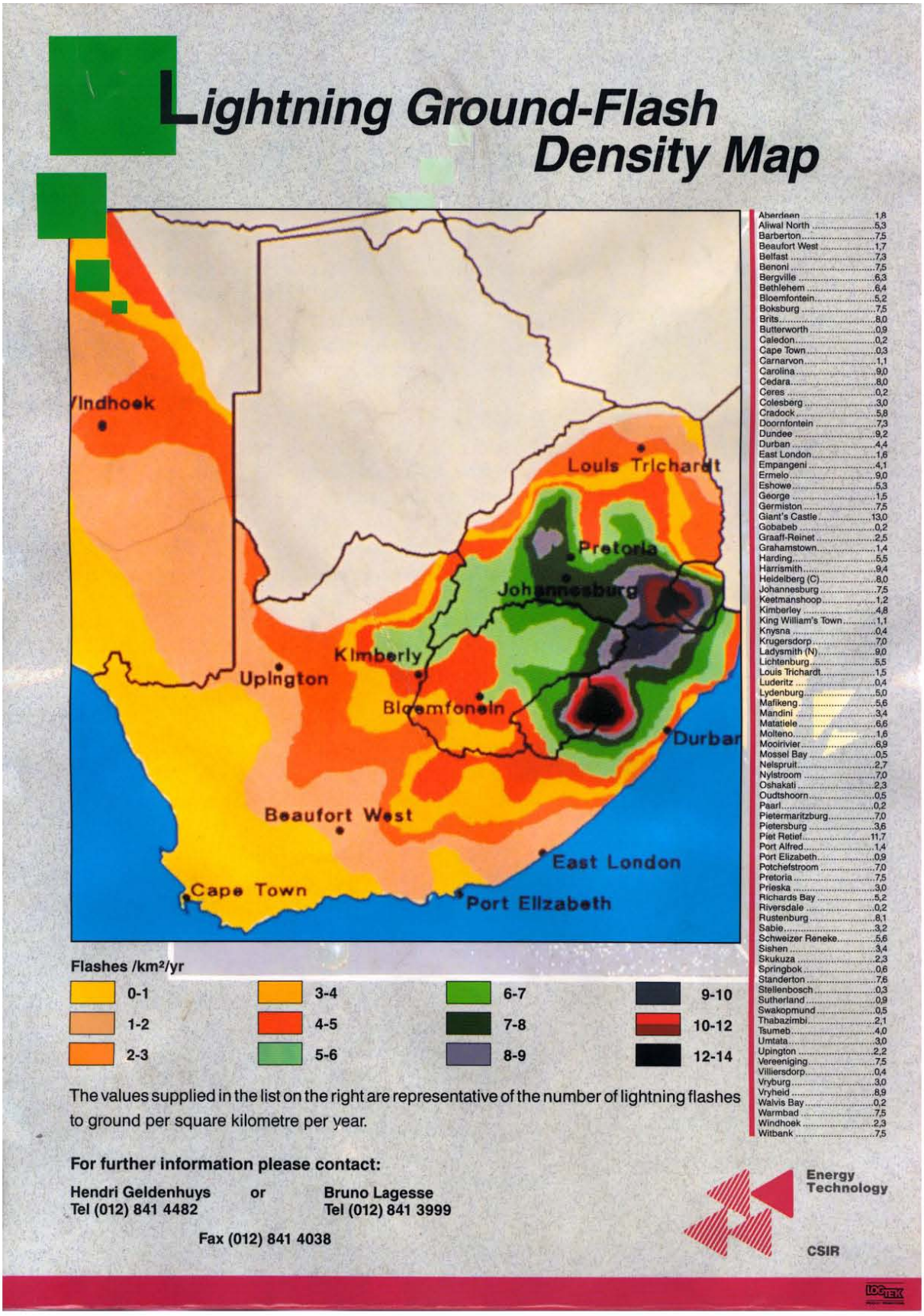

Figure C.0.1: South African Lightning flash density map [SAWS]

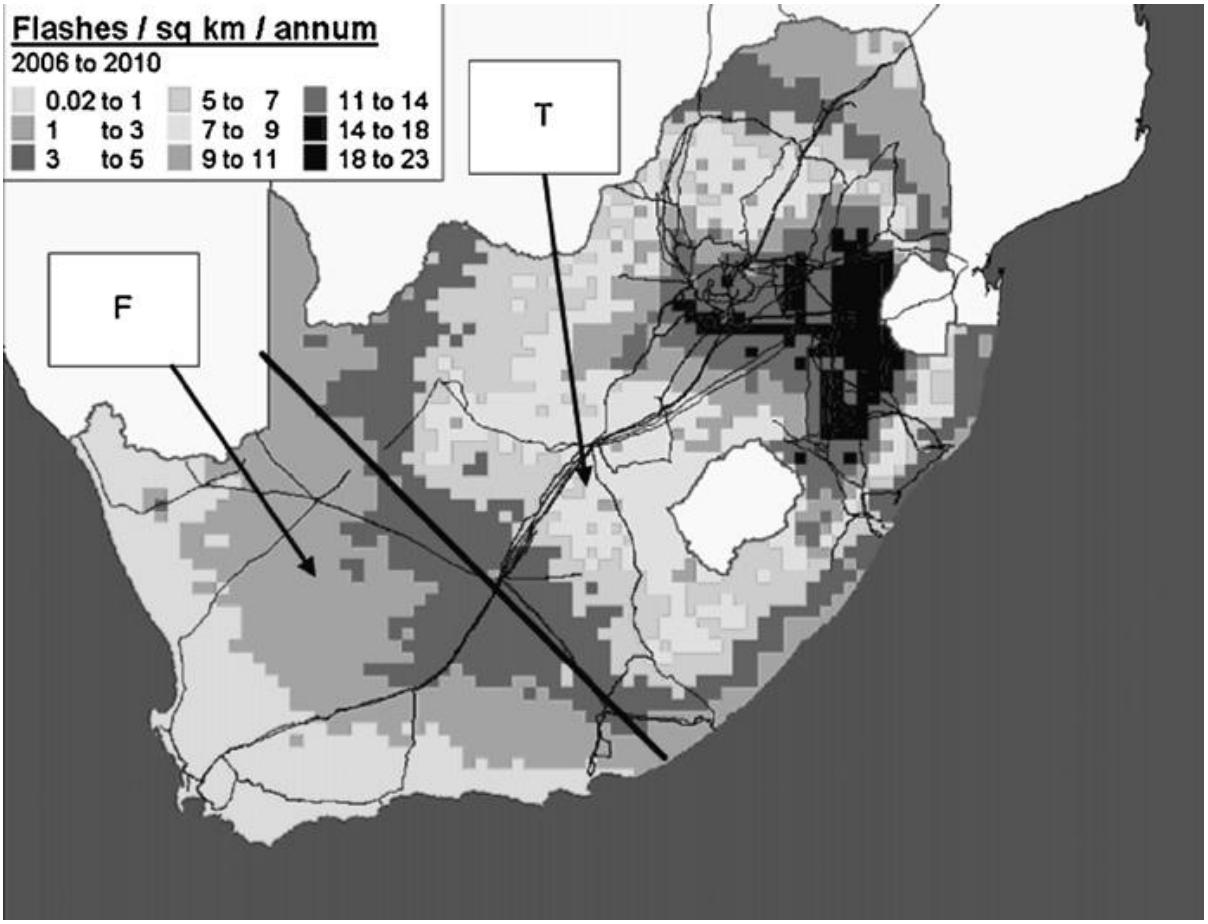

Figure C.0.2: South African Lightning flash density map based on climatic regions [Minnar et al, 2012]

C. PSEUDO NETWORK SPECIFICATIONS

C.1 Network component specifications

- **Transmission lines**

The transmission lines are rated at 400 kV and 1.7 kA. Table D.1 shows the transmission line conductor categories based on the resistance and reactance values.

Table E.1: Resistance and reactance conductor categories

Category	Resistance	Reactance	Number of lines
A	0.36	3.5	5
B	0.31	3.5	2
C	0.27	1.0	1
D	0.34	1.08	4
E	0.15	0.58	4
F	0.31	1.2	1
G	0.32	1.1	11
H	0.17	0.54	4

Table E.2: Bus-bus line connections and line lengths

From bus	To bus	Line length (km)	Category
11	12	12	A
	15	150	B
	19	280	C
12	13	154	A
	14	154	
16	19	130	B
17			A
18			
19	21	123	E
	31	246	F
	41	187	D
	22	123	E
	23	300	G
24	31	123	E
25		123	
31	32	203	H
	33	207	
	34	226	G
34	37	250	

35		207	H
36	53	203	
37		109	G
	38	82	
42	43	163	D
43	44	196	
	45	168	
46	47	171	G
49	51	163	
51	52	82	
52	53	40	
	54	31	
53		47	

C.2 Pseudo network frequency of failure data sets

Table E.4: Short-term transmission failure statistics for different climatic regions

Thunderstorm region												
S/P	**00:00-05:59**			**06:00-11:59**			**12:00-17:59**			**18:00-23:59**		
	mean	std	max	mean	std	max	mean	std	max	mean	std	max
January-March	17.8	6.73	58.2	3.6	2.47	15.6	7.9	5.79	36.3	12.6	5.33	44.6
April-June	13.9	9.39	59.5	8.4	2.99	28.8	7.8	7.69	44.6	9.1	5.17	37.1
July-September	7.4	4.13	35.8	8.4	4.43	39.6	26.4	12.36	86.4	5.8	2.69	22.2
October-December	10.9	5.12	40.1	3	2.01	17	13.4	4.39	40.2	12.1	5.65	44.1
January-December	**50**	**13.29**	**193.6**	**23.4**	**6.22**	**101**	**55.5**	**16.27**	**207.5**	**39.6**	**9.71**	**148**
Frontal region												
S/P	**00:00-05:59**			**06:00-11:59**			**12:00-17:59**			**18:00-23:59**		
	mean	std	max	mean	std	max	mean	std	max	mean	std	max
January-March	18.10	23.13	131.30	5.00	4.76	35.80	8.70	4.14	40.00	6.80	4.58	39.50
April-June	11.00	3.83	35.00	6.90	3.68	29.70	2.70	3.39	23.00	6.10	3.69	27.60
July-September	9.30	3.73	31.30	5.30	1.77	17.30	1.10	1.69	13.70	4.70	3.52	27.30
October-December	11.40	4.62	40.60	2.00	1.84	15.20	4.70	3.34	23.60	4.20	2.30	17.50
January-December	**49.80**	**24.18**	**238.20**	**19.20**	**6.54**	**98.00**	**17.20**	**6.53**	**100.30**	**21.80**	**7.22**	**111.90**

Table E. 5: Annual transmission failure statistic for local South African threats

Frontal region (January-December)												
Threat	00:00-05:59			06:00-11:59			12:00-17:59			18:00-23:59		
	mean	std	max	mean	mean	std	max	mean	mean	std	max	max
Birds	36.10	7.13	92.90	13.30	4.50	46.50	5.20	1.73	18.40	14.20	5.48	50.00
Lightning	4.00	3.06	26.40	2.00	1.66	13.60	4.60	4.89	47.20	2.20	3.27	27.20
Fire	0.30	0.48	3.90	0.70	0.90	7.50	4.10	2.96	26.10	0.50	0.84	5.30
Pollution	1.60	2.58	17.60	1.60	2.10	12.80	1.20	2.63	13.20	0.20	0.28	1.80
Thunderstorm region (January-December)												
Threat	00:00-05:59			06:00-11:59			12:00-17:59			18:00-23:59		
	mean	std	max	mean	mean	std	max	mean	mean	std	max	mean
Birds	37.80	12.31	129.40	12.50	4.36	46.50	2.00	1.84	16.40	19.10	6.85	70.00
Lightning	9.20	4.14	38.00	2.00	1.66	13.60	19.40	7.09	67.40	17.70	6.66	60.50
Fire	1.40	1.16	8.60	7.30	3.54	28.10	34.10	14.52	123.70	2.60	1.71	15.00
Pollution	9.40	22.90	115.00	3.20	4.35	30.40	1.20	2.63	13.20	2.60	3.29	25.00

D. LABORATORY EXPERIMENT SIMULATION TRANSFORMER GIC INJECTION

D.1 Experiments on single-phase transformers

The lab set up is shown in Figure F.1. The main purpose of the laboratory experiment was to observe the effect dc current (simulated GIC) injection on a transformer's outputs (voltage and current).

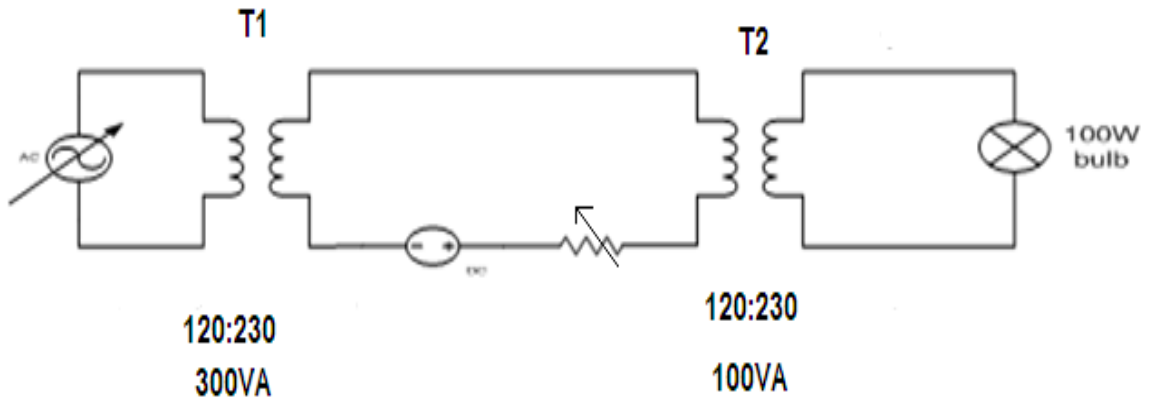

Figure F.1: Setup of experiment on single-phase transformers

The set up ensured that only the load transformer (T2) could be pushed into saturation by any dc injection. The output voltage and current profiles of the load transformer, before and after dc injection, are shown in Figure F.2. The profiles are clearly different. The rms and pk-pk values also show that the dc injection caused a drop in the magnitude of the load transformer's output voltage and current. The power output of a transformer would thus be lower than the rated value.

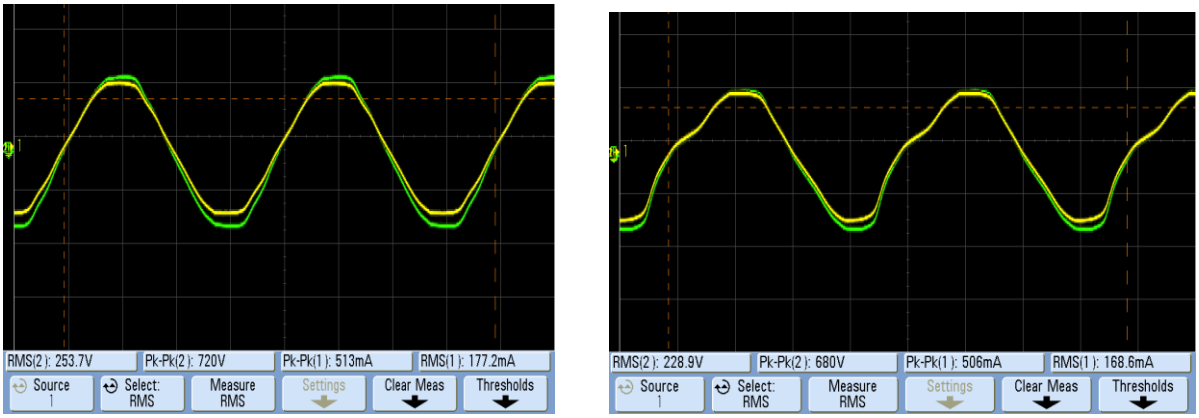

(a) **(b)**

Figure F.2: Load transformer output voltage and current waveforms (a) before GIC injection (b) after GIC injection

D.2 Experiments on three-phase transformer

In order to simulate the effects of GIC on a transformer with an earthed neutral, a bench scale laboratory test system was used. A significantly over-rated source transformer supplied power to a smaller load transformer an both transformers are a bank of three single phase transformers. The load transformer, which is the transformer under test, is being operated at its knee voltage as defined by McLyman as the point on the magnetization curve that touches a straight line from the origin whose slope is characterized by maximum permeability μ_r. The set up of this experiment is shown in Figure F.3.

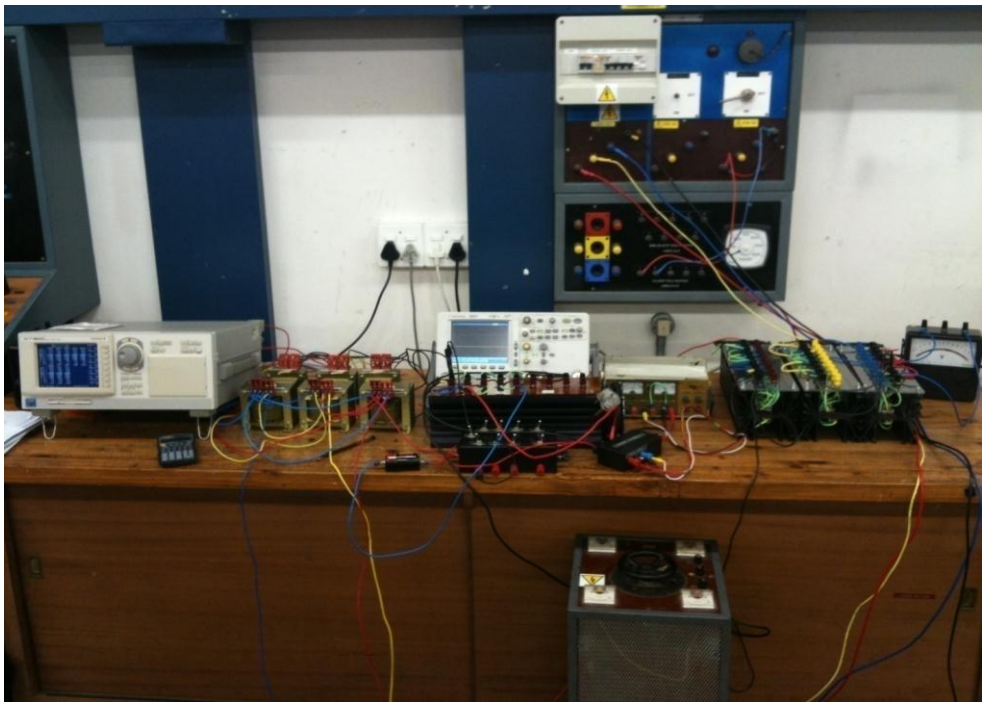

Figure F.3: Laboratory test system to simulate injection of GIC into the neutral of the load transformer. A DC battery is used to inject the direct current [Chisepo, 2012].

A small isolated three phase generator was used as the power supply and care was taken to ensure that the applied voltage across the load transformer did not correspond to over-excitation (approximately 30% below the nameplate rating) and therefore generate harmonics. The direct current that was injected was a percentage of the magnetizing current of the load transformer, namely 1.6 per unit. The justification for using an arbitrary resistive load (70% of VA rating) is that after a series of tests it was shown that non-active power absorbed by the load transformer was substantially independent of the load and increased more than linearly with the applied voltage, as expected.